





REVIEW

Battery Safety: Mechanisms, Monitoring, and Machine Intelligence

Hao Jing^{1,2}  | Shiqi Ou^{1,2}  | Zhilong Lv^{1,3}  | Haifeng Guo¹ | Andrew F. Burke⁴ | Jingyuan Zhao⁴ 

¹School of Future Technology, South China University of Technology, Guangzhou, Guangdong, China | ²Guangdong Artificial Intelligence and Digital Economy Laboratory (Guangzhou), Guangzhou, Guangdong, China | ³Hubei Longzhong Laboratory, Hubei University of Arts and Science, Xiangyang, Hubei, China | ⁴Institute of Transportation Studies, University of California Davis, Davis, California, USA

Correspondence: Shiqi Ou (sou@scut.edu.cn) | Jingyuan Zhao (jyzhao@ucdavis.edu)

Received: 27 December 2025 | **Revised:** 8 May 2026 | **Accepted:** 12 May 2026

Keywords: battery safety| cloud-edge collaboration| next-generation batteries| physics-informed neural networks| self-healing

ABSTRACT

Batteries constitute the foundation of electronic devices and electrified transportation. Nevertheless, aging and sudden faults can precipitate thermal runaway, making battery safety a global concern. This review elucidates failure triggering and evolution from the perspectives of multiphysics coupling and multiscale failure propagation, with emphasis on chemistry-specific heterogeneity in next-generation battery systems. To mitigate these risks, intrinsic-safety materials and structural designs are systematically examined, together with a graded evaluation of their maturity. System-level active protection is further discussed, highlighting the role of cloud-based Battery Management Systems in data governance and cloud-edge collaborative monitoring and control. Building on this architecture, an artificial intelligence-empowered monitoring and control framework is synthesized across four dimensions: (1) perception, which uses multimodal fusion to overcome the limitations of single-variable monitoring and enable holistic mapping of internal states; (2) algorithms, which adopt data-efficient paradigms such as self-supervised learning to address data scarcity in extreme fault scenarios; (3) mechanisms, which integrate physics-informed neural networks and digital twins to enhance interpretability and physical consistency; and (4) deployment, which leverages edge computing and federated learning to enable cloud-edge collaboration and swarm intelligence under privacy constraints. Finally, this review outlines prospects for next-generation safety testing standards, autonomous closed-loop safety management, self-healing technologies, and cross-domain safety management.

1 | Introduction

To mitigate fossil resource depletion and climate change, the transition toward efficient and reliable energy systems has become a central technological imperative [1–3]. Lithium-ion batteries (LIBs), owing to their high energy density, long cycle life, and low self-discharge, are widely deployed in electric vehicles (EVs), stationary energy storage, and portable electronics, and have emerged as a cornerstone technology for the energy transition [4–6]. In the EV sector, global sales in 2024 surpassed 17 million units, accounting for more than 20% of total vehicle sales, which

underscores the strong growth of the sector [7]. China continues to lead the electrification trajectory, with EVs accounting for nearly one-half of domestic new-vehicle sales. In the stationary storage sector, LIBs likewise dominate: as of 2024, they account for 96.4% of the commissioned energy-storage capacity in China, with an annual output of approximately 260 million kWh. With continued declines in LIB costs, global deployment is expected to expand further [8]. However, as deployment scales and cell-level energy density increase, safety risks have become increasingly salient, now constituting a principal constraint on the sustainable development of LIB technology [9–11].

Under abusive conditions such as overcharge or overdischarge, overheating, or mechanical damage, LIBs may undergo cascades of exothermic electrochemical reactions, leading to rapid internal temperature rise [12, 13]. If not promptly mitigated, these processes can trigger off-gas release, casing rupture, and, in severe cases, thermal runaway (TR) accompanied by ignition or explosion [14–16]. Between 2010 and June 2024, 511 verified EV battery fire incidents were recorded globally, elevating public and industrial concern regarding the intrinsic safety of battery systems [17, 18]. Accordingly, elucidating failure mechanisms under coupled electrochemical, thermal, and mechanical fields, identifying the origins of diverse failure modes, and integrating cross-disciplinary insights to support safety-by-design have become critical priorities in the development of next-generation high-safety batteries [19–22].

Current safety assurance frameworks continue to rely predominantly on traditional passive protection strategies [23, 24]. These strategies span multiple hierarchical levels, including material-level flame retardants and coatings, structural measures such as thermal insulation pads, firewalls, and cell spacing design, and system-level safeguards involving pressure relief devices and overvoltage/overcurrent protection circuits [25–27]. While effective in reducing accident probabilities under nominal conditions, these approaches exhibit diminishing protective efficacy under increasingly demanding scenarios involving high energy density, fast charging, and extreme temperatures [28, 29]. Fundamentally, passive strategies suffer from intrinsic response latency, which prevents timely intervention during the early stages of TR and allows localized abnormalities to evolve into irreversible chain reactions [30, 31]. In parallel, contemporary Battery Management System (BMS) remains largely dependent on threshold-triggered logic, limiting real-time perception and predictive capability for complex, multi-source signals and reducing sensitivity to localized or latent faults. Moreover, existing safety testing and certification standards emphasize isolated extreme conditions, with limited consideration of multiphysics coupling and long-term aging effects [32–34]. These limitations indicate that conventional material-level improvements and passive system-level protection are increasingly inadequate for emerging safety challenges, underscoring the need for active, cross-hierarchical safety management frameworks.

Recent advances in computing, communications, and artificial intelligence (AI) have created new opportunities for battery safety research [35–37]. Deep learning and large-model frameworks are increasingly applied to battery materials design, performance prediction, prognostics, and state estimation [38–40], enabling accurate prediction of the state of charge (SOC), state of health (SOH), and remaining useful life (RUL) for predictive maintenance [41–45]. However, safety events such as TR are high-consequence yet rare, leading to severe data scarcity that limits model generalization and reliability [46, 47]. Moreover, electrochemical and thermodynamic processes under multiphysics coupling remain complex; without physical constraints, model predictions may deviate from underlying mechanisms [48, 49]. Practical deployment is further constrained by computational resources, model interpretability, and real-time requirements [50]. These challenges indicate that data-driven safety management alone is insufficient for high-safety battery systems.

Despite the progress achieved in battery safety research in recent years, existing review articles have largely proceeded along relatively independent lines, such as failure mechanisms, intrinsic safety design, or intelligent monitoring, and have accumulated substantial findings within each of these directions. However, for advanced battery systems operating under demands of high energy density, long service life, and complex service conditions, safety issues are not merely localized problems at a single level, but rather constitute a complex systems problem that spans multiple scales, multiple hierarchical levels, and multiple disciplines, extending from materials and cells to the entire process of system operation. Although existing studies have separately elucidated the evolution of TR, aging-induced failure, and abuse responses, proposed safety-enhancement strategies such as material modification and structural protection, and explored the application of machine learning in areas such as state estimation, they have remained largely focused on their respective domains. As a result, a unified analytical framework that systematically links failure-triggering mechanisms, intrinsic safety boundaries, online monitoring signatures, and intelligent decision-making for battery safety remains lacking. Meanwhile, next-generation electrochemical systems also exhibit distinct characteristics in terms of failure-triggering conditions and risk manifestations. Moreover, as AI becomes more deeply integrated into battery safety research, attention has expanded beyond predictive capabilities to broader challenges, including data scarcity, limited interpretability, privacy protection, and secure deployment. These issues have not yet been discussed in a sufficiently systematic manner in existing reviews. Therefore, it is necessary to re-examine battery safety research from a perspective that integrates mechanisms, design, monitoring, and intelligent management to establish a more holistic, engineering-oriented conceptual framework.

Against this background, this work proposes a unified technical framework that combines failure-mechanism analysis, materials innovation, system design, and intelligent monitoring (Figure 1). Centered on multiphysics coupling and multiscale analysis, the framework systematically elucidates the initiation and evolution of safety issues such as TR, covering hierarchical levels from particle and interface to electrode, cell, and pack, and highlights the failure heterogeneity of next-generation battery chemistries (Section 2). On this basis, the study further explores frontier directions for enhancing intrinsic safety through material modifications and structural innovations, with a graded assessment of the maturity of safety technologies (Section 3), and, in conjunction with system-level operational monitoring strategies, proposes a multilayer coordinated safety-assurance scheme (Section 4). Additionally, this study traces the evolution of the BMS under an edge-to-cloud collaborative paradigm. It clarifies its key roles in large-scale monitoring, intelligent decision-making, and closed-loop data management. Finally, this study reviews intelligent battery safety monitoring methods and, from four dimensions including signal fusion, data-efficient algorithms, physics-informed integration, and engineering deployment, presents the core technical system and development trends of intelligent safety monitoring. The goal is to shift battery safety management from reactive response to proactive prediction, achieving more accurate and robust safety control (Section 5). Section 6 provides a forward-looking outlook on future directions for battery safety research and engineering practice.

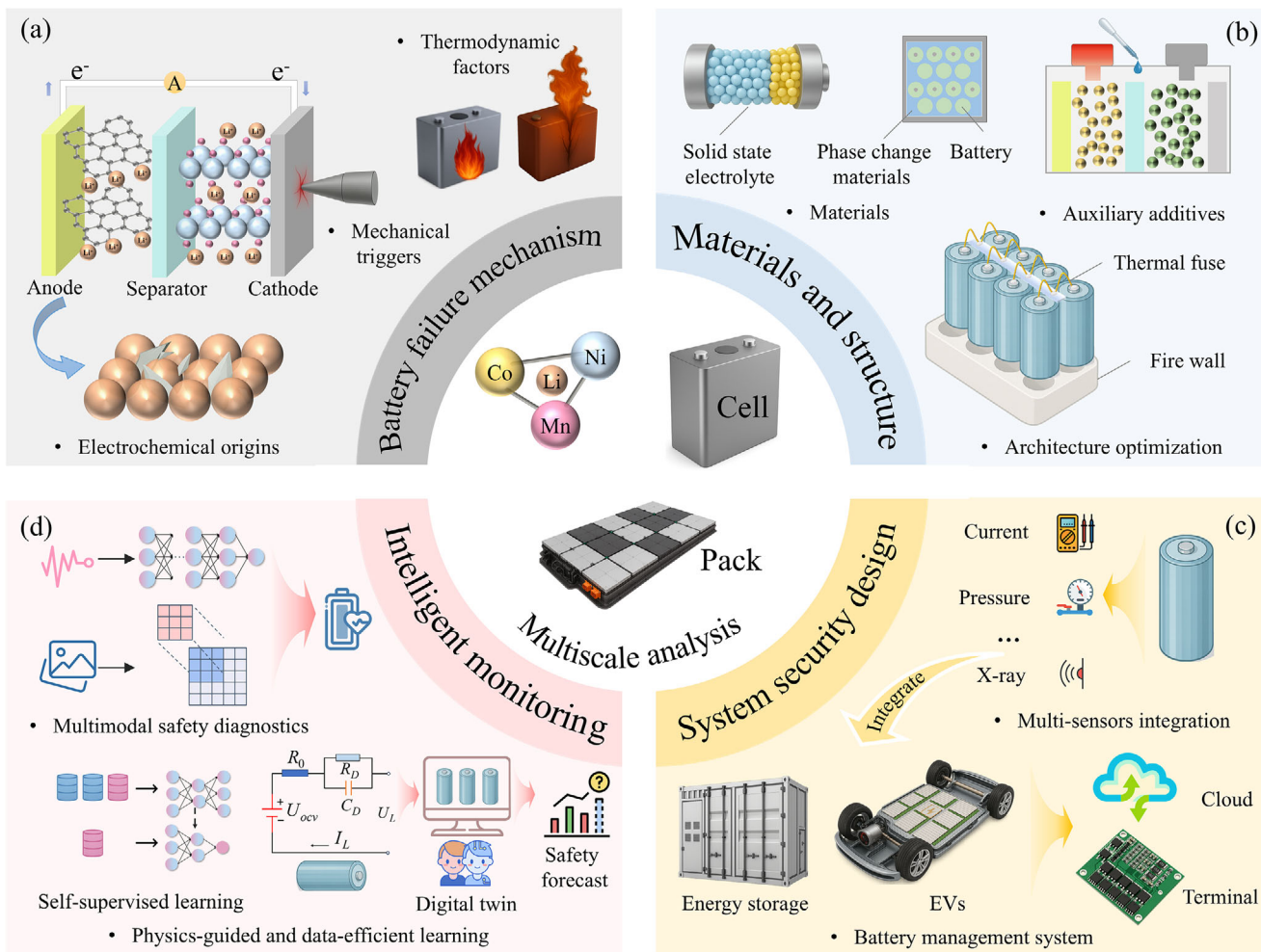


FIGURE 1 | Multilevel battery safety framework illustrating the interplay between degradation mechanisms, materials design, real-time monitoring, and intelligent management across cell, module, and system scales.

2 | Failure Mechanisms of Batteries

2.1 | Multiphysics Coupling Failure Mechanisms

LIBs are dynamically coupled systems governed by the concurrent interactions of charge transport, mass diffusion, heat generation, and mechanical response. Under normal operating conditions, their behavior is dominated by reversible electrochemical reactions accompanied by Joule heat generation [51, 52]. When subjected to external loads and abusive conditions, such as vibration or impact, as well as overcharge and elevated temperatures [53, 54], strong electrochemical–thermal–mechanical coupling emerges with pronounced nonlinear amplification (Figure 2). Exothermic side reactions induce thermal instability, mechanical damage leads to structural degradation and internal short circuits (ISCs), and heat accumulation further accelerates material decomposition and failure, collectively driving the transition from localized abnormalities to irreversible loss of control [55–57].

From an electrochemical perspective, cell-to-cell inconsistency increases susceptibility to overcharge or overdischarge, particularly under end-of-cycle conditions [58, 59]. Once the operating window is exceeded, rapid increases in temperature and pressure

trigger parasitic reactions, including oxygen release from the cathode, separator degradation, and rupture and decomposition of the solid electrolyte interphase (SEI), exposing fresh active surfaces [60]. These processes continuously consume electrolyte and cyclable lithium, resulting in capacity fade and increased internal resistance (Figure 2a) [61–63]. Within this framework, electrolyte decomposition constitutes one of the major sources of gas generation and associated safety hazards in rechargeable batteries. Specifically, the parasitic decomposition of the electrolyte exhibits pronounced interfacial dependence and compositional specificity [64]. At the cathode interface, high-voltage conditions promote the oxidative dehydrogenation of carbonate solvents, primarily releasing CO_2 and CO . Meanwhile, highly reactive oxygen species liberated during structural degradation of the cathode can further attack solvent molecules, thereby markedly intensifying the generation of CO_2 , CO , and H_2O . At the anode interface, solvent molecules undergo reductive bond cleavage upon electron uptake. In this process, two-electron reduction pathways predominantly generate CO , whereas one-electron reduction pathways are generally accompanied by the evolution of flammable hydrocarbon gases such as C_2H_4 , CH_4 , and C_2H_6 . In addition, protons generated by oxidative reactions at the cathode can migrate across the separator to the anode and be reduced there, which also constitutes an important

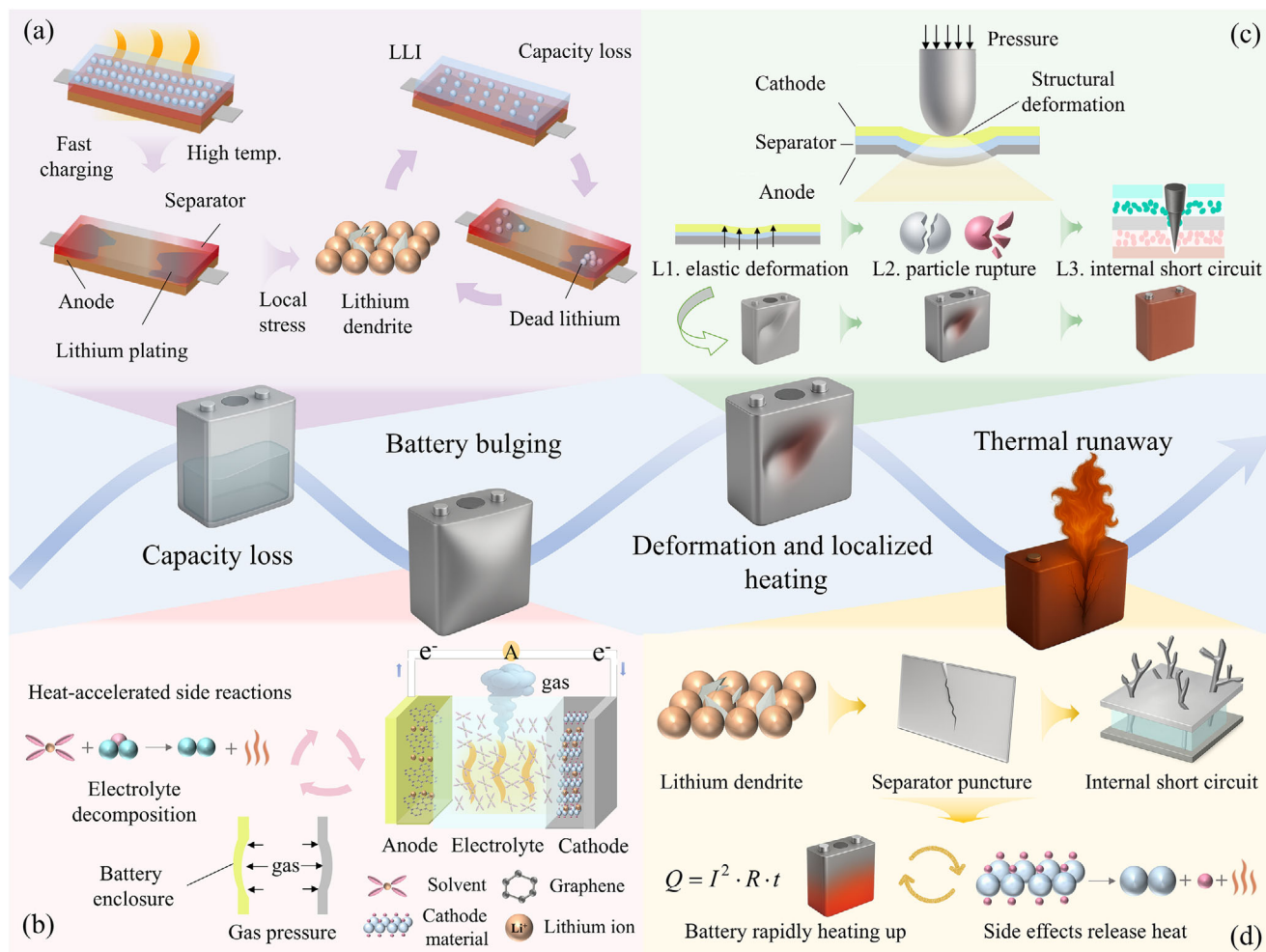


FIGURE 2 | Schematic of electrochemical–thermal–mechanical coupling in Li-ion battery safety. (a) Under fast-charging and elevated-temperature conditions, Li plating couples with local stress, causing dendrite growth, dead Li formation, and capacity loss. Adapted with permission [62]. Copyright 2022, Elsevier. (b) Electrolyte decomposition and heat-accelerated side reactions generate gases, increase internal pressure, and induce battery bulging. (c) Mechanical deformation damages cell components and promotes ISCs and localized heating. (d) Dendrite-induced separator puncture triggers ISCs, Joule heating, exothermic reactions, and TR.

source of H_2 within the system [65]. Beyond these direct interfacial reactions, chain decomposition reactions initiated by trace impurities in the electrolyte, particularly H_2O , are likewise non-negligible. Water can not only be directly reduced at the anode to evolve H_2 , but can also induce the hydrolysis of lithium salts such as $LiPF_6$, generating highly corrosive species including HF and POF_3 . The resulting HF can further attack inorganic carbonate components on electrode surfaces, inducing renewed CO_2 release and thereby forming a self-amplifying degradation loop [66]. Quantitative investigations based on in situ differential electrochemical mass spectrometry have demonstrated that both the identity and the amount of evolved gases depend strongly on electrode chemistry, electrolyte formulation, and operating conditions [64]. This effect is especially pronounced in battery systems employing alkali-metal anodes, in which gas evolution rates and accumulation effects are typically more severe. As shown in Figure 2b, if the generated heat and gas are insufficiently dissipated, cell swelling, casing rupture, and even TR or explosion may occur [67–69]. Overcharging further promotes metallic lithium deposition and lithium plating [70], which can evolve into dendrites that penetrate the separator,

induce ISCs, and constitute a critical trigger for TR (Figure 2d) [71].

From a mechanical perspective, compression, vibration, and penetration alter electrochemical behavior through structural and interfacial damage (Figure 2c). Prolonged vibration causes stress accumulation and damage to components or separators, inducing ISCs and accelerating resistance growth and capacity degradation [72, 73]. Severe mechanical damage disrupts the SEI and amplifies parasitic reactions [74], while even minor deformation can impede ion transport and accelerate degradation [75]. Under extreme mechanical abuse, such as penetration, direct anode–cathode contact leads to severe ISCs, intense heat release, and rapid temperature escalation, activating cascading side reactions and ultimately driving TR [76, 77].

From a thermal perspective, heat generation originates primarily from Joule heating and reaction enthalpy, with normal cycling producing limited heat [50, 78]. Under insufficient heat dissipation, localized heat accumulation initiates a sequence of exothermic reactions: SEI decomposition at approximately $80^\circ C$

[79], electrolyte decomposition with gas evolution near 100°C [80], and cathode decomposition accompanied by oxygen release around 180°C [81]. The superposition of these processes forms a positive thermal feedback loop that may culminate in TR [58]. Additionally, exposure to excessive ambient temperatures or thermal shock beyond the optimal 20–40°C window accelerates parasitic reactions, leading to capacity loss and increased internal resistance; sustained external heat input can further push the system toward TR [82].

More importantly, these physical fields do not operate independently, but are tightly coupled through a series of mutually reinforcing pathways. Among them, electrochemical–thermal coupling constitutes one of the principal interaction routes. Joule heating, changes in reaction enthalpy, and heat released from parasitic reactions directly alter the battery’s internal temperature field, while temperature variations, in turn, strongly regulate electrochemical reaction kinetics. Elevated temperature not only accelerates electrode reactions and ion transport but also promotes parasitic processes such as SEI decomposition, electrolyte degradation, and oxygen release from the cathode, thereby forming a positive feedback loop in which electrochemical side reactions lead to heat accumulation, which further intensifies side reactions [83]. Thermal–mechanical coupling represents another important route through which multiphysics interactions are further amplified. Non-uniform thermal stresses induced by temperature rise can lead to mechanical damage such as interfacial delamination and separator thermal shrinkage [84]. These structural failures, in turn, disrupt local heat transfer and dissipation within the battery and may induce ISCs, thereby releasing additional Joule heat and causing more severe heat accumulation. Meanwhile, electrochemical–mechanical coupling serves as a critical link between microscopic interfacial behavior and macroscopic failure manifestations. Volume changes associated with lithium-ion insertion and extraction can result in current collector debonding and repeated rupture of the SEI, whereas the resulting mechanical damage can further hinder ion transport, aggravate local current heterogeneity, and promote lithium dendrite growth [53]. This gives rise to a bidirectional coupling process involving electrochemical cycling, volume strain, structural damage, and accelerated electrochemical degradation. These three coupling pathways are deeply intertwined and act synergistically. In particular, gas evolution arising from electrolyte decomposition serves as an important coupling medium linking electrochemical, thermal, and mechanical fields. The increase in internal pressure caused by gas generation can aggravate cell swelling and interfacial contact failure, which, in turn, intensifies local current heterogeneity and heat accumulation, ultimately forming a self-accelerating cycle involving all three fields. Under extreme conditions such as overcharge, overdischarge, elevated temperature, and mechanical abuse, an initial perturbation in a single physical field can be rapidly amplified through this multiphysics coupling network, thereby triggering cascaded positive-feedback failure across multiple fields and ultimately leading to catastrophic safety events such as TR.

2.2 | Multiscale Failure Propagation

As complex, dynamic, multiscale systems, LIBs exhibit cascade-type failure behavior, characterized by a progression from micro-

scopic origins through mesoscopic evolution to macroscopic outbreaks [85]. As illustrated in Figure 3, the cross-scale failure propagation chain spans the entire process from atomic-scale material degradation to system-level thermal propagation. During electrochemical cycling, in addition to reversible intercalation and deintercalation, manufacturing defects and complex operating conditions jointly induce microscopic parasitic reactions and structural damage. These early degradation signatures accumulate and amplify with cycling, gradually evolving into mesoscopic electrode structural deterioration and interfacial instability, and ultimately manifesting at the macroscopic level as performance degradation, structural swelling, accelerated capacity fade, and even TR, thereby posing severe safety risks [86–88]. Importantly, this cross-scale propagation is not a simple sequential accumulation process, but a coupled amplification chain governed by several key control nodes, including particle integrity, interfacial stability, separator robustness, gas and pressure buildup, localized hot-spot formation, and thermal coupling between neighboring cells, among others. Once these nodes are destabilized, microscopic perturbations can be rapidly amplified into macroscopic system-level failure. By comparatively analyzing two representative evolution pathways—abnormal capacity fade and TR (Figure 3)—the nonlinear amplification mechanisms and propagation routes through which microscopic physicochemical instabilities translate into macroscopic system failures can be elucidated.

For the abnormal capacity fade chain shown on the left of Figure 3, the microscopic origins may be attributed to impurity defects introduced during manufacturing and to chemo-mechanical coupling damage at the atomic and particle scales. The cross-scale correlation mechanism of this pathway is primarily driven by a coupled feedback loop among mechanical strain, interfacial structure, and electrochemical impedance. During cycling, active particles undergo repeated volumetric expansion and contraction due to lithium-ion intercalation and deintercalation [67]. Taking the anode as an example, particle expansion induces compressive stress at contact points. At the same time, constraints imposed by binders and conductive additives further exacerbate stress accumulation [53, 89–91], promoting crack initiation and propagation that ultimately lead to particle fragmentation and pulverization [92]. Particle fracture transforms the electrode structure from dense to porous, weakening the electronic and ionic transport networks and causing a pronounced increase in internal resistance [93]. Meanwhile, exposure of fresh surfaces continuously drives electrolyte decomposition and SEI reformation, resulting in the irreversible loss of lithium inventory (LLI) and accelerated SEI thickening, leading to rising interfacial impedance. The cumulative effects of these microscopic defects and mesoscopic structural degradation ultimately cause rapid capacity decay and resistance growth at the cell level. When such degraded cells are present within a module, their deterioration—regulated by BMS balancing strategies—can be further amplified to the module and pack levels, potentially inducing severe safety hazards such as swelling and ISC during long-term operation [94, 95]. In this pathway, several key control nodes determine whether degradation remains slow and manageable or evolves into rapid system-level failure, including intrinsic material structural stability and defect control, electrode–electrolyte interfacial stability, electrode structural integrity, mitigation of cell-to-cell inconsistency, and system-level fault isolation capability.

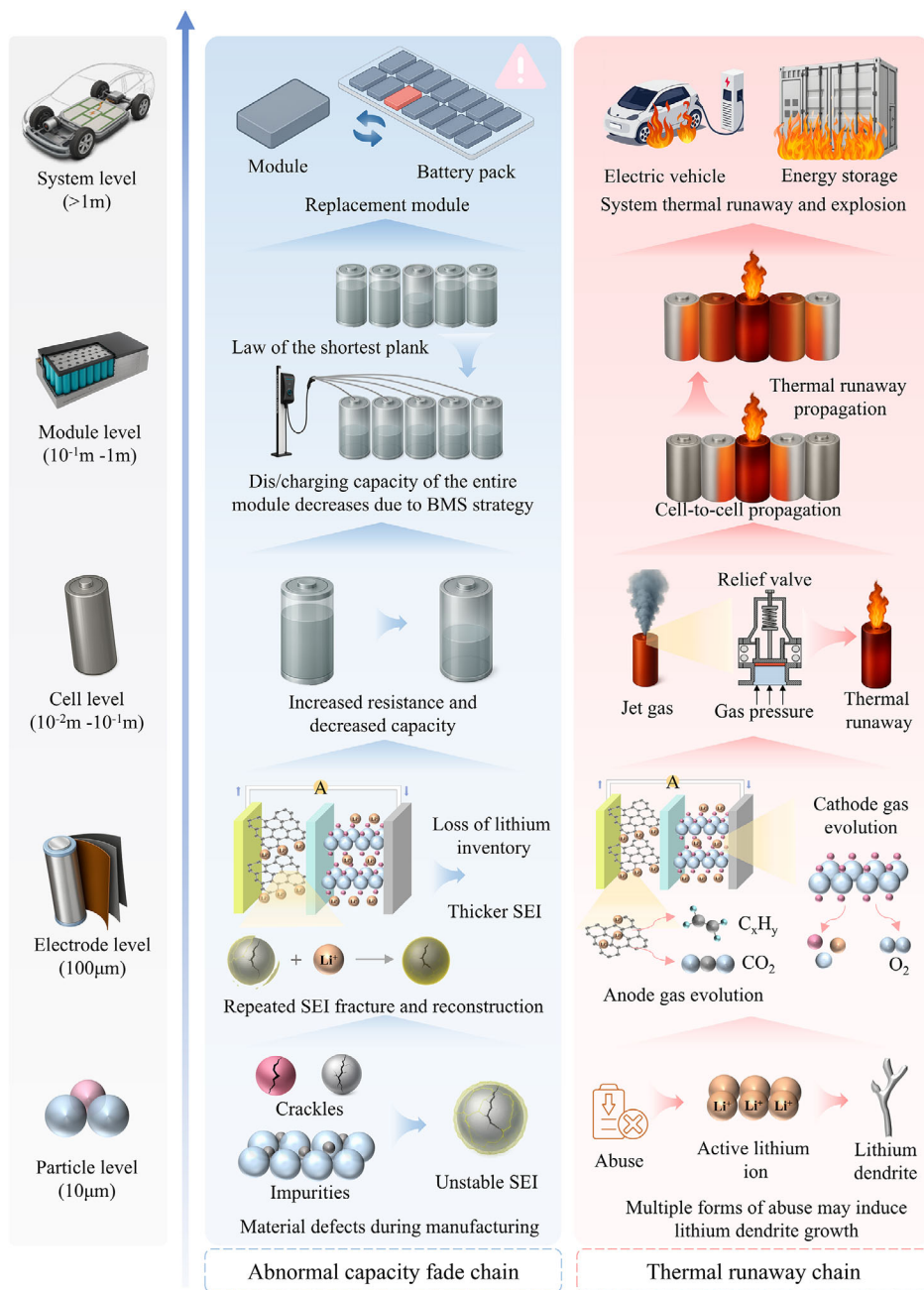


FIGURE 3 | Multiscale failure propagation chain from the particle scale to the electrode, single-cell, module, and full battery-pack levels, illustrating two representative evolution pathways. The left pathway corresponds to abnormal capacity fade, involving repeated volume changes, particle fracture, subsequent growth in interfacial impedance, cell capacity decay, and eventual module-level failure. The right pathway illustrates TR propagation, involving localized electrochemical instability, ISCs, and inter-cell thermal coupling that progressively amplify toward system-level destabilization.

Simultaneously, the TR propagation chain on the right side of Figure 3 represents a higher-risk cross-scale amplification process. Its correlation mechanism is characterized by a cascading amplification of electrochemical instability, intense heat release, and multiphysics thermal coupling. Under abusive conditions, such as overcharging or low-temperature operation, microscopic lithium plating leads to dendritic growth. Penetration of the separator by lithium dendrites can trigger mesoscopic internal micro-short circuits and generate localized hot spots. Concurrently, gas evolution from cathode phase transitions at elevated temperature and pressure, together with gas generation from electrolyte decomposition, intensifies internal pressure accumu-

lation, potentially activating pressure relief mechanisms and ejecting high-temperature gases and sparks [66]. At this stage, key control nodes include lithium plating and dendrite penetration, separator failure, localized hot-spot formation, gas and pressure accumulation, and the strength of thermal coupling between adjacent cells.

These nodes determine whether an initial localized abnormality is confined to the cell level or escalates to module-level propagation. Once inter-cell thermal coupling becomes dominant, the intense heat released from a failed cell can rapidly propagate to neighboring cells. In the absence of effective thermal barriers, this

TABLE 1 | Quantitative comparison of TR risks and toxic gas emissions among different battery systems.

Battery systems ^a	TR trigger temperature (°C)	TR maximum temperature (°C)	Total gas release ^b	Major toxic gas species	Concentration of toxic gases (ppm) ^c
Liquid electrolyte lithium iron phosphate (LFP) battery	196–280 [98, 99, 100]	417–511 [99, 101]	~0.6–2.5 L Ah ⁻¹ [98, 102, 103]	HF, CO [102, 103]	>130 (HF) [104]
Lithium nickel cobalt manganese oxide (NCM523) battery ^d	165–253 [100, 101]	544–850 [98, 100, 101]	~1.74–5.0 L Ah ⁻¹ [98, 102]	HF, CO [102, 103]	>130 (HF) [104, 105]
Sulfide-based solid-state battery ^e	150–313 [106, 107]	500–700 [98, 106, 108]	~0.8–1.5 L Ah ⁻¹ [98]	H ₂ S, SO ₂ [104, 109]	<25 (H ₂ S) [109]
Sodium-ion battery ^f	157–271 [100, 103]	466–794 [101, 110]	~1.8–5.1 L Ah ⁻¹ [102, 103]	HCN, HF, CO [104, 111]	<100 (HCN) [104]
Potassium-ion battery ^f	100–120 [112, 113]	325–500 [112, 113]	~51.4 wt% mass conversion ^b [111]	HCN, HF, CO [111]	<100 (HCN) [104]

^aThe data presented in this table represent typical reference ranges derived from recent literature. The exact TR temperatures and associated gas emission yields may vary depending on factors such as chemical composition, electrolyte formulation, cell design, SOC, and testing conditions, including heating rate, atmosphere, and chamber configuration.

^bSpecific gas emission yields are typically normalized to cell capacity. However, for emerging potassium-ion batteries, gas emission data are predominantly reported at the material level as mass loss. Upon thermal decomposition, fully charged hexacyanoferrate cathodes release toxic cyanide-containing gases corresponding to roughly 51.4 wt% of the cathode mass.

^cThe measured gas concentrations (ppm, volume basis) are influenced by the testing environment, including factors such as chamber volume and experimental configuration. Therefore, the reported values are intended to provide a quantitative reference for comparison with established safety thresholds such as IDLH limits, while comparisons across different battery chemistries should be made with appropriate consideration of differences in experimental conditions.

^dNCM523 refers to LiNi_{0.5}Co_{0.2}Mn_{0.3}O₂.

^eData for sulfide-based solid-state batteries are based on NCM cathode materials and lithium phosphorus sulfide chloride solid electrolytes.

^fSodium-ion and potassium-ion batteries release toxic HCN gas when Prussian blue analogues (PBAs) are used as cathode materials.

leads to domino-like thermal propagation, ultimately resulting in system-level fire or explosion [96, 97].

These two representative pathways together show that battery failure is inherently a nonlinear multiscale propagation process. Microscopic defects, interfacial instabilities, and localized thermal or electrochemical abnormalities do not remain isolated, but are progressively amplified through mesoscopic structural degradation and cell-level heterogeneity. Their evolution is controlled by several scale-bridging nodes, and once these nodes lose stability, the system can transition rapidly from reversible degradation to irreversible failure. Elucidating these multiscale propagation mechanisms and their key control nodes, therefore, provides a fundamental theoretical basis for the design of high-safety battery systems and for the identification of effective intervention points across scales.

2.3 | Failure Specificity of Next-Generation Battery Chemical Systems

As battery technologies evolve toward solid-state electrolytes (SSEs) and emerging chemistries, failure modes exhibit pronounced chemistry-specific characteristics. Under identical thermal, electrical, and mechanical abuse triggers, substantial divergence can arise in TR onset thresholds, reaction kinetics, jetting behavior, and hazard manifestations. To provide a quantitative illustration of these differences, Table 1 presents a systematic comparison of the TR risk thresholds and toxic gas emissions

between mainstream liquid-based batteries and next-generation batteries.

For emerging battery systems based on highly reactive alkali metals, such as Na, Li, and K, the intrinsic chemical reactivity and interfacial instability can lead to failure via pathways such as dendritic growth or rapid SEI degradation, and they are highly sensitive to ambient moisture and oxygen [114, 115]. This intrinsic reactivity and fragile interface directly contribute to a reduction in system-level thermal safety thresholds. As shown in Table 1, the TR trigger temperature of potassium-ion batteries is only 100–120°C, which is significantly lower than that of conventional LIBs. One potential mechanism is related to the relatively large ionic radius of potassium ion, which gives rise to substantial volumetric stresses during potassiation of the carbon host. These stresses can readily rupture the SEI on the anode surface, expose highly reactive intercalated potassium phases to the electrolyte at relatively low temperatures, and thereby trigger vigorous exothermic side reactions that promote TR [112]. On the other hand, despite the high intrinsic modulus of many SSEs, they still face the risk of lithium dendrite penetration, which constitutes a pathway for ISCs and TR. In solid-state systems, dendrite evolution transcends classical macroscopic elasticity criteria. It is governed by an electrochemical–mechanical coupling process involving microscale defect-driven fracture mechanics and the dynamic viscoplastic behavior of lithium metal [116, 117]. This process can be divided into two stages: initiation and propagation. During the initiation stage, dendrite formation is highly defect-dependent [118]. Lithium preferentially deposits at pre-existing

micropores or nanoscale cracks near the electrolyte surface. These regions exhibit concentrated local electric fields and current focusing, providing favorable sites for dendrite initiation [117, 118]. Constrained lithium deposition generates high local stress within these spaces, and when this concentrated pressure exceeds the local fracture strength of the solid electrolyte, initial microcracks are triggered. In the propagation stage, lithium continues to exert wedge-like deposition pressure, driving crack tip regions to unstable growth. Moreover, atomistic simulations indicate that rapid consumption of lithium ions at crack tips may transiently increase local fracture toughness, leading to intermittent or rate-dependent crack propagation. In polycrystalline systems, cracks tend to deflect along grain boundaries, producing a mixed tensile–shear failure mode that enhances intergranular sliding and delamination [119]. Ultimately, the accumulation of microcracks and continued lithium filling within crack networks compromises the structural integrity of the electrolyte, leading to direct electronic contact between anode and cathode, violent energy release, and TR. Although solid-state batteries may extend intrinsic material-level thermal stability windows, certain oxide solid-electrolyte systems can exhibit intensified transient heat-release behavior during TR, with peak heat-release rates escalating from the 10^2 kW range to the 10^3 kW regime, reflecting markedly faster kinetics [120, 121]. Moreover, thermal stability is no longer governed primarily by the decomposition temperature of the electrolyte alone, but instead depends critically on cathode–electrolyte interfacial compatibility. For example, sulfide solid electrolytes coupled with high-nickel layered cathodes can trigger violent reactions at approximately 150°C , whereas pairing with phosphate cathodes can elevate the instability threshold to around 350°C [107]. These contrasts indicate that a higher material-level stability window does not necessarily translate into lower system-level failure risk. In addition, increased solid-phase content may enhance the erosive effects of solid-particle ejection, thereby altering the dominant thermal-propagation pathways.

Beyond thermal characteristics, the toxic evolution of gas species generated during failure has emerged as a critical safety concern for next-generation batteries. Under TR or abuse conditions, gas compositions vary substantially across material systems, shifting the dominant risk dimension from flammability alone toward toxicity and environmental impact. As shown in Table 1, fluorinated electrolyte systems in LIBs predominantly release highly corrosive gases such as HF, with reported concentrations exceeding 130 ppm, far above the immediately dangerous to life and health (IDLH) threshold of 30 ppm established by the U.S. National Institute for Occupational Safety and Health [122, 123]. For emerging chemistries, sodium- and potassium-ion batteries employing Prussian blue-type cathode materials may release HCN at concentrations below 100 ppm under elevated temperature or high SOC conditions, which may still exceed the corresponding IDLH threshold of 50 ppm [123]. In addition, sulfide-based solid-state batteries can emit H_2S when heated or exposed to humid air, with concentrations below 25 ppm, which are close to the associated safety threshold of 20 ppm [104, 124]. These findings reveal substantial differences in gas evolution kinetics and concentrations across battery chemistries, resulting in distinct toxic exposure risks in enclosed environments. Since conventional safety assessment frameworks have primarily focused on fire and explosion hazards, future

testing standards should explicitly incorporate the evaluation of chemistry-specific toxic emission profiles in next-generation electrochemical systems.

Moreover, failure modes in next-generation chemistries may exhibit a stronger dependence on cycling history. Prolonged cycling, fast charging, extreme temperatures, and mechanical loading can substantially modify interfacial structures, dendrite morphology, and the distribution of reactive species, thereby reshaping failure initiation pathways and evolution dynamics. For example, porous or fractured dendritic networks formed on alkali-metal anodes during cycling can reduce TR thresholds and accelerate reaction kinetics [125]. At the same time, the accumulation of microcracks and electrically isolated metallic phases within solid electrolytes may degrade mechanical integrity and alter thermal response behavior [126]. Consequently, the safety assessment of next-generation batteries should treat SOC and aging history as decisive variables and adopt a material–interface–history coupled perspective to establish chemistry-specific and stage-resolved failure description frameworks, thereby enabling more targeted testing standards and system-level protection strategies.

3 | From Materials to Structures: Multiscale Design of Intrinsic Safety

Batteries inherently pose several safety risks due to the materials and structures used, including highly reactive electrode materials, volatile electrolytes, and flammable separators. Therefore, systematically improving and innovating the internal materials and structures of the battery, starting from the fundamental nature of the materials, has been widely regarded as a key approach to overcoming performance limitations and achieving intrinsic safety enhancements [127, 128]. Accordingly, this section reviews several pathways, including electrode and interface engineering, active lithium compensation, self-healing batteries, electrolyte systems, thermal management materials, and structural design, and summarizes the mechanisms, safety benefits, representative implementations, and intrinsic safety maturity readiness level (IMRL) in Table 2. To improve the transparency of the maturity grading in Table 2, the definition, classification criteria, and representative assignment basis of IMRL are provided in Section S1 of the Supporting Information and in Tables S1–S2.

3.1 | Electrode and Interfacial Materials

In the complex multi-component architecture of LIBs, the cathode and anode materials serve as host matrices for reversible lithium-ion intercalation and deintercalation. They serve not only as the primary determinants of energy density and power characteristics but also as critical bottlenecks that constrain safety and cycling stability across the full lifecycle. The intrinsic physicochemical properties of electrode materials—encompassing the thermal stability of the crystal structure, microscopic phase transition mechanisms, and electrochemical compatibility at the electrode/electrolyte interface—directly define the safety boundaries of the battery system. Consequently, grounded in a profound understanding of structure-property relationships, precise structural design and modification of electrode

TABLE 2 | Summary and IMRL grading of material and structural strategies for intrinsic battery safety.

Specific strategy	Functional mechanisms	Safety benefits	Representative implementations	IMRL ^a
Cathode modification	Element doping: regulates electronic structure/ion pathways to stabilize the lattice.	Improved thermal stability, mitigated overcharge-induced degradation, and TR.	Elemental doping (Mn, Na, Zr, Ti) and multi-element co-doping [137–139].	4-5
	Surface coating: creates a physical barrier to buffer interface reactivity.	Reduced parasitic heat generation, lower gas evolution, and extended cycling stability.	Fluorides, phosphates, transition metal oxides [141].	4-5
Anode SEI engineering	In-situ stabilization: electrolyte additives decompose to form specific passivation layers.	Mitigated dendrite-induced short circuit, lower gas/heat release, and extended cell life.	Fluoride/Nitride/Sulfide forming LiF/Li ₃ N/Li ₂ S-rich SEI [151].	4-5
	Artificial interface: Protects anode surface from electrolyte attack and suppresses SEI rupture/regrowth.	Lower interfacial heat generation, reduced impedance rise, improved long-term stability.	ALD-derived Al ₂ O ₃ and functional interlayers on graphite/Si-based anodes [155].	3-4
Active lithium compensation	Pre-lithiation: introduces an extra Li source during manufacturing to offset initial SEI loss.	Compensates ICE and improves cycle life.	Li-Naphthalene [160]. Li-(4,4'-dimethylbiphenyl) [161].	3-4
	External Li supply: uses sacrificial additives to release Li+ during charging via anodic oxidation.	Dynamically restores aged batteries and enables Li-free cathodes without breaking seals.	Additive: Lithium trifluoromethylsulfinate (LiSO ₂ CF ₃) [164].	1-2
Solid-state electrolytes	Non-flammable solid media with high mechanical strength, suppressing dendrite penetration.	Eliminated leakage or flammability, enhanced high-temperature stability.	Ceramic, sulfide, phosphate SSEs. PEO/PAN-based SPEs [171, 172].	2-3
Self-healing polymer electrolytes	Reversible bond exchange heals interfacial cracks and delamination.	Maintains interfacial integrity, prevents local hotspots and impedance growth.	Polyether urethane with dynamic disulfide/hydrogen bonds [175].	1-2
Gel polymer electrolytes	Polymer network immobilizes solvent while preserving ionic conductivity.	Reduced leakage/flame risk, enhanced interfacial wettability, and thermal stability.	Matrix: PEO, PMMA [179]. Salts: LiPF ₆ , LiBF ₄ , LiBOB [167, 180].	3-4
Phase change materials	Absorbs excess heat via solid-liquid phase transition (latent heat storage).	Buffers temperature spikes, ensures uniform thermal distribution, and passively suppresses thermal feedback.	Materials: Paraffins, PEG [183]. Composites: paraffin with graphene/CNTs for enhanced conductivity [184].	3-4
Thermal insulation	Uses materials with ultra-low thermal conductivity to block heat transfer.	Delays heat propagation between cells during TR and acts as a fire retardant barrier.	Silica aerogels (<0.03 W/m·K) and flame-retardant modified aerogels [188].	5

(Continues)

TABLE 2 | (Continued)

Specific strategy	Functional mechanisms	Safety benefits	Representative implementations	IMRL ^a
Electrical architecture	Integrates thermal fuses in current paths that melt upon overcurrent.	Physically isolates faulty cells to prevent cascading electrical failures.	Thermal fuses, current-interrupt devices integrated in cell circuits [189].	5
Physical structure & geometry	Geometry: Enlarged heat-dissipation area and shortened heat-transfer path.	Reduces internal heat accumulation, improves space utilization and cooling efficiency.	BYD “Blade Battery” (long, thin rectangular cells) [192].	5

^aIMRL ranges from 1 to 5, with higher scores indicating higher maturity.

materials remain the central research focus for overcoming existing performance limitations and achieving intrinsic safety upgrades [129].

The cathode material, as the main source of lithium ions during electrochemical reactions, plays a decisive role in determining the voltage platform and cycling stability. At present, widely used cathode materials include ternary oxides, such as nickel cobalt aluminum (NCA) oxide and nickel cobalt manganese oxide (NCM), which offer high specific capacity and energy density, as well as olivine-structured LiFePO₄, which exhibits high structural and thermal stability and a long cycle life. These materials have been extensively applied in energy storage systems (ESS) and electric transportation [130, 131]. However, existing cathode materials still face multiple technical challenges in practical applications. In particular, insufficient structural stability and severe interfacial side reactions with the electrolyte have become major limiting factors for battery safety [132]. These issues may lead to undesirable outcomes such as oxygen release, transition metal dissolution, and structural collapse of the electrode, thereby posing significant risks to thermal stability and intrinsic safety under high-rate and high-temperature operating conditions [133, 134]. To address these performance bottlenecks, current strategies for cathode material modification primarily focus on two approaches: elemental doping and interfacial engineering [135]. Elemental doping can regulate the electronic structure and ion migration pathways at the lattice level, thereby improving structural stability and charge transport efficiency [136]. For instance, studies have demonstrated that Manganese-doped LFP (LiFe_{0.92}Mn_{0.08}PO₄) exhibits only 0.43% capacity fade after 100 charge–discharge cycles at 0.1C [137]. Sodium ion doping can expand crystal channels and reduce the lithium-ion diffusion barrier, thereby enhancing ion mobility and thermal stability [138]. Co-doping with multiple elements, such as zirconium and titanium, can significantly improve the structural integrity of the electrode, thereby enhancing cycling stability and extending service life [139]. In addition, surface coating techniques aim to construct a stable interfacial barrier between the active material and the electrolyte, effectively suppressing undesirable side reactions and improving interfacial compatibility and cycling performance [140]. Electrochemically inert materials such as fluorides, phosphates, and transition metal oxides can serve as coating layers that buffer the interface and reduce the reactivity between cathode materials and the electrolyte. This results in improved cathode safety and durability [141].

Regarding anode materials, carbon-based materials have been successfully applied in commercial LIBs for nearly two decades [142]. However, under practical operating conditions, the SEI often suffers from structural instability and inhomogeneous growth [143]. These defects can lead to localized current density concentration and promote lithium dendrite formation. Continuous dendrite growth may penetrate the separator, causing ISC and ultimately leading to TR [144]. Therefore, enhancing the structural and chemical stability of the SEI is essential for ensuring the safety and long-term stability of LIB anodes [145]. Current SEI stabilization strategies are mainly categorized into two types: in-situ stabilization and artificial interface construction [146–148]. The in-situ approach aims to improve the integrity of naturally formed SEI films through precise electrolyte formulation, optimization of the electrochemical formation process, and modulation of electrode surface microstructure [149]. For example, the addition of fluoride-related functional additives can decompose preferentially during initial charging, forming a LiF-rich or polymeric network-based SEI on the graphite surface. These SEI films exhibit uniform and dense morphology, along with excellent mechanical strength and lithium-ion conductivity [150]. In addition to fluorides, other additives, such as nitrides, phosphides, and sulfides, have been used to form SEI layers enriched with Li₃N, Li₃P, and Li₂S, respectively, demonstrating improved interfacial and thermal stability [151]. Furthermore, strategies such as high-concentration or localized high-concentration electrolytes, optimized formation temperature and current density, and engineered electrode porosity have been adopted to enhance SEI uniformity and stability, suppress dendrite growth, reduce interfacial resistance, and prolong cycle life [152]. In terms of artificial interface construction, techniques such as surface coating and interlayer design are commonly employed. Among these, atomic layer deposition (ALD) has been widely applied for anode surface modification due to its precise thickness control and uniform film formation [153, 154]. Relevant studies have demonstrated that, through standard ALD cycles involving the sequential introduction of an aluminum precursor pulse, purging of residual precursor, introduction of an oxygen precursor pulse, and purging of residual oxygen precursor, together with the self-limiting surface reaction mechanism, a dense Al₂O₃ coating can be grown in situ on the graphite surface with high precision. This conformal coating can effectively suppress the penetration of electrolyte solvent molecules, reduce the occurrence of parasitic interfacial side reactions, and significantly enhance the intrinsic thermal stability of the electrode–electrolyte interface [155]. In

experimental tests, graphite anodes modified by ALD exhibited only about 2% capacity fade after 500 charge–discharge cycles, indicating excellent interfacial protection and cycling performance [156]. In addition, ALD-based interfacial engineering strategies are not limited to LIBs; they have also achieved notable success in emerging ESSs, such as sodium-ion batteries [157].

Beyond strengthening the structural and chemical stability of the SEI film through interface engineering and pre-lithiation strategies, which serve as active intervention mechanisms capable of compensating for lithium inventory loss at the source, these strategies possess decisive significance for overcoming the capacity and lifespan bottlenecks of high-specific-energy batteries. During the initial charging of the battery, the reductive decomposition of the electrolyte on the surface of the low-potential anode forms the SEI film. This process inevitably consumes active lithium ions originating from the cathode, leading to a significant reduction in the initial coulombic efficiency (ICE) and causing a permanent deficit of cyclable lithium resources within the full-cell system. Consequently, the introduction of additional lithium sources before battery cycling to compensate for this irreversible loss has emerged as a critical technological pathway for reshaping battery energy density and cycle life [158, 159]. Regarding chemical pre-lithiation at the electrode manufacturing level, to address the challenge of low ICE in hard carbon anodes due to their high specific surface area and abundant defect sites, relevant research has proposed a mild chemical pre-lithiation strategy using a lithium naphthalene solution. Experimental characterization and theoretical calculations indicate that this strategy not only effectively compensates for lithium-ion loss during SEI formation but also drives lithium ions to pre-react with micro-graphitic domains, oxygen-containing functional groups, and defect sites within the hard carbon. This induces the formation of a dense and robust interfacial film rich in lithium fluoride and lithium carbonate on the electrode surface. Benefiting from this multifunctional pre-compensation mechanism, the pre-lithiated carbon nanofiber anode exhibited an ICE of up to 93.89%. It showed almost no capacity decay after 1,500 cycles, thereby significantly enhancing the cycling stability of the battery [160]. Furthermore, targeting anode-free lithium metal batteries, which pursue ultimate energy density, recent research constructed a heteroatom (boron, nitrogen, fluorine) co-doped porous graphene host and employed lithium-(4,4'-dimethylbiphenyl) as a novel high-efficiency reagent for deep chemical pre-lithiation. This strategy optimized the nucleation kinetics of lithium deposition through defect sites and raised the equivalent ICE of the host electrode to over 100% via an over-compensation mechanism, thereby completely offsetting the irreversible loss of the initial cycle [161]. Moreover, the role of pre-lithiation is not limited to compensating for the initial lithium loss. Relevant studies have shown that pre-lithiation can induce the formation of stable interphases with compositions and microstructures distinct from those generated during the conventional first-cycle film-formation process, such as LiF-rich SEI layers or mosaic interfacial structures composed of lithium silicates and related species. Such interphases generally exhibit enhanced chemical stability, mechanical robustness, and interfacial ionic transport capability, thereby helping to mitigate continuous interfacial evolution, suppress impedance growth, and improve the long-term stability of full cells. At the same time, the safety benefits associated with pre-lithiation are strongly method-dependent. For highly reactive pre-lithiation reagents

or inadequately controlled pre-lithiation processes, potential issues such as lithium deposition, insufficient air stability, and limited process compatibility may still arise. Therefore, the safety implications of pre-lithiation should be evaluated with caution in the context of specific pre-lithiation pathways [162, 163].

However, the aforementioned static pre-lithiation strategies, based on electrode manufacturing or battery assembly stages, provide only one-time compensation and struggle to dynamically address the continuous depletion of active lithium due to side reactions during long-term cycling. To address this technological limitation, a breakthrough study proposed an external Li-supply strategy to achieve dynamic lithium equilibrium throughout the full lifecycle. This method enables flexible, non-destructive lithium-ion injection at the battery level by dissolving a specific organic lithium salt— LiSO_2CF_3 —into the electrolyte as a sacrificial additive. Its core mechanism utilizes the anodic oxidation reaction of LiSO_2CF_3 during the charging process, releasing active lithium ions while expelling organic ligands in gaseous form, thereby completing in-situ lithium replenishment without compromising the battery sealing structure or leaving solid residues. This technology not only successfully empowered intrinsically lithium-free, high-specific-energy cathode materials but also restored performance in aged commercial LFP batteries, extending their cycle life to over 11,818 cycles with a capacity retention rate of 96.0%. This universal strategy, which decouples lithium source supply from electrode material design, fundamentally reshapes the lithium-deficit compensation mechanism in batteries and provides a revolutionary technological pathway for maintaining high safety and ultra-long life in ESSs [164].

3.2 | Electrolyte

Currently, LIBs predominantly employ liquid electrolytes as the medium for ion transport [165]. Earlier research has largely focused on optimizing the performance parameters of liquid electrolytes, particularly ionic conductivity, to enhance charge–discharge efficiency and prolong cycle life. However, with the growing deployment of LIBs in EVs and large-scale ESSs, their intrinsic safety concerns have become increasingly prominent. The frequent occurrence of TR and safety incidents in recent years has highlighted the inherent drawbacks of liquid electrolytes, particularly their flammability, volatility, and limited thermal stability. These issues have consequently prompted heightened attention to the safety performance of electrolytes and spurred deeper reflection on alternative designs [166–168].

SSEs and quasi-SSEs, also known as gel polymer electrolytes (GPEs), have emerged as major research hotspots due to their non-volatility, superior mechanical strength, enhanced thermal stability, and reduced flammability, making them promising candidates for improving battery safety [169]. SSEs are primarily classified into two categories: solid inorganic electrolytes (SIEs) and solid polymer electrolytes (SPEs) [170]. SIEs typically comprise ceramic, nitride, sulfide, or phosphate materials, which offer rigid frameworks conducive to efficient ion transport between the anode and cathode [171]. In contrast, SPEs are mixtures of Li salts with polymers such as polyacrylonitrile (PAN). These materials exhibit higher flexibility and better processability, making them more compatible with diverse battery architectures

[172]. However, the practical application of SSEs continues to face significant challenges related to mechanical and interfacial stability. Although the polymer matrix is flexible, the repetitive volumetric expansion and contraction of electrode active materials during long-term electrochemical cycling generate substantial localized stress. Such stress accumulation is prone to initiating and propagating microcracks within the electrolyte, leading to rupture of ion-transport channels and physical delamination at the solid-solid interface. This, in turn, triggers a precipitous increase in internal resistance and potentially leads to battery failure.

To address mechanical failure, incorporating self-healing capability has emerged as a promising strategy to enhance the safety and cycling life of solid-state batteries. These biomimetic mechanisms encompass diverse pathways, including inter-chain diffusion of polymers, microcapsule-based healing, reversible covalent bond reorganization, and supramolecular dynamic chemistry [173, 174]. A representative study innovatively designed a polyether urethane-based self-healing polymer electrolyte based on the synergistic effect of dynamic covalent disulfide bonds and hydrogen bonds. Through the reversible scission and recombination of dynamic bonds, combined with a dual integration strategy at the electrode/electrolyte interface, this material achieved the autonomous repair of interfacial micro-cracks and the dynamic maintenance of intimate contact. Experimental results indicate that solid-state lithium-sulfur batteries utilizing this strategy retained a capacity as high as 93% after 700 cycles at a rate of 0.3 C, verifying the significant advantages of the self-healing mechanism in preserving interfacial integrity and electrochemical stability [175]. Despite the aforementioned advancements in material modification, the large-scale commercialization of pure SSEs remains constrained by several critical bottlenecks. First, issues of low ionic conductivity at room temperature and high contact impedance at the solid-solid interface remain fundamentally unresolved, directly limiting the battery's rate performance and power output. Second, the fabrication processes for SSE films are complex and impose stringent requirements on the manufacturing environment, resulting in persistently high production costs. Consequently, the development of low-cost SSE systems that possess high ionic conductivity, excellent interfacial compatibility, and amenability to scalable manufacturing remains a focal direction requiring urgent resolution in this field [176, 177].

GPEs, which lie between conventional liquid electrolytes and SSEs, are composed of a polymer matrix embedded with a liquid phase, combining the benefits of both systems. The liquid component plays a crucial role in enhancing ionic conductivity and stabilizing the electrode–electrolyte interface, while the polymer matrix provides mechanical strength and structural integrity [178]. GPEs are typically formulated using polymer frameworks, lithium salts, and organic solvents [167]. In this system, the selection and modification of the polymer matrix are critical, as it is required to provide high thermal stability, robust electrochemical performance, and sufficient mechanical strength to withstand external stress and inhibit lithium dendrite formation. Commonly used polymer matrices include PAN, polyethylene oxide (PEO), and polymethyl methacrylate (PMMA), etc. [167, 168, 179]. The choice of lithium salt is equally important, as it directly affects the energy density and cycling stability. Lithium salts

with high ionic conductivity and chemical stability, including lithium hexafluorophosphate (LiPF_6), lithium tetrafluoroborate (LiBF_4), and lithium bis(oxalate)borate (LiBOB), are commonly used in GPE systems. [167, 168, 180]. At present, due to their favorable ionic conductivity and interfacial compatibility, GPEs are considered a more practical and commercially viable transitional solution in the development of all-solid-state batteries. GPEs enhance battery safety while retaining certain advantages of liquid systems, such as ease of processing and adaptability to existing manufacturing infrastructure. Looking ahead, with continuous advancements in SSE technologies—particularly in ionic conductivity, interface stability, and material processing—there is significant potential to realize truly safe, high-energy-density batteries. Such progress is expected to fundamentally address the risks associated with TR and accelerate the adoption of next-generation energy storage technologies.

3.3 | Thermal Management Materials

Effective thermal management not only maintains the battery within its optimal operating temperature range, thereby enhancing electrochemical performance and cycle life, but also serves as a critical line of defense against thermal feedback loops and TR. Beyond reliance on system-level external thermal control strategies, the rational design and application of high-efficiency thermal management materials, based on intrinsic material characteristics, have emerged as a pivotal technological pathway for achieving precise temperature regulation and ensuring the system's intrinsic safety.

For thermal absorption and buffering, phase change materials (PCMs) are widely utilized in the interstitial spaces between battery cells due to their significant latent heat storage capacity [181]. As illustrated in Figure 1b, during charge and discharge cycles, PCMs undergo a solid-to-liquid phase transition by absorbing excess heat without causing a sharp temperature rise. This phase transition provides effective thermal buffering and enables uniform temperature distribution. In their liquid state, PCMs exhibit superior thermal conductivity compared to their solid counterparts, thereby facilitating efficient heat transfer among adjacent cells, reducing the formation of local hot spots, and enhancing overall thermal stability [58, 182]. Furthermore, this process is passive and requires no external power input. Commonly used PCMs include paraffins, nitrates, polyethylene glycol (PEG), and certain metallic PCMs [183]. However, conventional PCMs typically exhibit low intrinsic thermal conductivity, thereby limiting their thermal responsiveness. To overcome this limitation, researchers have focused on developing composite PCMs by incorporating high thermal conductivity additives such as graphene, carbon nanotubes (CNTs), and metal particles [58, 184]. For example, paraffin-based composites with embedded graphene nanosheets have demonstrated significantly enhanced thermal conductivity and accelerated phase change dynamics [185]. However, the thermal safety effect of PCM is strongly stage-dependent. PCM is primarily applicable during normal battery operation stage or before the onset of TR, where its main function is to mitigate local hot spots, improve temperature uniformity, and delay TR initiation. In contrast, during the propagation stage of TR, if the PCM exhibits a high effective thermal conductivity, it may accelerate heat transfer to adjacent cells and thereby

increase the propagation rate of TR. Therefore, PCM-based thermal management systems require a balance between heat buffering and TR propagation suppression, and are typically co-designed with thermal insulation layers or propagation-blocking structures [186].

In scenarios where TR becomes unavoidable, the application of thermal insulation materials is crucial for preventing the propagation of heat to adjacent cells or modules [187]. Aerogels, known for their ultralight weight and highly porous structure, possess extremely low thermal conductivity—typically below 0.03 W/m·K—and are considered among the most efficient thermal insulators currently available [188]. In battery thermal management, aerogels can function as effective thermal barriers between cells, modules, or between cells and outer casings, thereby delaying the transmission of heat during thermal events and suppressing thermal propagation. Additionally, certain modified aerogels exhibit excellent flame-retardant properties. Under high-temperature conditions, these materials can form carbonized layers or thermal shields, which help delay flame spread and provide additional response time for emergency intervention. Such attributes further enhance the overall thermal safety of battery systems.

3.4 | Mechanical and Structural Designs

Innovative structural designs play a pivotal role in enhancing the intrinsic safety of battery systems, particularly by effectively interrupting risk propagation pathways when individual cells experience failure. Such design strategies can be realized through two key dimensions: electrical architecture optimization and thermal insulation in the physical structure. From the perspective of electrical architecture, thermal fuses can be introduced between individual cells to prevent the cascading effects of ISC or abnormal overcurrent events [189]. As illustrated in Figure 1b, thermal fuses are embedded within the current path between adjacent cells. When the operating current exceeds a predetermined threshold, the thermal fuse rapidly melts, disconnecting the faulty cell from the rest of the module. This disconnection prevents abnormal current from propagating to neighboring cells, significantly reducing the likelihood of chain-reaction failures. By achieving cell-level electrical isolation, this approach improves the module's fault tolerance and enhances overall electrical safety.

In terms of physical structural design, as shown in Figure 1b, thermal transfer between adjacent cells during TR propagation can be effectively reduced by introducing thermal barriers, such as fire-resistant walls, or by maintaining appropriate spacing between neighboring cells. In the event of TR in a single cell, the thermal barrier can partially contain the generated heat, thereby delaying thermal propagation and limiting incident spread. This passive protection strategy is particularly critical in high-energy-density battery modules, where the consequences of TR are severe [189, 190]. However, it should also be noted that, under normal operating conditions, thermal barriers may reduce the overall heat dissipation efficiency of the system to some extent, reflecting an inherent trade-off between thermal management performance and safety protection under extreme conditions [191]. In addition to insulation strategies, optimizing the geometric design of battery cells can also enhance thermal dissipation

and mitigate TR risks. A representative example is BYD's blade battery, which restructures conventional cylindrical or prismatic cells into ultra-thin, elongated rectangular formats [192]. This design increases the surface-area-to-volume ratio, enhancing heat dissipation and accelerating thermal transport from the cell interior. Consequently, it mitigates localized temperature rise, promotes more uniform temperature distribution at the module level, and improves both thermal safety and space utilization, achieving a balanced integration of safety and packing efficiency.

Notably, the transferability of intrinsic-safety strategies from LIBs to next-generation chemistries is not guaranteed. Changes in reaction kinetics, thermal stability windows, gas and particulate emissions, and interfacial compatibility can shift dominant failure modes and hazard metrics. As a result, materials and structural solutions proven effective for LIBs may deliver diminished benefits, require re-optimization, or even introduce new risk pathways when applied to solid-state, alkali-metal, sulfur-based, or other emerging systems. Therefore, intrinsic-safety design should be chemistry-aware, and maturity should be interpreted under the specific chemistry and operating envelope rather than assumed to be universally applicable.

3.5 | Compatibility and Coupling Effects of Intrinsic Safety Strategies

Intrinsic safety design in batteries increasingly relies on the integration of multiple material strategies, in addition to individual approaches. While individual strategies such as SEI engineering, SSEs or GPEs, and thermally functional materials have demonstrated effectiveness in enhancing safety, their combined application introduces complex interdependencies that require systematic consideration.

From the perspective of synergistic design, the integration of multiple material strategies may provide complementary benefits beyond those achievable by individual approaches alone. Taking SSE as an example, although SSEs can enhance energy density to a certain extent and eliminate the risks associated with volatility and leakage of conventional liquid electrolytes, interfacial instability between lithium metal and SSEs remains a critical challenge in all-solid-state lithium metal batteries. By introducing multiple SEI engineering strategies in a coordinated manner, such as crystal-facet-regulated SEI formation and prelithiation-induced interphase construction, a stable and ion-conductive interphase can be established at the solid–solid interface. This effectively suppresses side reactions and mitigates dendrite formation, thereby improving both cycling stability and safety [193–195]. Furthermore, in sulfide-based all-solid-state batteries, the cathode interface often suffers from severe interfacial reactions and limited ionic transport. Through multiscale cathode interfacial engineering, the strategy can evolve from inert protective coatings to functional solid electrolyte coatings with ionic conductivity. Such an approach enables the simultaneous stabilization of interfacial chemistry and enhancement of ionic transport, leading to synergistic improvements in interfacial stability, electrochemical performance, and safety [196, 197]. In addition, for high-nickel layered cathode materials, pronounced interfacial side reactions and structural degradation present significant challenges. Single surface modification strategies are

often insufficient to simultaneously ensure interfacial stability and structural integrity. By combining surface coating with near-surface elemental doping, a synergistic modification strategy can be achieved, which not only constructs a stable interfacial layer but also optimizes the crystal structure and stress distribution. This synergistic modification effectively suppresses side reactions and structural degradation, thereby enhancing both safety and cycling durability [198, 199].

However, the integration of multiple intrinsic safety strategies is not necessarily additive. If not properly coordinated, their combination may introduce trade-offs or even new failure modes. For instance, when phosphorus-containing flame-retardant additives, such as trimethyl phosphate (TMP), are used together with SEI-forming additives possessing relatively low reduction potentials, such as ethylene carbonate (EC), EC may not be able to preferentially form a dense SEI before the co-intercalation of TMP occurs, because its reduction potential (approximately 0.95 V) is substantially lower than the onset potential for TMP co-intercalation (approximately 1.4 V). The co-intercalation of TMP not only enlarges the graphite interlayer spacing and increases the reactive surface area, but also lowers the reduction stability of the system and accelerates the decomposition of TMP, ultimately resulting in the failure of the intended SEI protection mechanism [200, 201]. Moreover, adverse coupling effects may also arise between prelithiation and interfacial regulation strategies. Although prelithiation can compensate for lithium loss and improve the initial interfacial condition, when applied in systems with limited interfacial ionic transport, it may aggravate localized lithium accumulation, thereby increasing the risk of lithium plating and thermal instability [202, 203].

Based on the above analysis, the distinct underlying mechanisms and optimization objectives of different intrinsic safety strategies indicate that both synergistic and antagonistic interactions may emerge during their combined implementation. Therefore, the design of advanced battery systems with enhanced safety requires a system-level perspective for the coordinated integration of multiple strategies, guided by several general design principles. In this context, interfacial stability is of central importance, as interfaces often serve as the primary sites for electrochemical reactions and thermal degradation. At the same time, continuous and low-resistance ionic transport pathways must be maintained to prevent localized current density buildup and the resulting thermal hotspots [204]. Furthermore, mechanical compatibility among different components is also essential, as it can mitigate stress accumulation and suppress structural cracking as well as interfacial delamination. In addition, a multiscale design framework is required, in which material-level strategies are systematically coordinated with thermal management and structural design at the cell and module levels.

4 | System-Level Safety Design and Monitoring

Driven by the increasing diversification of application demands, battery cells are typically assembled in series, parallel, or a combination of both configurations to achieve the required power and energy outputs, thereby meeting the performance requirements of EVs, ESSs, and portable electronic devices [205, 206]. However, as the structural complexity and energy density of battery systems

increase, these multi-cell assemblies also face significant safety challenges. In particular, when an individual cell exhibits abnormal behavior such as rapid capacity degradation or localized TR, the resulting failure can propagate swiftly to neighboring cells, triggering chain reactions that ultimately lead to system-level failure and even catastrophic events. Although intrinsic safety design strategies can mitigate such risks to some extent, relying on these measures alone is insufficient to fully eliminate potential safety hazards. Consequently, achieving high-precision monitoring, real-time sensing, and dynamic management of battery states during operation has emerged as a critical issue in battery technology development [207, 208]. To this end, a systematic multi-level design approach is required, encompassing accurate acquisition of sensor data, advanced data processing and state estimation, optimized system protection strategies, and rapid response of execution units. Such an integrated system-level safety monitoring and management framework is essential for ensuring the long-term stability of battery systems and maintaining their operation within predefined optimal conditions [209].

4.1 | Sensor Integration

The accuracy of BMS control algorithms is primarily determined by the reliability and stability of sensor measurements. To enable efficient monitoring and early fault detection, modern battery systems integrate various sensors, such as temperature, voltage, current, and gas sensors, forming the first line of defense in battery safety. These sensors continuously monitor key parameters, identifying abnormal signals and issuing warnings before failures reach irreversible stages. As battery systems grow more complex, greater demands are placed on sensor networks regarding spatial distribution, measurement precision, and electromagnetic interference immunity, all of which directly affect BMS performance. Thus, developing high-reliability multimodal sensing frameworks is essential for advancing next-generation intelligent BMS [210].

4.1.1 | Multimodal Sensor Types, Monitoring Objectives, and Physical Deployment

The primary sensors integrated into battery systems include electrical and temperature sensors, which are essential for monitoring battery operation. Electrical sensors measure individual cell voltages and total pack voltage, while current sensors monitor branch and bus currents. Voltage analysis helps assess cell health, such as capacity degradation or increased internal resistance, while current measurements detect faults, such as overcurrent and short circuits, aiding system-level protection decisions [211]. Temperature sensors, typically mounted on the battery surface, enable real-time monitoring of cell temperatures. By tracking temperature values and changes, TR and other heat-related failures can be predicted. Anomalies in temperature distribution may also indicate defective cells [212]. However, the recent increase in fires in EVs and ESSs highlights the limitations of relying solely on electrical and thermal signals. Failures often involve electrolyte decomposition and gas generation in addition to thermal anomalies. Gas and pressure sensors near the battery pack vents or relief valves detect leakage, swelling, or gaseous

byproducts from side reactions, providing early fault detection at the pack level [213]. However, these sensors primarily monitor macroscopic external responses, and irreversible damage may occur before anomalies are detected. To enable earlier fault detection, acoustic sensing technology has been explored. Acoustic sensors mounted on the battery casing or terminals operate by detecting acoustic emission signals generated during material damage. When electrode materials undergo quasi-brittle fracture, such as crack initiation or propagation, transient elastic waves are released. These waves originate from the damage source, propagate through the medium to the material surface, and induce time-varying voltage signals in the sensing element via the piezoelectric effect. The sensor output is typically amplified by a preamplifier, and the nominal resonant frequency of such sensors generally ranges from 50 to 200 kHz. Owing to this capability, acoustic sensors can identify ISCs and arcing phenomena induced by separator rupture or lithium dendrite penetration, thereby providing a basis for early fault intervention [214, 215]. In addition, both infrared thermography and X-ray imaging enable nondestructive monitoring. Infrared thermography is based on Planck's law of thermal radiation, with a temperature resolution of up to 0.03°C and a frame rate exceeding 30 fps, making it suitable for identifying thermal abnormalities such as local overheating in battery cells [216]. X-ray imaging, by contrast, is based on differences in X-ray attenuation coefficients among materials, with a response time of less than 0.2 s, and can be used to monitor structural changes such as electrode damage and separator integrity [217, 218]. These multimodal sensing technologies support the development of a multi-tiered battery health monitoring system, enhancing system safety and reliability.

4.1.2 | Key Challenges and Constraints in Sensor Deployment

Measurement data from sensors often suffer from deviations, limiting the optimization of BMS performance. For example, current sensing may exhibit zero offset drift when no load is connected, caused by factors such as temperature fluctuations, component aging, bias voltage, analog-to-digital converter resolution limits, and electromagnetic interference. Although these drifts are generally small, they can introduce systematic errors in state estimations, reducing fault detection accuracy. To mitigate this, measures such as automatic zero calibration, electromagnetic shielding, low-pass filtering, single-point grounding, and environmental compensation should be employed to enhance the robustness and integrity of sensor data [219]. In large battery packs, equipping each cell with sensors increases wiring complexity and costs. For instance, installing temperature sensors on all cells provides high spatial resolution but is often impractical due to cost and maintenance challenges. To balance accuracy and cost, optimizing sensor layout strategies is essential. By strategically placing sensors and combining thermal models with data interpolation, temperature distribution within battery packs can be reconstructed, enabling precise thermal anomaly detection. This approach is crucial for improving manufacturability, cost-effectiveness, and reliability, especially in high-energy-density pack designs [220]. In addition, sensors, like batteries themselves, are subject to service-life limitations. In high-load, long-duration operating scenarios such as commercial vehicle fleets and grid-

scale ESSs, sensors are continuously exposed to harsh conditions, which can accelerate aging and lead to signal drift, reduced sensitivity, and increased measurement noise. Among them, temperature and gas sensors are particularly susceptible to aging and contamination, which can weaken the ability of BMS to perceive and monitor critical states. In fluorine-containing battery systems, the corrosive internal environment can further accelerate sensor degradation. Accordingly, it is necessary to systematically evaluate the long-term stability of materials such as silica optical fibers, chalcogenide optical fibers, and plasmonic metal coatings under harsh battery chemical environments, and to develop further innovative coating materials that combine excellent chemical and thermal stability to improve sensor reliability and durability under complex service conditions. At the same time, measures such as durable material selection, optimized packaging processes, anti-interference circuit design, periodic calibration, and sensor health monitoring are also required to identify performance degradation in a timely manner and initiate maintenance actions, thereby ensuring the long-term stable operation of battery safety monitoring systems [221, 222].

4.1.3 | Next Generation Battery Monitoring Sensor Systems

Most current BMS sensors function as passive data acquisition nodes. However, future battery systems may require sensors to evolve into intelligent terminals capable of active perception and collaboration. To address the limitations of existing sensors, which are prone to measurement deviations due to electromagnetic interference and temperature fluctuations, next-generation sensors should integrate localized computing and edge intelligence. By implementing real-time anomaly detection and in-situ data correction through embedded algorithms, these sensors can ensure data accuracy at the source. Furthermore, to overcome the latency of surface monitoring and the issues faced by wired sensors, a miniaturized wireless sensing system integrated within the cell jelly roll is proposed. Using power line communication, this system transmits signals via battery tabs, enabling real-time internal temperature and strain monitoring without affecting electrochemical performance. Compared to surface monitoring, this technology allows precise localization of mechanical failures and improves sensitivity to localized ISC, enhancing early detection of TR. This “intelligent front-end” design, combining edge intelligence with in-situ sensing, is expected to reduce the computational burden on the BMS, improving response time and system robustness [223].

For large-scale ESSs with stringent safety requirements, TR of a single cell can trigger catastrophic chain reactions. In such cases, distributed sensing technologies such as fiber optic sensor networks can be employed. Fiber Bragg grating sensors, for example, operate on the principle of Bragg wavelength shift. Variations in temperature, strain, and pressure inside the battery can alter the grating period, thereby causing a shift in the reflected wavelength. By analyzing these wavelength changes, temperature, pressure, and strain information can be decoupled. Among these approaches, in situ infrared fiber-optic detection exhibits rapid response capability, with a detection time of only about 4 s [215]. These systems offer long-distance coverage, high spatial

resolution, and strong resistance to electromagnetic interference, enabling continuous monitoring and early warning at the battery pack level [224]. In contrast, wearable devices, flexible electronics, and miniature robots impose strict constraints on size, weight, and flexibility. Printed electronic sensors, with their low cost, lightweight, and flexible characteristics, hold significant potential for meeting the monitoring requirements of next-generation miniaturized battery systems [225]. Furthermore, quantum sensing exploits the high sensitivity of microscopic quantum states to minute variations in external electromagnetic fields and temperature, thereby enabling ultrahigh-precision detection beyond the limits of classical measurement. For example, a high-sensitivity current measurement with a precision of 10 mA over a range of 1000 A has been demonstrated. Owing to its high sensitivity and nondestructive detection capability, this technology shows strong potential for real-time monitoring of early battery faults. It can also complement printed electronic sensors, thereby promoting the development of miniaturized monitoring systems [226].

Finally, as AI becomes more deeply integrated into battery management, efficient and standardized data flow from sensors is increasingly critical. Designing sensors that support standardized bus interfaces such as Controller area network (CAN) and inter integrated circuit (I2C) may allow seamless integration with BMS and higher level AI algorithms. This approach ensures high precision, high speed, and low latency data transmission. The resulting synergy between hardware and software is expected to drive the evolution of battery management toward greater intelligence and reliability.

4.2 | Battery Management System

The BMS is essential in modern battery systems, ensuring optimal performance, safety, and longevity. It monitors the health and status of individual cells in real-time, managing the entire battery system. A traditional BMS, embedded in EVs or ESS, controls charging and discharging to enable real-time system management [227]. However, as battery technology advances and application scenarios diversify, the operating conditions for BMS have become more complex, requiring higher performance. As battery systems expand from EVs to renewable ESS and portable power sources, BMS is required to adapt to increasingly varied environments, requiring enhanced real-time capabilities, intelligent control, and high stability. Concurrently, the rise of big data, AI algorithms, and increased computational resources has led to the development of cloud-based BMS, which leverages big data analytics, machine learning, and predictive algorithms to optimize battery management [228]. Cloud-based BMS enables large-scale data processing, predictive analytics, and remote monitoring, improving fault detection and decision-making. The integration of onboard and cloud-based systems is expected to play a critical role in optimizing battery performance, safety, and longevity.

4.2.1 | Onboard BMS

The onboard BMS is an integrated electronic system installed directly in EVs or ESSs. It interfaces with various sensors through communication protocols such as CAN and I2C, facilitating effi-

cient, real-time data transmission at fixed sampling intervals. This system enables real-time sensing, state estimation, rapid feedback control, and data uploading, making it a critical component for ensuring battery safety and performance management [229]. As shown in Figure 4, the onboard BMS consists of multiple functional modules, with the most critical functionalities including the following aspects:

4.2.1.1 | Real-Time Sensing. The performance of the onboard BMS relies on accurate and efficient signal acquisition, with strict requirements for critical parameter measurements. For instance, bus current resolution should be at least 0.1 A, total voltage should have a resolution of 0.1 V, and individual cell voltages should be measured with high precision (1 mV) for detailed monitoring. Different battery chemistries, such as LFP, require specific measurement precision, as small voltage changes can cause significant errors in remaining capacity estimation. In addition to precision, high sampling frequencies are essential for capturing rapid events like TR, which can occur within seconds. Therefore, temperature, voltage, and current should be sampled at around 1000 Hz. However, higher sampling rates increase power consumption and system complexity, so lower frequencies may be used for non-critical signals to reduce system load. Signal transmission in BMS systems is often susceptible to electromagnetic interference, potentially leading to data distortion. To mitigate this, the BMS is required to perform anomaly detection and preprocessing, such as filtering and noise reduction. Future improvements in electromagnetic compatibility, including better circuit layouts and enhanced shielding and grounding, are expected to further enhance data reliability and provide accurate input for processing [230].

4.2.1.2 | State Estimation and Online Prognosis. One of the core functions of the BMS is to provide real-time and accurate estimation of the operational status of both individual battery cells and the entire battery pack. These state parameters include SOC, SOH, state of power (SOP), state of function (SOF), end of life (EOL), and state of energy (SOE), among others [208, 227, 231–235]. However, most of these state parameters cannot be directly measured and rely primarily on the calculation or derivation of SOC and SOH. Since SOC and SOH are not directly available, their estimation typically involves indirect calculation based on measurable signals such as voltage, current, and temperature [227, 236]. Among the existing SOC estimation methods, the amp-hour integration method is the most successful and widely used commercial method in onboard BMS systems with limited computational power due to its simple logic and low computational load [227, 237]. However, this method is highly dependent on the accuracy of current measurements, which can introduce cumulative errors. To mitigate this issue, multiple correction strategies are often employed. For example, when the battery is in a resting state, its terminal voltage gradually stabilizes. This characteristic can be used in conjunction with the relationship between open-circuit voltage (OCV) and SOC at different temperatures for static correction of SOC. Additionally, strategies such as full charge correction and full discharge correction are commonly used to further improve estimation accuracy [238]. In addition to the amp-hour integration method, model-based SOC estimation methods are also widely applied in onboard BMS systems. These methods primarily include

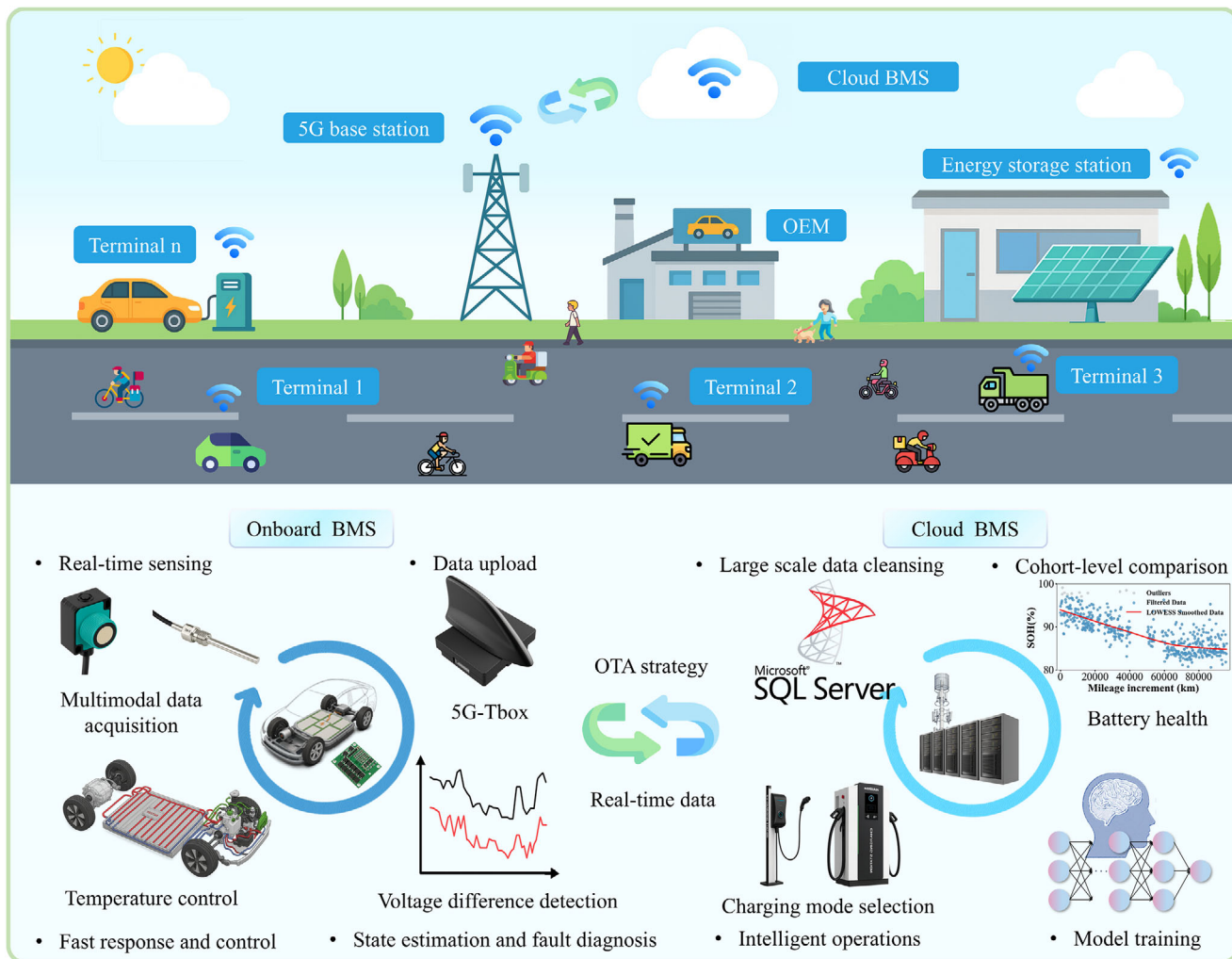


FIGURE 4 | Schematic of hybrid battery management architecture integrating onboard BMS and cloud BMS for multi-layered safety diagnostics. Onboard BMS performs real-time sensing, safety inference, and rapid fault response at the vehicle level. Cloud BMS aggregates fleet data, performs large-scale trend analysis, trains deep safety models, and distributes updates across systems. The integration of these two layers enables both fast reaction and long-term intelligence evolution.

equivalent circuit models (ECMs) and electrochemical models [208, 239]. Among these, ECMs are the mainstream solution due to their relatively low computational complexity and convenient parameter acquisition. This method represents the dynamic behavior of the battery using circuit elements such as resistors and capacitors, and combines voltage, current, and temperature measurements to identify model parameters, thereby formulating state equations and performing dynamic SOC estimation by means of optimization algorithms such as Kalman filtering [240]. In contrast, electrochemical models offer deeper insights into the physical and chemical processes inside the battery, providing higher accuracy. However, these models are complex, difficult to parameterize, and computationally intensive, which presents significant challenges to their application in onboard BMS systems [241]. For SOH estimation, the vehicle-mounted onboard BMS primarily uses capacity degradation as the key indicator. Battery capacity degradation is closely related to calendar life and the number of cycles. Battery manufacturers typically provide empirical capacity degradation curves based on experimental tests, correlating the degradation with the number of cycles. The BMS relies on these empirical data to estimate SOH. However, such

methods also face the issue of gradually increasing cumulative errors during long-term operation.

In addition to the evaluation of SOH, accurate prediction of battery EOL is also critical for maintenance decisions and safe, reliable operation. Existing studies have shown that capacity fading trajectories and EOL can be predicted online using only the historical operating data of an individual battery, with average errors for degradation trajectory and EOL as low as 2.8% and 8.2%, respectively [242]. Under more complex practical conditions, adaptive frameworks that combine offline global models with online individualized updating have achieved test errors as low as 0.93% and 1.41% on laboratory data and real-world fleet data, respectively, while online adaptation can further reduce the error by up to 13.7% [243]. Moreover, Liu et al. proposed a time-series-decomposition-based ensemble lightweight learning model for cases with limited labeled data. The model does not require an offline training dataset. It can achieve high-accuracy EOL prediction using only a small amount of historical data from a single battery, and it also provides a certain degree of degradation diagnostic capability [244]. Furthermore, the significance of

online prediction is no longer limited to providing a single EOL point. Rather, it lies in continuously characterizing the future degradation evolution of batteries by integrating historical and field-operating data. Based on this capability for lifetime extrapolation under subsequent operating conditions, BMS can further support health-conscious operational optimization, maintenance, and warranty decisions, as well as post-retirement assessment of suitability for second-life use and determination of recycling timing. As these capabilities continue to advance, their application scope is expected to extend beyond the operational stage to broader lifecycle management domains, including design and manufacturing, smart-grid dispatch, and resource circularity, thereby improving system-level economic performance and resource allocation efficiency [34, 245]. Meanwhile, with advancements in data transmission technology and computational power, uploading signals collected by the onboard BMS to the original equipment manufacturer (OEM) for large-scale centralized data analysis and updating algorithms and parameters via remote Over-the-Air (OTA) methods has gradually become an important direction for achieving high-precision state estimation and dynamic optimization of battery performance [246].

4.2.1.3 | Fast Feedback Control. Based on high-precision real-time sensor signals collected by the BMS and the estimated battery states, fast feedback control is another core function and critical task of the onboard BMS. The primary control functions can be summarized into three main modules: thermal management, balancing control, and fault diagnosis [227, 247].

For thermal management, the ideal operating temperature range for LIBs is typically 20°C to 25°C. However, due to fluctuations in environmental temperature and the heat generated during battery operation, it is often difficult to maintain the battery temperature within this ideal range. When the temperature falls below 15°C, the viscosity of the electrolyte increases significantly, hindering lithium-ion migration and leading to increased internal resistance and capacity degradation. Conversely, excessively high temperatures may trigger thermal feedback, potentially resulting in TR. Therefore, an efficient thermal management system is required not only to monitor battery temperature in real time but also to regulate heating or cooling actuators when anomalies occur, keeping the battery within a healthy operating temperature range and controlling temperature differences between cells to prevent extreme TR events [248–250]. Currently, the most common method for battery heating is positive temperature coefficient (PTC) heating. This method uses thermistors as heating elements that are in direct contact with the battery [251]. Research has shown that, when combined with adaptive self-preheating algorithms embedded in the onboard BMS, PTC heating can achieve an average temperature rise rate exceeding 40°C/min, maintaining the battery at approximately 30°C even in extreme environments as low as -40°C, with a temperature difference between cells controlled within 1.5°C [252]. However, PTC heating consumes energy from the battery itself, with parasitic power typically accounting for 5% to 15% of the total vehicle drive power, which limits its application in energy-sensitive scenarios such as EVs [253]. Consequently, researchers have explored more efficient heating methods. For example, one study proposed a motor waste heat recovery system, which reduces PTC energy consumption by 68.7%, 49.98%, and 35.97% at -5°C, -15°C, and -25°C, respectively [254]. Furthermore, thermal management

control algorithms are also critical. One study proposed a PTC power control strategy based on a feed-forward neural network, which effectively reduced parasitic PTC power by 6.74% [255]. In addition to PTC, air heating and liquid heating are also applied; the former transfers heat by heating air, while the latter heats liquid using electric heating wires, which then transfers heat to the battery. However, neither of these methods matches PTC in heating rate efficiency. In cooling, onboard BMS often deploys solutions such as air cooling, PCM cooling, and liquid cooling [256, 257]. Air cooling has a simple structure and low cost, but limited cooling efficiency, making it suitable for small or low-power battery packs. PCM cooling absorbs heat through latent heat during phase transitions, offering the advantage of no additional energy consumption, but with high cost and limited cooling capacity, it is commonly used in compact battery systems where complex cooling systems cannot be installed [258, 259]. Liquid cooling, however, offers high cooling efficiency and good temperature uniformity, making it the mainstream choice and widely used in large-capacity, high-power battery packs. The realization of efficient liquid cooling relies on optimized pipeline structures, refrigerant properties, and the collaborative design of embedded control algorithms. For example, one study proposed a novel distributed inlet immersed liquid cooling method, which, when combined with fluid dynamics, backpropagation neural networks, and a reference vector-guided evolutionary algorithm, reduced the maximum battery temperature by 5.9%, the temperature difference by 4.3%, and significantly lowered the additional power consumption caused by liquid cooling compared to traditional strategies under 5C charging conditions [260]. Whether for heating or cooling, the control is dependent on sensor signal inputs, with the embedded algorithms of the onboard BMS performing calculations and driving actuators to take the corresponding actions. Therefore, given a relatively fixed battery hardware architecture, continuously optimizing the BMS thermal management control algorithms is crucial for ensuring the stability, efficiency, and safety of the entire battery system.

Despite significant advancements in current battery manufacturing processes, there remains a degree of capacity variation among cells produced in the same batch, which often intensifies during use. To address inconsistencies arising from both the manufacturing and usage processes of battery cells, battery pack balancing control was developed [261]. The primary goal is to prevent certain battery cells from entering overcharge or overdischarge states too early during charge and discharge cycles, which would lead to premature shutdown of the battery pack and reduce overall capacity utilization efficiency. The objectives of battery pack balancing control can be summarized into three categories: balancing the voltage, SOC, and capacity across cells [262]. Since SOC and capacity are often difficult to measure directly, they are typically estimated. Therefore, most commercial BMS use a voltage-based balancing strategy, ensuring, through longitudinal BMS, that the voltage difference between cells does not exceed a preset threshold during battery pack operation, thus avoiding voltage inconsistencies between cells. Balancing control technology can be divided into passive balancing and active balancing methods [227, 261, 263]. Passive balancing works by dissipating excess energy from higher-voltage cells through resistors on the BMS circuit board when voltage differences between cells exceed the set threshold, thereby equalizing the voltage across all cells. This method has the advantages of a

simple structure, good stability, ease of implementation, and low cost, and is widely used in commercial vehicle-mounted BMS. However, the principle of passive balancing inherently requires the dissipation of some energy to balance the cells, making it inefficient. Additionally, this process generates extra heat, which may affect the stability and safety of the BMS control board [264]. In contrast, active balancing uses power electronic devices integrated into the BMS hardware to transfer energy. Compared to passive balancing, active balancing offers higher energy efficiency and is especially suited for large battery systems. Despite its more complex control algorithms and structure, active balancing can achieve efficient balancing without wasting battery energy [261, 265]. Active balancing techniques can be categorized into three main architectures based on the energy transfer actuators: capacitive-based, inductive/transformer-based, and converter-based methods [261, 266]. The capacitive-based active balancing technique uses capacitors as intermediaries for energy storage and transfer. It stores excess energy from the higher-voltage battery cells in the capacitors and releases it to the lower-voltage cells to maintain energy balance. This method typically balances one pair of selected battery cells at a time, resulting in lower efficiency [267]. To address this, researchers have proposed the dual-layer switched capacitor method, which reduces the balancing time by 50% [261, 268]. The inductive or transformer-based active balancing technique utilizes the continuous, gradual variation of current in inductive elements to redistribute energy between cells. Unlike other components, the balancing current in inductors is not affected by the reduction in voltage differences between cells, ensuring a relatively constant current output and preventing fluctuations in dynamic response caused by voltage convergence. Additionally, this method enables bi-directional energy flow between cells [261, 269]. The converter-based active balancing technique is the most complex but can achieve energy balance through efficient step-up/down conversions. This method allows for voltage and current adjustments over a wide range, ensuring efficient energy transfer [270]. Apart from the differences in balancing actuators, the balancing algorithms embedded in the BMS also significantly impact balancing efficiency. For example, one research utilized inductors for energy transfer and applied a particle swarm optimization algorithm to dynamically optimize the balancing process, thereby obtaining the optimal energy path for balancing. Research shows that this method improved balancing speed by 36% and reduced energy loss by 2.39% [271]. However, the active balancing technology, which relies on numerous power electronic devices, significantly increases the cost of the onboard BMS, and balancing speed generally correlates positively with circuit complexity and cost. Therefore, optimizing the balancing architecture and strategy remains a crucial direction for the development of BMS technology to achieve a balance between cost and efficiency in different application scenarios.

In large-scale series-parallel battery systems, the onboard BMS needs to continuously monitor the internal state of the battery and identify potential faults and their types, including ISC, external short circuits, excessive voltage differences, temperature differences, and TR issues [272]. Depending on the severity of the fault, the onboard BMS is likely to execute appropriate control strategies and report the fault. However, due to computational limitations, the onboard BMS typically detects faults only from real-time sensor data residuals and from whether those residuals

exceed preset thresholds. For example, one standard for detecting TR is whether cell temperature exceeds a predefined threshold [273]. This method, which directly uses statistical analysis and threshold judgment based on sensor data, has the advantages of a simple structure, low computational requirements, and strong interpretability. Therefore, it has been widely applied in EVs and ESSs. However, traditional methods are limited in the types of faults they can identify and, more importantly, cannot provide early warnings. They generally only capture fault data after the fault has occurred. In particular, for TR and other faults, fault propagation is extremely fast. Even if the onboard BMS can detect and then control the TR, the isolation measures taken at that point may not effectively curb the spread of the fault [274]. With advances in machine learning and the increasing computational power of onboard BMS chips, machine learning-based fault prediction methods are becoming feasible. For example, one study proposed a method that combines Long Short-Term Memory (LSTM) networks and Convolutional Neural Networks (CNNs) to predict battery temperature. It successfully achieved a 27-minute early fault warning for potential TR risks in battery packs [275]. Zhao et al. proposed a multi-fault diagnostic method for battery packs based on deep neural networks and autoencoders, specifically targeting soft short circuits and external short circuits. In external short-circuit fault diagnosis, the F1 score reached 93.74%, while the rapid diagnosis score for soft short circuits reached an impressive 99.13% [276]. With ongoing algorithm optimization and increasing data volume, machine learning-based fault prediction methods are expected to more accurately identify potential faults and enable preventive measures in advance, enhancing the safety of battery systems.

4.2.1.4 | Data Transmission and Cloud Connectivity.

Lastly, serving as a pivotal bridge between physical battery entities and the digital domain, the onboard BMS is critical for transmitting high-fidelity data from the edge to the cloud. It is required to execute the standardized encapsulation and compression of acquired multi-dimensional time-series data, including voltage, current, temperature, and fault alarms, in strict accordance with unified Internet of Vehicles communication protocols. Leveraging the high-bandwidth, low-latency transmission channels provided by onboard 5G T-BOX (Telematics box) units or intelligent gateways, these data are uploaded in real time to OEMs or third-party cloud servers. This process not only facilitates off-site disaster recovery backup and traceability management of critical operational data but also furnishes an indispensable data foundation for conducting large-scale parallel computing, constructing high-precision digital twins, and training large battery models in the cloud.

4.2.2 | Cloud BMS

In contrast to the onboard BMS, which targets individual vehicles and is constrained by limited embedded computational power and storage resources, the cloud-based BMS utilizes an elastically scalable computing and storage architecture (Figure 5). This capability enables the centralized governance, in-depth analysis, and decision dissemination of large-scale operational data across fleets. With the maturation of wireless communication technologies, such as 5G, alongside cloud computing

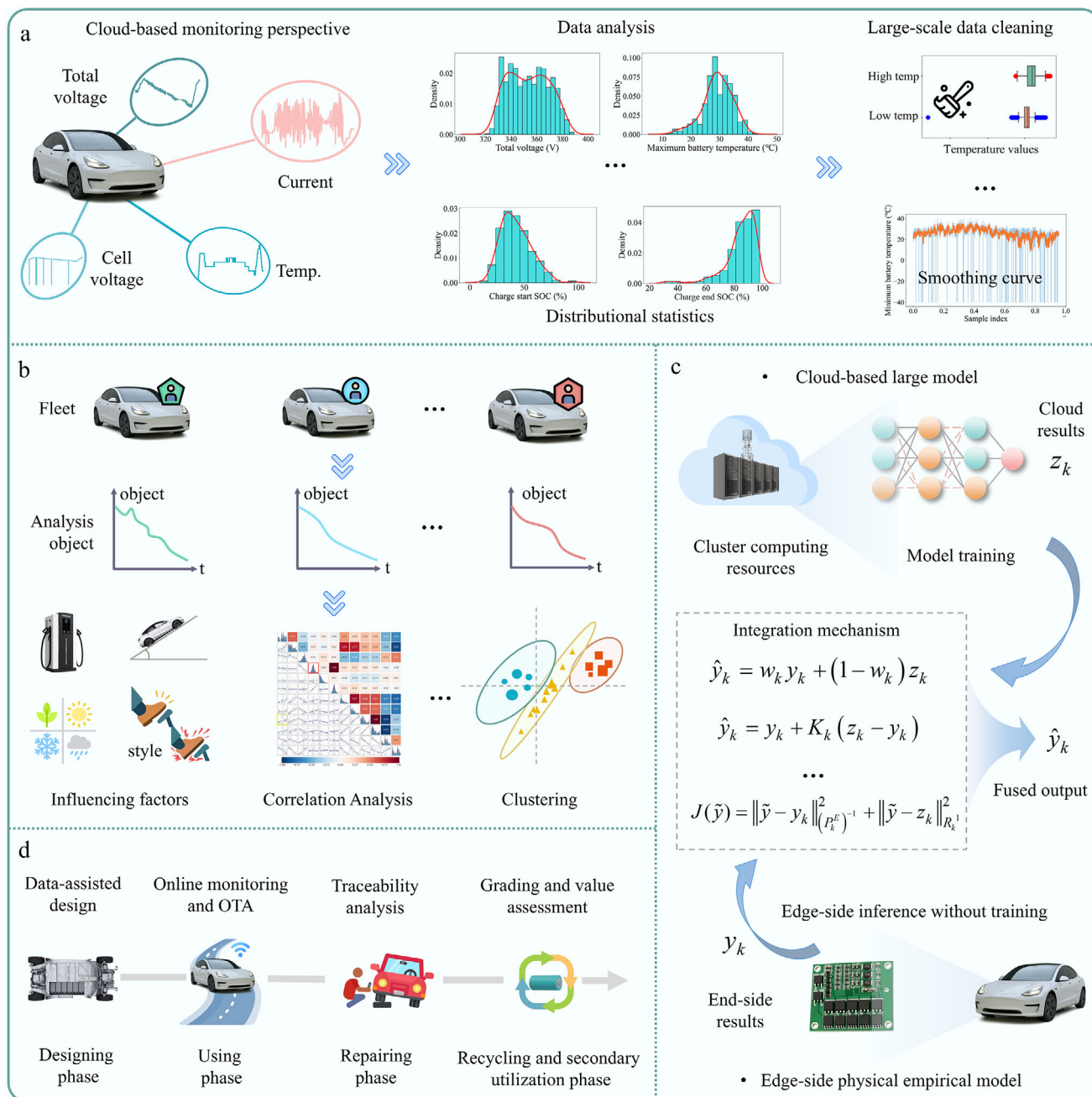


FIGURE 5 | Overall architecture and functional mechanism of cloud BMS for enhancing battery safety. (a) Cloud-based monitoring and data cleaning, including multi-source signal acquisition, distributional analysis, and data preprocessing. Adapted with permission [297]. Copyright 2025, Elsevier. (b) Fleet-level comparison and pattern recognition, involving influencing-factor analysis, correlation analysis, and clustering. Adapted with permission [297]. Copyright 2025, Elsevier. (c) Cloud-based large-model training and edge-cloud collaborative calibration, integrating cloud learning with edge-side inference. (d) Intelligent operation and maintenance across the full lifecycle, including data-assisted design, online monitoring and OTA updating, traceability analysis, and grading and value assessment for recycling and second-life utilization.

infrastructure, the deployment costs of cloud-based BMS have significantly decreased. This reduction enables the system to perform computationally intensive tasks, including large-scale data cleaning, fleet-level battery state assessment, fault prediction, parameter calibration, and complex model training, as illustrated in Figure 4. Furthermore, through wireless communication, the system implements remote OTA updates, thereby providing terminal users with continuously evolving battery management services [277].

4.2.2.1 | Large-scale Data Cleansing. The onboard BMS transmits real-time operational data via onboard communication terminals, such as the T-BOX, in accordance with unified standards, including the Chinese National Guidelines (GB/T 32960) series specifications. This data encompasses critical signals including voltage, current, temperature, and insulation status. Upon reception, the cloud platform must first perform protocol parsing, field mapping, timestamp synchronization, and metadata management to ensure that the data meets consistency

and traceability requirements before ingestion into the data lake [278]. However, constrained by complex vehicle operating environments, such as obstruction by high-rise buildings and tunnels, as well as adverse weather conditions and electromagnetic interference, the raw uploaded data frequently exhibits quality issues. These issues, including packet loss, abnormal drift, and duplicate uploads, severely constrain the accuracy of downstream modeling [279–281]. To address this bottleneck, the cloud BMS implements a multi-tiered data-cleaning strategy that leverages distributed storage and computing frameworks, as illustrated in Figure 5a. First, the system accurately identifies and eliminates outliers using statistical methods, such as the interquartile range and box plots, in conjunction with residual analyses derived from electrochemical or thermal-mechanism models. Second, the system repairs missing fragments of time-series data by employing linear interpolation, Lagrange interpolation, or generative models based on deep learning, followed by deduplication and resampling processes. Finally, the system performs spatiotemporal alignment of vehicle operational data with environmental information, such as meteorology, road gradient, and altitude. It subsequently performs data slicing and condition labeling based on operating modes—including charging, discharging, and resting—thereby constructing highly available, standardized datasets. In this domain, a study on EV cloud platforms designed an integrated battery data-cleaning framework. Through a multi-level screening mechanism, this framework achieved an anomaly sample detection rate exceeding 93.3% and controlled the data repair error to within 2.11%, significantly enhancing data quality [282]. Addressing SOH prediction tasks, another related work introduced standardized outlier-elimination and invalid-value-cleaning procedures for modeling data uploaded from terminals. Furthermore, it incorporated refined slicing processing combined with ambient temperature data, effectively mitigating the interference of noisy data on model training [283]. It is noteworthy that vehicle data is typically uploaded at a high frequency of 1 Hz, with a single vehicle generating millions of data frames annually. Confronted with the petabyte-scale data deluge resulting from the concurrent uploads of massive fleets, relying on the robust elastic computing capabilities of the cloud for real-time and efficient data governance constitutes a prerequisite for achieving high-precision battery management and excavating value throughout the full lifecycle.

4.2.2.2 | Cohort-level Comparison and Pattern Recognition. Upon the completion of cleaning and standardization governance, multi-source heterogeneous data enters the stage of cohort-level analysis (Figure 5b). This constitutes the core advantage distinguishing the cloud BMS from traditional terminal management systems. Unlike the local perspective of the terminal side, which can observe only a single vehicle or battery pack, the cloud BMS relies on operational data aggregated at a macro scale from tens of thousands of EVs and energy storage units to construct a high-dimensional spatiotemporal data space across time, regions, and environments. On this basis, utilizing cross-sectional comparison and longitudinal tracking, the system can systematically decouple the coupled influence mechanisms of multiple factors, such as ambient temperature, driving behavior, charging patterns, and manufacturing consistency differences—on battery aging trajectories, fault evolution, and potential safety risks [284, 285]. To extract critical degradation features and anomaly indicators from large datasets, the cloud BMS leverages

statistical and machine learning algorithms. For correlation analysis, Pearson and Spearman correlation coefficients are commonly used to quantify linear and nonlinear relationships between usage behavior parameters and SOH, the internal resistance growth rate, and TR risk. In pattern recognition, principal component analysis is used to reduce the dimensionality of high-dimensional features. Dynamic time warping is employed to address similarity measurement in non-aligned time-series data, in conjunction with density-based clustering algorithms to accurately identify outlier operating modes and latent failure characteristics, thereby uncovering the evolution of key aging factors and hidden faults [286–289]. Multiple empirical studies have verified the effectiveness of cohort-level analysis in revealing statistical laws of battery performance degradation. For instance, a study using one year of operational data from 525 EVs in Shanghai, China, identified 14 behavioral indicators, including average driving duration and cumulative throughput. The analysis results confirmed that cumulative mileage and charging time exhibited a significant negative correlation with the SOH, revealing a linear degradation trend under urban operating conditions [290]. Regarding environmental sensitivity, another three-year longitudinal analysis of fleet-level data discovered a significant nonlinear “U-shaped” relationship between ambient temperature and battery energy consumption. Specifically, energy consumption rises significantly at low temperatures (below 0°C), while energy efficiency is optimal within the 15–20°C [291]. Furthermore, regarding the impact of SOC management strategies, a long-cycle study covering ten years pointed out, through the analysis of operational data from new energy vehicles, that the proportion of time the SOC remains in the 50%–60% range is significantly negatively correlated with the battery aging rate, providing data support for optimizing the SOC window [292]. These statistical laws, based on cohort big data, provide a solid empirical foundation for constructing environment-adaptive life prediction models and energy consumption optimization strategies.

It is worth emphasizing that the cohort analysis of the cloud BMS does not stop at descriptive statistics but is progressively evolving deeply toward mechanism-based association and predictive modeling. Using multi-source data fusion and residual analysis techniques, the system can identify microscopic feature signals that are highly correlated with specific electrochemical degradation mechanisms. For example, under similar SOC and temperature conditions, by comparing the voltage response trajectories and temperature distribution curves of cells from the same batch, weak but continuous abnormal drift signals can be detected. If the monitored unit exhibits a trend of gradually increasing voltage hysteresis or persistent localized hot spots, it can be inferred that early faults, such as micro-short circuits, may be occurring internally. Such early diagnosis strategies based on feature evolution can not only block risk propagation through active maintenance and replacement before faults occur but also feedback failure features to the cell manufacturing and quality control stages through full-lifecycle data reverse tracking, thereby realizing the closed-loop optimization of safety management from manufacturing to usage to operation and maintenance [293, 294].

4.2.2.3 | Model Training and State Calibration. Upon completion of cohort-level feature extraction, the cloud BMS further constructs data-driven generalized state-mapping models,

which constitute a core component for achieving precise state perception across diverse systems and devices. Although the majority of current onboard BMS incorporate state estimation algorithms based on physical empirical formulas, as illustrated in the lower portion of Figure 5c, the parameters of these models are typically calibrated using data derived from controlled experimental conditions. Consequently, they struggle to adapt to complex real-world operating environments. Furthermore, owing to significant variations among users regarding factors such as driving behavior, ambient temperature, load characteristics, and charging and discharging strategies, terminal-side models frequently exhibit accuracy degradation during long-term operation [34, 295]. More critically, the data-processing capability of an onboard BMS is limited to a single vehicle or battery pack, making it difficult to capture macroscopic operational features and global degradation patterns across a cohort. This limitation in data visibility severely constrains the generalization capability and prediction accuracy of the system under dynamic operating conditions. In contrast, as depicted in the upper portion of Figure 5c, the cloud BMS leverages large-scale data aggregation and high-performance computing capabilities to conduct deep mining on multi-source data across vehicle models, chemical systems, and geographical regions. This enables the extraction of common factors influencing the evolution of key state parameters, including SOC, SOH, and SOP, among others, under varying operating conditions, thereby facilitating the construction of cloud-based large models possessing robust transferability [292, 296].

At the level of cloud-based model training, to fully exploit the latent mechanistic information inherent in multi-dimensional time-series data, mainstream research typically adopts a hybrid strategy that integrates deep learning with statistical modeling. The system captures long- and short-term memory dependencies of the battery throughout its full lifecycle by performing feature extraction and high-dimensional embedding of variables such as voltage gradient, incremental capacity (IC), charging frequency, and energy consumption rate. For instance, a study based on real-world on-road operational data developed a three-dimensional feature framework encompassing vehicle attributes, driving behaviors, and electrochemical responses. It introduced a temporal convolutional network and an improved Transformer architecture. Using a multi-head attention mechanism, this method precisely captures the multivariate coupling among voltage, temperature, and charge-discharge rates in complex dynamic environments. Consequently, it generates high-precision cloud-based prediction results, significantly enhancing the generalization robustness of the model across multiple vehicle models and diverse chemical systems [297]. Such modeling frameworks, underpinned by cloud-based big data, transcend the limitations inherent in traditional methodologies that excessively rely on static calibration parameters derived from laboratory conditions and prior expert rules. By transitioning toward the autonomous learning of nonlinear evolutionary laws from massive empirical data, these frameworks establish a robust foundation for intelligent health management across diverse devices and systems. However, despite the high precision of large cloud-based models, their direct application to millisecond-level real-time control is constrained by communication latency. Consequently, the edge-cloud collaborative architecture has emerged as a critical pathway for resolving the trade-off between real-time performance and

model accuracy. As illustrated by the fusion mechanism depicted in the central region of Figure 5c, this architecture establishes a bidirectional closed loop consisting of cloud-based offline training and terminal-side online correction. Within this framework, numerous empirical studies have demonstrated distinct collaborative strategies. One study constructed a cloud-edge collaborative framework for SOH estimation, employing the Kalman filter algorithm as the core corrector. This approach periodically transmits prediction results from the cloud-based data-driven model back to the terminal, integrating them into the terminal-side empirical model to enable dynamic online parameter correction. While maintaining a low computational load on the terminal, this strategy effectively overcame the drift issues associated with fixed-parameter models, thereby constraining the mean absolute error (MAE) to within 2% [298]. To further enhance precision, another study proposed a more refined dual-layer update strategy. This methodology integrates multi-feature fusion with Transformer models, combining a high-precision deep learning model in the cloud with a dual-exponential empirical model on the terminal side. Regarding the collaborative mechanism, the Kalman filter and the Unscented Kalman filter are used to implement, respectively, the dual-layer updates of model parameters and states. Experimental results indicate that this dual correction mechanism achieves an excellent equilibrium between real-time performance and accuracy, further reducing the prediction error to less than 1% [299]. These studies show that joint modeling between the cloud and the edge can handle data drift and distribution shift in dynamic, complex environments and deliver adaptive evolution and high-accuracy state estimation.

Overall, Model training and state calibration based on cohort analytics transform a cloud BMS from a local monitoring tool into an intelligent decision system with global perception and predictive capabilities. By mapping key factors from cohort comparison to data-driven models and utilizing edge-to-cloud collaboration for cross-chemistry parameter transfer and remote calibration, a cloud BMS provides unified health assessment and proactive optimization across various operating environments and electrochemical systems. This approach enhances state estimation accuracy and robustness, establishing a foundation for a continuously learning and adaptively evolving battery management ecosystem.

4.2.2.4 | Intelligent Operations and Lifecycle Management. Intelligent operations and lifecycle management build on the cohort awareness and model adaptivity of the cloud BMS. The objective is to extend the observable, interpretable, and predictable view of battery health and risk into an actionable, optimizable, and closed-loop management practice. At the operations level, the cloud system uses large-scale data mining, physics, and data fusion models to continuously evaluate and version core parameters, including thermal control thresholds, balancing strategies, power limits, charge and discharge windows, and alarm thresholds. In this way, the system can form differentiated operations and maintenance strategies for vehicle platforms, chemistries, and climate zones. Using cloud-based simulation together with digital twins for joint verification, these strategies are validated for safety margins and reliability, then delivered to edge controllers through secure OTA updates. The process enables dynamic updates to software parameters with online

rollback protection, so that strategy evolution proceeds with low risk and minimal interruption, without disturbing real-time control logic. For fleet-scale applications, the cloud BMS can employ phased pilots, A/B testing, and staged rollouts to compare the effectiveness of alternate strategies. With closed-loop data returned from the edge, the system performs causal attribution and statistical analysis of key indicators, including energy consumption, temperature differentials, alarm rates, early service request rates, and capacity retention. It then consolidates validated strategies into scenario-specific templates for typical operating conditions, thereby supporting large-scale deployment and long-term operations [300]. In the algorithmic practice within this domain, relevant research has demonstrated the immense potential of data-driven decision-making. For instance, addressing the cloud-based charging recommendation problem for EVs, a study developed an intelligent agent based on reinforcement learning. This algorithm dynamically optimizes to achieve the dual objectives of minimizing the battery degradation rate and charging costs, provided that the user's driving requirements are met. Experimental results indicate that this strategy can significantly reduce the annual battery degradation rate from 1.3819‰ to 0.8037‰ [301]. Furthermore, if embedded within the cloud BMS and integrated with spatiotemporal distribution information of charging stations, this approach can provide vehicle owners with personalized and optimal charging plans. Moreover, targeting complex micro-mobility scenarios such as shared transportation, another study proposed a lithium large model of the billion-parameter scale. By conducting unsupervised masked pre-training on more than 10 million entries of real-world BMS time-series data, this model acquires universal representations of battery states. Consequently, by utilizing precise range prediction and health assessment capabilities, it enables intelligent battery recommendations and decision-making for battery-swapping services [302]. These contributions substantiate the core value of cloud intelligence in enhancing the overall energy efficiency and operational efficiency of fleets.

As the scope of operations expands from one-time repair and static warranties to lifecycle governance, the cloud BMS extends across the full chain from pre-commissioning acceptance to second life use and recycling and remanufacturing (Figure 5d). In the early phase, the cloud system applies factory consistency assessment and early break in monitoring to identify structural defects and abnormal degradation trajectories, which reduces early failure rates and returns for service at the source. During service, RUL prediction and risk grading enable preventive maintenance and dynamic provisioning of spare parts, thereby reducing unplanned downtime and increasing vehicle availability. At retirement, the cloud system uses long-term SOH trajectories, equivalent full-cycle counts, temperature and stress-exposure histories, and incident logs to stratify quality, select cells for second life, and provide SOH-matching guidance and safety constraints for grid-connected and islanded storage. In reuse and recycling, lifecycle traceability data support materials recovery assessment, carbon accounting, and remanufacturing process optimization. These functions create a closed-loop data system that spans manufacturing, use, and regeneration. Through lifecycle-wide measurement and intervention, the cloud BMS balances safety, availability, and economics and advances battery asset management toward high efficiency, low environmental impact, and intelligence [303, 304].

Despite its advantages in computation and data integration, cloud-based BMS architectures remain constrained by communication reliability and data security. Variable network latency arising from coverage limits, bandwidth contention, and interference can undermine real-time state estimation and delay safety-critical responses, particularly under high-rate operation and extreme thermal conditions. Wireless packet loss and data integrity issues further disrupt time-series continuity, degrading cloud-based modeling and diagnostic accuracy. In parallel, large-scale deployment raises persistent concerns regarding data security and privacy, as battery operational data may expose sensitive user and asset information [305]. Battery operational data often contains sensitive information, including location traces, driving patterns, charging behavior, and equipment identifiers; inadequate protection may expose personal privacy or commercial confidentiality. To mitigate these risks, multilayer defense strategies—such as encrypted communication, mutual authentication between edge and cloud, and hierarchical access control—have been proposed. Future research should further advance ultra-reliable communication, edge–cloud collaboration, and privacy-preserving computing to enable secure, trustworthy, and truly real-time intelligent battery management [277].

5 | Intelligent Battery Safety Monitoring: Algorithms to Deployment

Confronted with increasingly heterogeneous operating conditions and progressively stringent safety and reliability standards, battery management technology is accelerating its evolution from passive monitoring toward autonomy and intelligence. Driven by the rapid advancement of computational intelligence, advanced algorithms, such as machine learning, have deeply permeated the field of battery safety monitoring, paving novel technological pathways to transcend the performance bottlenecks of traditional methodologies. In contrast to traditional deterministic diagnostic methods that rely on fixed rules or static thresholds, AI technologies offer robust nonlinear modeling capabilities. These technologies facilitate the autonomous extraction of latent features from large-scale, high-dimensional heterogeneous data, the identification of weak early-stage risk signals, and the construction of cognitive models endowed with continuous learning and self-evolutionary capabilities. Despite the significant advantages demonstrated by data-driven approaches, their practical engineering implementation faces severe challenges, including difficulties in multi-source data fusion, constraints on computational resources, insufficient physical model interpretability, and issues regarding system deployment security [306–308].

Consequently, this section focuses on the next-generation AI-based battery safety monitoring system, aiming to systematically elucidate the technical framework and evolutionary trends of this domain across four core dimensions: perception, algorithms, mechanisms, and deployment. This endeavor seeks to construct a comprehensive research landscape encompassing the spectrum from underlying signal acquisition to top-level intelligent coordination, as illustrated in Figure 6. Specifically, at the perception level, the monitoring paradigm extends beyond the acquisition of single physical quantities, such as voltage and current, to multimodal fusion perception that encompasses multidimensional information, including electrochemical, thermodynamic,

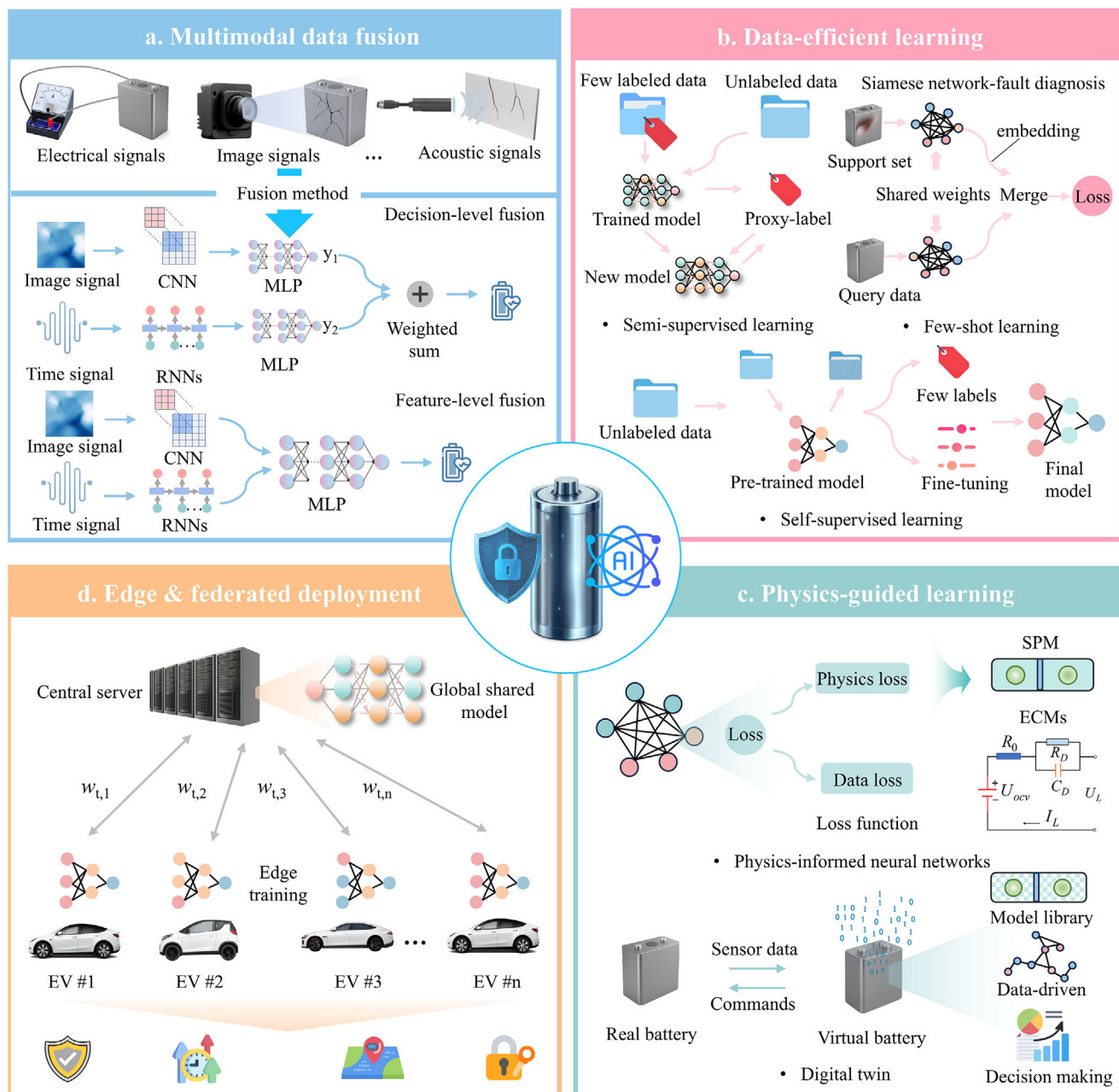


FIGURE 6 | System-level AI framework for intelligent battery safety monitoring. (a) Multimodal sensor inputs for safety diagnosis. (b) Learning paradigms for data-efficient safety prediction: few-shot learning, semi-supervised learning, and self-supervised learning. (c) Physics-informed machine learning and digital twins. (d) Scalable deployment via edge and federated learning.

acoustic, and optical data. This expansion aims to transcend the observational limitations of single-source signals and achieve a holistic mapping of the internal state of the battery. Concurrently, at the algorithmic level, to address the critical issues of scarce real-world safety event samples and exorbitant annotation costs, the modeling paradigm is progressively shifting from supervised learning that relies on large-scale labels toward data-efficient paradigms such as few-shot learning, semi-supervised learning (Semi-SL), and self-supervised learning (Self-SL). This transition aims to enhance the generalization capability of models under long-tail fault distributions. Furthermore, at the mechanism level, to address the deficiencies of purely data-driven mod-

els in physical consistency and interpretability, the research focus is shifting toward physics-informed learning, digital twin technologies, and post-hoc methods. By deeply integrating electrochemical mechanisms with data-driven models, this approach seeks to construct hybrid modeling architectures that possess both precision and physical credibility. Finally, at the deployment level, leveraging edge computing and federated learning technologies can address computational bottlenecks and data privacy challenges. This promotes distributed intelligent collaboration across devices and fleets, thereby realizing the continuous evolution of battery safety management systems throughout their full lifecycle.

5.1 | Multimodal Safety Diagnostics

With the exponential growth in the scale of battery systems and the increasing complexity of operating conditions, traditional diagnostic methods relying on single-modal signals, such as voltage and current, struggle to effectively capture early, weak anomaly features induced by multi-physics coupling. To address this challenge, modern battery packs have integrated multi-dimensional perception networks including pressure, gas, acoustic, and image sensors, among others (Figure 6a). These heterogeneous sensors provide rich data sources across electrochemical, thermodynamic, mechanical, and optical dimensions, containing complementary fault-indication information [309–312]. Therefore, utilizing multimodal fusion technology to break the observational limitations of single physical quantities and build a robust, high-sensitivity risk identification framework has become a key direction for enhancing intrinsic battery system safety. Unlike single-channel diagnosis, multimodal intelligent diagnosis aims to extract latent correlations and spatiotemporal evolution laws among data through cross-modal information interaction at the feature or decision layer, thereby achieving precise risk prediction and trend locking when fault symptoms are still in a concealed stage. In the architectural design of multimodal safety diagnosis, paradigms are typically classified into feature-level fusion and decision-level fusion based on the stage where fusion occurs (Figure 6a). Feature-level fusion utilizes neural networks to directly learn nonlinear coupling relationships between different modal signals after raw data input, constructing a unified high-dimensional feature space and outputting prediction results based on a shared classifier or regressor, realizing deep integration and collaborative representation of multi-source information. In contrast, decision-level fusion allows each modality to perform feature extraction and inference independently. Then it employs strategies such as neural network ensembles, weighted voting, or Bayesian inference to synthesize a judgment at the result level, thereby obtaining diagnostic conclusions with higher confidence.

In the application of feature-level fusion, to address the issue that single signals struggle to comprehensively depict battery aging paths, a study proposed a battery SOH prediction framework based on multimodal feature fusion. This method maps current, voltage, and temperature signals to a unified feature space, uses CNNs to extract local features, combines bidirectional LSTM (BiLSTM) networks to capture long-term temporal dependencies of degradation, and introduces spatiotemporal attention mechanisms to weight the importance of different modalities dynamically. This architecture effectively extracted the intrinsic laws of battery health evolution, realizing multi-step degradation prediction, with estimation accuracy in the early degradation stage improved by more than 65% compared to benchmark single-modal models [313]. To address the alignment challenge between infrared images and temperature sequences for TR prediction, another study developed a model that fused two-dimensional heatmaps and one-dimensional temperature sequences. This model employed ResNet18 and one-dimensional CNN to extract spatial and temporal features, respectively, and achieved semantic alignment of cross-modal features through bidirectional cross-attention mechanisms. Ultimately, through temperature trend prediction via a multi-scale gating fusion

module, the root mean squared error (RMSE) was reduced by 91.07% compared to traditional methods, fully verifying the precision advantage of deep feature-level fusion in processing high-dimensional heterogeneous data [314]. Unlike feature-level fusion, decision-level fusion offers greater flexibility in processing multi-domain signals. A study on early TR warning proposed a decision-level diagnostic method based on the fusion of time-domain and frequency-domain signals. This approach first applied phase space reconstruction to transform time-domain voltage signals and frequency-domain features into high-dimensional representations, followed by weighted fusion of the dual-domain signals after independent inference using a squeeze-and-excitation network-gated recurrent unit (GRU) cross-modal fusion classifier. By introducing cross-attention mechanisms to capture deep correlations between time-frequency features, the method significantly improved the identification of TR propagation paths, providing a warning an average of 7954 s earlier than TR onset, thus highlighting the significant advantage of decision-level fusion in early risk detection [315].

Notably, multimodal fusion not only improves diagnostic sensitivity and robustness but also provides an important technical interface for connecting data-driven models with physical mechanisms. By explicitly mapping multimodal features to physical domain variables such as temperature gradients, electrochemical potentials, or mechanical stress distributions, the fusion model enables the inversion and interpretation of degradation mechanisms, thereby endowing the AI model with higher interpretability and engineering credibility. Simultaneously, addressing challenges such as modality asynchrony, mismatching sampling rates, and signal absence prevalent in practical applications, cross-modal representation learning has become a hotspot of frontier research. By learning modality-invariant representations in a latent embedding space, the model can maintain inference stability using complementary information even when partial inputs are missing. For instance, multimodal variational autoencoders realize the generation and reconstruction of complementary features between modalities through shared latent variable structures, whereas contrastive learning and co-attention mechanisms adaptively allocate weights during modal interaction to highlight key modalities and suppress noise interference [316]. These methods significantly enhance the generalization capability and transferability of the model in multi-source heterogeneous and non-ideal data environments.

However, as multimodal deep learning model architectures become increasingly complex, issues of parameter redundancy and low computational efficiency have gradually become prominent. Many multimodal models introduce a large volume of redundant parameters while pursuing precision, posing severe challenges to the edge computing resources of the BMS. Therefore, improving training and inference efficiency through techniques such as model pruning and knowledge distillation while ensuring model performance remains a key problem that urgently needs a solution in the future. Overall, research on multimodal intelligent diagnosis is driving battery safety monitoring from simple multi-source signal acquisition toward deep cognitive fusion, laying a solid foundation for building a next-generation BMS characterized by comprehensive perception, autonomous prediction, and high reliability.

5.2 | Learning Paradigms for Data-efficient Safety Prediction

Battery safety events are typically characterized by the dual attributes of rarity and high risk. Consequently, traditional deep learning methodologies often struggle to achieve effective generalization in practical scenarios when sufficient labeled data is absent. Particularly in critical domains such as battery fault prediction and TR analysis, the extreme scarcity of relevant scenarios often results in a severe data shortage for modeling. The paucity of labeled data not only constrains the training performance of deep learning models but also significantly elevates the risk of overfitting. Furthermore, the annotation process itself often entails exorbitant costs, which further exacerbates the difficulty of data acquisition. In this context, the introduction of data-efficient machine learning methodologies has emerged as a critical approach to addressing the aforementioned challenges. These methodologies are capable of effectively utilizing unlabeled data or an extremely limited number of labeled samples to achieve precise identification and prediction of faults and safety events, even under conditions where labeled samples are severely restricted [317].

5.2.1 | Semi-Supervised Learning With Limited Labels

Semi-SL represents a pivotal branch of data-efficient learning paradigms, aiming to establish a knowledge transfer mechanism between supervised signals and unsupervised distributions. This approach provides core technical support for overcoming the critical bottleneck of scarce labeled samples and high annotation costs in the field of battery safety monitoring. This paradigm emphasizes the extensive mining of intrinsic structural information and dynamic evolution laws contained within massive and easily accessible unlabeled operating data, under the constraint of relying solely on a limited quantity of high-quality labeled samples. In practical engineering scenarios, such unlabeled data typically accounts for more than 90% of the total dataset, encompassing multi-dimensional monitoring signals such as voltage time-series sequences, temperature dynamic response curves, and transient current characteristics throughout the full lifecycle of the battery. The theoretical foundation of Semi-SL is established upon the manifold assumption, positing that battery monitoring data exhibits specific low-dimensional manifold structures or distributional characteristics within a high-dimensional feature space [318]. For instance, voltage-capacity curves across different states of health exhibit clustered distributions along degradation trajectories, while thermal signals during fault evolution phases exhibit significant correlation in the temporal dimension. By introducing unlabeled data, the model can acquire a more comprehensive prior of data distribution, thereby capturing the essential characteristics of battery state evolution more accurately and effectively mitigating the risks of overfitting and limited generalization capabilities caused by insufficient labeled samples.

At the methodological level, Semi-SL typically adopts a collaborative training framework in which labeled data provide supervision. In contrast, unlabeled data are exploited through constraint-based regularization, including consistency enforce-

ment, entropy minimization, and generative modeling. Consistency regularization encourages prediction invariance under small input perturbations (e.g., noise injection or temporal masking), enhancing robustness to distributional variations. Entropy minimization drives confident predictions on unlabeled samples, thereby sharpening decision boundaries. At the same time, generative modeling captures the underlying data manifold to synthesize representative samples and implicitly expand the effective training set. Together, these mechanisms enable Semi-SL models to leverage unlabeled data to learn smoother and more discriminative representations of multi-dimensional battery states [319]. Under this general framework, the self-training strategy stands as one of the most widely applied methods in the field of battery safety, as illustrated in Figure 6b. An initial model trained on limited labeled data iteratively assigns pseudo-labels to high-confidence unlabeled samples, which are then incorporated into subsequent training cycles. This closed-loop process expands data coverage and improves generalization under complex operating conditions without incurring substantial annotation costs [320].

Based on the aforementioned theoretical framework, Semi-SL has demonstrated significant engineering utility across multiple battery safety tasks. To address scenarios with insufficient early-cycle data for newly produced batteries, a study proposed a joint estimation framework that combines Semi-SL with an LSTM network. This method utilized a multi-graph Laplacian semi-supervised algorithm to extract seven-dimensional health features from voltage and IC curves, achieving an SOH estimation error of less than 4% under conditions where the proportion of labeled data was less than 15%. Subsequently, the generated capacity evolution sequence was input into the LSTM network for degradation dynamics modeling, achieving high-precision RUL prediction with an MAE as low as 0.06 cycles. This strategy requires only approximately one-sixth of the labeled volume to reach an accuracy approaching that of fully supervised models, providing a cost-effective pathway for early life prediction [321]. Another study proposed the partial Bayesian co-training method, constructing a dual-view linear model system. This approach utilizes a partial view composed of key degradation features to generate pseudo-labels, guiding the training of the full view model. Through maximum a posteriori probability optimization, the method achieved an accuracy improvement of 21.9% compared to the traditional Lasso method while relying on only about ten groups of labeled data, and effectively identified key physical features related to energy dissipation. This framework reduces full-lifecycle testing requirements by approximately 80% while ensuring precision, significantly saving research and development testing costs [322]. In the field of fault diagnosis, Semi-SL exhibits similarly superior performance. Related research proposed a model based on the densely connected contrastive observer for detecting resistance anomalies and voltage faults in VRLA batteries. This method introduced a horizontal axis cropping data augmentation strategy to enhance the self-learning capability of time-series image features, achieving a diagnostic accuracy of 95.63% in one-shot scenarios, which is significantly superior to existing industrial-grade methods [323].

In summary, Semi-SL demonstrates unique advantages in battery safety monitoring. Under constraints of high annotation costs

and scarce fault samples, it can fully utilize the unlabeled portion of massive operational data, significantly improving the robustness of fault identification and SOH estimation. However, practical application still faces challenges. On one hand, the minimum threshold for the quantity of labeled samples and quality standards lacks systematic quantification, and the minimum effective scale of annotation required to avoid performance degradation remains to be studied in depth. On the other hand, pseudo-labels inevitably contain noise; thus, constructing a learning framework robust to noisy labels to suppress the risk of error propagation and ensure decision reliability is a key problem urgently awaiting solution. In the future, combining technologies such as multimodal data fusion, graph structure learning, and physics-constrained learning, Semi-SL is expected to realize efficient knowledge transfer under more complex cross-platform operating conditions, laying a solid foundation for building a highly credible and self-evolving intelligent BMS.

5.2.2 | Few-Shot Learning for Rare Events

Few-shot learning represents a machine learning paradigm specifically engineered for scenarios characterized by an extreme scarcity of samples or long-tail distributions within high-dimensional feature spaces. Distinct from Semi-SL, which relies on the iterative optimization of large-scale unlabeled data and pseudo-labels, few-shot learning aims to preserve the core discriminative performance and generalization capability of models under boundary conditions where labeled resources are severely restricted or impossible to expand. This paradigm possesses significant applicability and necessity within the domain of battery safety monitoring. High-risk faults, such as localized overheating, micro-short circuits, and TR, exhibit evolution processes that are simultaneous, sudden, concealed, and irreversible. Consequently, acquiring complete observational data and high-quality labeled samples during actual operation is extremely difficult, and available samples remain at minimal levels. In this context, traditional deep learning methods driven by massive labeled data struggle to converge effectively and cannot construct fault diagnosis models with reliable generalization capabilities. To address this critical bottleneck, few-shot learning eliminates the direct dependence on large-scale labeled data. Instead, it employs strategies such as transfer learning and meta-learning to extract generalizable feature representations or optimization strategies from source tasks with relatively abundant data, thereby acquiring rapid adaptive capabilities. In target fault diagnosis tasks, the model requires only a minimal number of labeled samples (typically a support set of fewer than 5) to achieve effective identification of novel fault modes and parameter adaptation. This ensures that high-precision fault diagnosis capabilities and robustness are maintained even under constraints of severely limited labeled resources [9, 324, 325].

As a key enabler of few-shot learning, transfer learning reuses model parameters, feature representations, or optimization strategies learned in a source domain and adapts them to a target task, typically via fine-tuning. Its central premise relaxes the independent and identically distributed assumption under-

lying conventional machine learning by allowing knowledge transfer across domains or tasks. By aligning shared representations, transfer learning substantially reduces the reliance on large labeled datasets and improves model generalization across varying operating conditions or battery systems [326]. In the context of generalization across chemical systems, one study proposed a fusion transfer network based on CNNs and FlashAttention-2. This method abandoned reliance on complete cycle data, utilizing only partial charging segments from 80% SOC to the cutoff voltage as input features. Combined with transfer learning strategies, it successfully migrated aging features of LFP batteries to NCM and NCA batteries. On the LFP dataset, this model achieved an RMSE of 0.109% with extremely low video memory usage and power consumption, and the full-lifecycle diagnosis required only 57 milliseconds, verifying the efficiency of partial data sampling strategies in cross-system SOH estimation [35]. Addressing the temporal challenge of scarce early cycle data and variable operating conditions, another study constructed a multi-scenario transfer prediction framework based on few-shot learning. This method first utilized the full lifecycle curves of single cells to generate a large volume of pseudo-degradation trajectories via polynomial functions for pre-training the deep network. Subsequently, it constructed a hybrid model integrating a GRU and a one-dimensional CNN. By freezing the GRU layer and utilizing data from the first 100 cycles of the target battery to fine-tune the CNN layer, the model achieved rapid adaptation to new scenarios. In cross-condition validation using the MIT dataset and laboratory NCM battery datasets, this method achieved precise prediction of full-lifecycle trajectories, effectively resolving the cold-start problem of data-driven models under variable conditions [327]. Furthermore, facing the extreme scenario where real TR data is scarce, and distribution differences are significant, related work proposed a multi-source domain transfer learning diagnosis framework based on few-shot learning. This method first designed a data distribution metric strategy based on segmented voltage differences to select source domains with high relevance from multiple historical TR cases, thereby avoiding negative transfer. Subsequently, it utilized stage adversarial networks and risk adversarial networks to extract domain-invariant features of time-series data under few-shot conditions. This achieved an average early warning lead time of 13.8 min for TR across different battery types and abuse conditions [328]. In summary, transfer learning effectively breaks down data barriers between source and target domains through feature alignment and parameter reuse, providing a data-efficient solution for state assessment under variable conditions and across systems.

Complementary to transfer learning, which focuses on parameter and feature reuse, meta-learning is a paradigm designed to endow models with the capacity to “learn to learn.” Its objective is not to directly solve a specific task but to acquire transferable initialization parameters, optimization strategies, or metric spaces via training on a series of source tasks. Consequently, when confronting a new task, the model can converge to the optimal solution using only minimal labeled data. In few-shot scenarios, meta-learning typically employs an episodic training mechanism, organizing data into multiple N-way K-shot tasks to simulate the realistic scarcity conditions of the target phase. This enables the model to learn how to efficiently

extract common features and suppress overfitting across the task distribution, thereby achieving rapid adaptation and high-precision identification of rare fault modes [329–331]. Regarding the enhancement of adaptive feature extraction capabilities, a study proposed a prediction framework combining meta-learning with adaptive feature selection to address the challenge of battery lifecycle prediction. This framework dynamically adjusts feature weights through a meta-learning mechanism, effectively capturing critical degradation indicators from a small amount of labeled data. Experimental results demonstrated that by optimizing feature selection, the model significantly improved generalization capabilities, with the MAE and RMSE reduced by factors of 13.04 and 12.69, respectively. Moreover, when using data from only the first five cycles, the prediction performance approached that of traditional fully supervised methods [332]. Considering that real-world battery operation data often contains various types of noise and environmental interference, another study specifically proposed the Bayesian meta random graph model, aiming to solve the RUL prediction problem under conditions where few-shot data and uncertainty coexist. This model integrates a meta-learning framework with stochastic graph networks, enhancing the robustness of feature extraction in limited-data and uncertain environments by introducing random feature functions and graph structure optimization. Tests on the National Aeronautics and Space Administration and the Center for Advanced Life Cycle Engineering datasets indicated that this model improved the RMSE and MAE by more than 40%. On the Massachusetts Institute of Technology dataset, it controlled the prediction error within an extremely low range, demonstrating superior performance in complex noise environments [333]. Overall, meta-learning endows the model with potent, rapid adaptation capabilities through high-order optimization at the task distribution level, enabling it to quickly establish precise mapping relationships using very few observational samples when facing entirely new fault modes or degradation trajectories.

Although few-shot learning has successfully addressed the prediction challenges of rare events such as battery faults by extracting transferable knowledge from minimal labeled samples, it still faces several limitations in large-scale practical deployment. For instance, when the distributional discrepancy between the source and target domains is excessive, “negative transfer” may occur, leading to a decline rather than an improvement in the model’s performance. Furthermore, existing methods are predominantly based on pure data-driven approaches and lack explicit constraints related to the internal electrochemical mechanisms of the battery, resulting in insufficient physical interpretability of predictions under extreme operating conditions. Future directions involve the deep integration of few-shot learning with PINNs, leveraging physics-based constraints to compensate for the insufficiency of data information, which is expected to be a key direction for enhancing model reliability. Simultaneously, leveraging the powerful representation capabilities of large language models (LLMs) or pre-trained foundation models to construct cross-modal, multi-scale universal battery feature extractors holds promise for further breaking through the performance ceiling of few-shot learning, thereby realizing more robust, transparent, and precise intelligent battery safety monitoring.

5.2.3 | Self-Supervised Representation Learning

Self-SL is a learning paradigm that can extract supervisory signals from the data itself without manual annotation. Its core philosophy is to drive the model to learn feature representations with strong transferability by constructing rational pretext tasks, thereby establishing a high-quality feature foundation for downstream tasks. Distinct from Semi-SL and few-shot learning, Self-SL completely eliminates dependence on external labeled data during its initial pre-training phase. It requires neither guidance from a small amount of label information nor collaborative training between supervised and unsupervised data, but rather directly utilizes the intrinsic structural attributes or spatiotemporal consistency of the data to automatically generate pseudo-labels as supervisory signals. Notably, unlike traditional unsupervised learning, which focuses on data distribution clustering or simple dimensionality reduction, Self-SL emphasizes guiding the model to learn useful representations rich in semantic information through ingenious task design, rather than being limited to sample clustering or low-dimensional mapping. Common pretext tasks include time-series sequence prediction, image patch reorganization based on spatial relationships, construction of positive and negative sample pairs for contrastive learning, and masked reconstruction. By solving these tasks, the model can deeply capture the low-dimensional manifold structure, semantic consistency, and dynamic evolution laws of the data, thereby constructing feature representations with high generalization capability regarding input signals [9, 334–336]. As illustrated in Figure 6b, representations acquired via Self-SL typically exhibit excellent transferability, enabling efficient application to downstream classification, prediction, or anomaly-detection tasks through fine-tuning or linear probing. While significantly reducing annotation costs, this paradigm effectively enhances the generalization capability and robustness of the model in few-shot, non-stationary, or cross-condition scenarios.

Leveraging the aforementioned significant advantages in feature extraction and generalization, Self-SL offers a new technical pathway to break the data bottleneck in battery monitoring and has achieved substantial progress in key tasks such as fault diagnosis and health state assessment. First, in the domain of discrete battery fault diagnosis, addressing detection challenges in non-ideal data environments, a study proposed a multi-source self-supervised domain adaptation network. This method innovatively combines multidimensional collaborative Self-SL with multi-source adaptive transfer learning to address data scarcity and class imbalance issues encountered in practical applications of valve-regulated lead-acid batteries. Through robust features extracted via self-supervised tasks and domain adaptation via transfer learning, this model significantly improved fault detection performance, with experimental results indicating a diagnostic accuracy of 99.71% in the target domain [337]. Extending the application scope from discrete fault detection to continuous state estimation, Self-SL also demonstrates data efficiency in SOH estimation. A study developed a self-supervised framework with weak labels that enhances input features by introducing signal-processing techniques such as Gramian angular fields and differential calculation, and uses a Vision Transformer as a feature extractor for self-supervised pre-training. Empirical research shows that, by effectively capturing latent features

through self-supervised pre-training, this method reduced the MAE and RMSE by 0.5219% and 0.6085%, respectively, compared to traditional fully supervised learning methods, while using only 30% labeled data, thereby validating its data efficiency in label-constrained scenarios [338]. Furthermore, to address special scenarios characterized by data fragmentation and label scarcity under privacy-regulation constraints, another study proposed a self-supervised pre-training framework based on segment-similarity-weighted masked reconstruction. This method first uses segment-level contrastive learning to capture high-level semantic similarity among fragmented charging segments. Then it forces a BiLSTM encoder to learn both fine-grained charging patterns and global correlation features simultaneously through a similarity-weighted masked reconstruction task. Under the condition of using only 10% labeled data for fine-tuning, this model reduced the testing error by 31.9% compared to state-of-the-art benchmark models in complex domain shift scenarios involving cross-manufacturer and whole-lifecycle battery aging. This strategy effectively exploits the potential of large-scale, unlabeled, privacy-preserving data to achieve high-capacity estimation under low-resource constraints [339]. Although the aforementioned studies have achieved significant progress under laboratory and restricted-dataset conditions, validating their effectiveness in real-world road operation environments remains a key link between theory and practice. To address the high dynamics and complexity of real-world vehicle data, a study proposed an aging diagnosis method based on self-supervised machine learning. This method uses large-scale unlabeled charging data, combined with IC analysis, to effectively extract aging features from charging sequences for capacity estimation. Under optimal configuration, this method improved the RMSE and MAE by 74.54% and 60.50%, respectively, compared to supervised learning benchmarks, requiring labeled data from only two EVs to complete model fine-tuning, demonstrating the immense potential of Self-SL in resolving the engineering challenge of abundant real-vehicle data but scarce labels [340].

Overall, as related technologies mature, the core advantages of Self-SL in large-scale fleet data mining and full lifecycle management have become increasingly prominent. However, the field currently faces several critical challenges urgently requiring solutions. First, regarding the non-stationary characteristics of battery time-series data, designing pretext tasks that are both universal and efficient remains particularly challenging, and the feature sensitivity of specific pretext tasks to different downstream fault types varies, limiting generalization efficacy. Second, self-supervised pre-training often entails high computational resource consumption and storage overhead, and achieving efficient training and lightweight model deployment on massive, scale-heterogeneous unlabeled data remains a key bottleneck constraining practical application. Looking forward, deeply integrating the Self-SL paradigm with the Large battery models foundation, and utilizing Transformer architectures to conduct universal feature pre-training on massive heterogeneous data, holds the promise of overcoming the limitations of traditionally hand-crafted pretext tasks. Simultaneously, by introducing physics-informed constraints and multimodal data fusion mechanisms, the interpretability and physical consistency of feature representations can be further enhanced, thereby propelling the next generation of BMS toward a higher order of intelligence and autonomy.

It should be noted that the applicability of different learning paradigms in battery safety tasks is strongly scenario-dependent. Specifically, few-shot learning is more suitable for rapid warning and cross-scenario adaptation in extreme fault scenarios, such as TR and ISC, where labeled samples are highly scarce. Semi-SL is more appropriate for scenarios in which a limited number of labeled samples coexist with large amounts of unlabeled operational data, and is particularly suitable for state estimation, fault identification, and early warning at the battery-pack and even fleet levels. Self-SL, by contrast, is better suited to large-scale, continuous time-series data that lack manual annotations. Through pretraining, it can acquire general representations with strong generalization capability, thereby providing a foundation for subsequent anomaly identification, degradation diagnosis, and safety-state assessment. Therefore, in battery safety tasks, the selection of a learning paradigm fundamentally depends on label availability, fault rarity, data organization, and deployment objectives.

5.3 | Physics-Informed and Interpretable Machine Learning

LIBs are inherently highly nonlinear, time-varying, and complex dynamic systems characterized by strong multiphysics coupling. Their internal mechanisms involve ion migration at the microscopic level, electrochemical reactions at electrode interfaces, and heat generation and transfer at the macroscopic level. These processes are intertwined and continuously evolve alongside aging throughout the full lifecycle. Traditional modeling methods based on first principles or pure physical mechanisms, such as the pseudo-two-dimensional model, possess scientific rigor and interpretability, yet they typically involve the solution of high-dimensional systems of partial differential equations, resulting in extremely high computational complexity. Furthermore, the high sensitivity of model parameters to different chemical systems and aging states makes parameter identification difficult, thereby rendering real-time control in vehicle-embedded systems with limited computing power challenging to achieve. On the other hand, pure data-driven models have demonstrated potential in battery state assessment by virtue of their powerful nonlinear fitting capabilities and flexibility. However, they are essentially “black box” models, and their performance is highly dependent on massive and high-quality labeled data. Under out-of-distribution operating conditions not covered by the training data, purely data-driven models are extremely prone to overfitting. They may even yield predictions that violate physical laws such as mass conservation or energy conservation, thereby severely lacking robustness and safety assurance [341–343]. More importantly, in battery safety-related tasks, high predictive accuracy alone is insufficient to support practical deployment. Models must also be able to establish relatively clear links among input features, prediction outputs, and underlying failure mechanisms, thereby enhancing the interpretability, verifiability, and engineering transferability of the results [344]. To achieve a more appropriate balance among computational efficiency, generalization capability, predictive accuracy, and model interpretability, increasing attention has been directed toward physics-informed learning, digital twins, and post-hoc interpretability analysis. Among these, physics-informed learning constructs deeply integrated mechanism–data hybrid models by embedding physical governing equations,

boundary conditions, mechanistic constraints, or features with explicit physical meaning into data-driven frameworks. Such approaches not only comply with fundamental physical laws but also enable dynamic correction based on measured data. Digital twins further realize dynamic characterization of the complex physicochemical states and evolutionary processes within batteries through virtual–real mapping and online updating. Meanwhile, post-hoc interpretability methods, such as Shapley Additive exPlanations (SHAP) and feature importance analysis, provide important complementary tools for revealing the basis of model decisions, identifying key influencing factors, and improving model transparency. Collectively, these approaches are driving intelligent battery modeling beyond a sole emphasis on predictive accuracy toward a more balanced paradigm that also incorporates physical consistency, mechanistic understanding, and engineering trustworthiness, thereby providing more reliable technical support for next-generation intelligent BMS [345, 346].

5.3.1 | Physics-Informed Neural Networks

PINNs represent a modeling paradigm that integrates physical priors with data-driven learning in a deeply unified manner. In contrast to traditional purely data-driven black-box models, PINNs explicitly or implicitly incorporate physical constraints, such as governing equations, boundary conditions, and conservation laws, into their network architectures and training procedures. This enables them to capture complex nonlinear relationships while remaining consistent with the intrinsic electrochemical, thermodynamic, and mass-conservation principles of battery systems. For battery fault diagnosis and health-state estimation, these characteristics improve model generalization across a wide range of operating conditions, particularly under extreme or out-of-distribution scenarios, and significantly enhance physical interpretability [347, 348].

As illustrated in Figure 7, existing applications of PINNs in battery modeling can be broadly categorized into three methodological classes. The abbreviations and mathematical symbols used in Figure 7 are defined in Section S2 of the Supporting Information. The first class, shown in Figure 7a, incorporates explicit physical constraint terms into the loss function. By reformulating heat-conduction equations, electrochemical kinetic equations, mass-conservation equations, and other governing relations into residual form, these constraints are optimized jointly with data-fitting errors, guiding the network to satisfy physical laws while achieving predictive accuracy. The second class, depicted in Figure 7b, embeds neural networks as nonlinear approximation components within model structures that possess explicit physical meaning, such as ECMs or mechanism-based electrochemical models. In these gray-box or semi-physical formulations, the physical model provides the macroscopic structural framework. At the same time, the neural network compensates for parameters or submodules that are difficult to model precisely. The third class, illustrated in Figure 7c, directly incorporates physically meaningful internal state variables, such as electrode-surface lithium-ion concentration or ohmic resistance, as model inputs, thereby embedding physical semantics in the feature space and improving both the credibility and interpretability of the model outputs.

Building on the overall framework described above, existing studies have explored these three methodological directions to develop targeted approaches for intelligent battery fault diagnosis and state assessment. For the first category of methods based on physics-constrained loss functions, the body of research is particularly extensive. One line of work imposes constraints on the trend of the estimated variables by leveraging prior relationships, such as the monotonicity between physical quantities. For example, a study proposed a lightweight two-stage PINN that uses relaxation voltage from an ECM and the peak values of IC curves as features, and employs the monotonic relationship between IC peaks and the SOH to construct the physical loss constraint, and this method achieved an MAE of approximately 0.68% across LIBs with different chemistries [349]. Another line of research moves beyond trend constraints and introduces explicit physical governing equations directly into the loss function to further ensure the physical consistency of the estimation results. In battery-temperature prediction, addressing the challenge that large-format cells exhibit highly nonuniform temperature fields that are difficult to measure directly, a study combined a battery thermal-balance physical model with an LSTM network. By incorporating the thermal model residuals as physical constraints into the loss function, real-time estimation of temperature distributions under various operating conditions was achieved, with both RMSE and MAE remaining below 0.6°C [350]. However, when dealing with more complex physical processes, such as multiphysics coupling, it is often necessary to handle multiple physical parameters and governing equations simultaneously, and these parameters and equations are not always easy to obtain or define precisely in practice. To address this challenge, some studies approximate the complex physical processes using neural networks while incorporating partial mechanistic constraints to enhance physical plausibility. For instance, one study developed a PINN architecture composed of a feature-to-SOH mapping function and a degradation-dynamics nonlinear function. It introduced a partial differential equation loss based on the relationship between SEI film growth rate and battery-aging kinetics, thus ensuring consistency with degradation mechanisms. In experiments involving more than 300 cells covering a wide range of chemistries and charge–discharge protocols, this method achieved a mean absolute percentage error (MAPE) of 0.87% [351]. In the context of rechargeable-battery health-state estimation, Zhu et al. proposed a two-stage framework that integrates PINNs with Bayesian calibration. A degradation model based on porous electrode theory was first used to generate simulation data for PINN pretraining, followed by fine-tuning on experimental data using a Bayesian SOH estimation model. Monte Carlo dropout was used to quantify uncertainty, leading to a MAPE of 1.45% and an RMSE of 0.0142, representing a substantial improvement relative to conventional methods [352]. For the second category of gray-box modeling methods that embed neural networks within physically meaningful model structures, existing research indicates clear advantages in interpretability and data efficiency. One study proposed an interpretable PINN constructed on an ECM, in which physical quantities, including charge, SOC, OCV, and polarization resistance, are explicitly embedded in the network architecture. Because the forward computation strictly follows ECM equations, physical consistency is ensured without requiring additional physics-based loss terms. Even with only about 30 samples, the model was able to adaptively learn system parameters and achieve high-accuracy voltage and

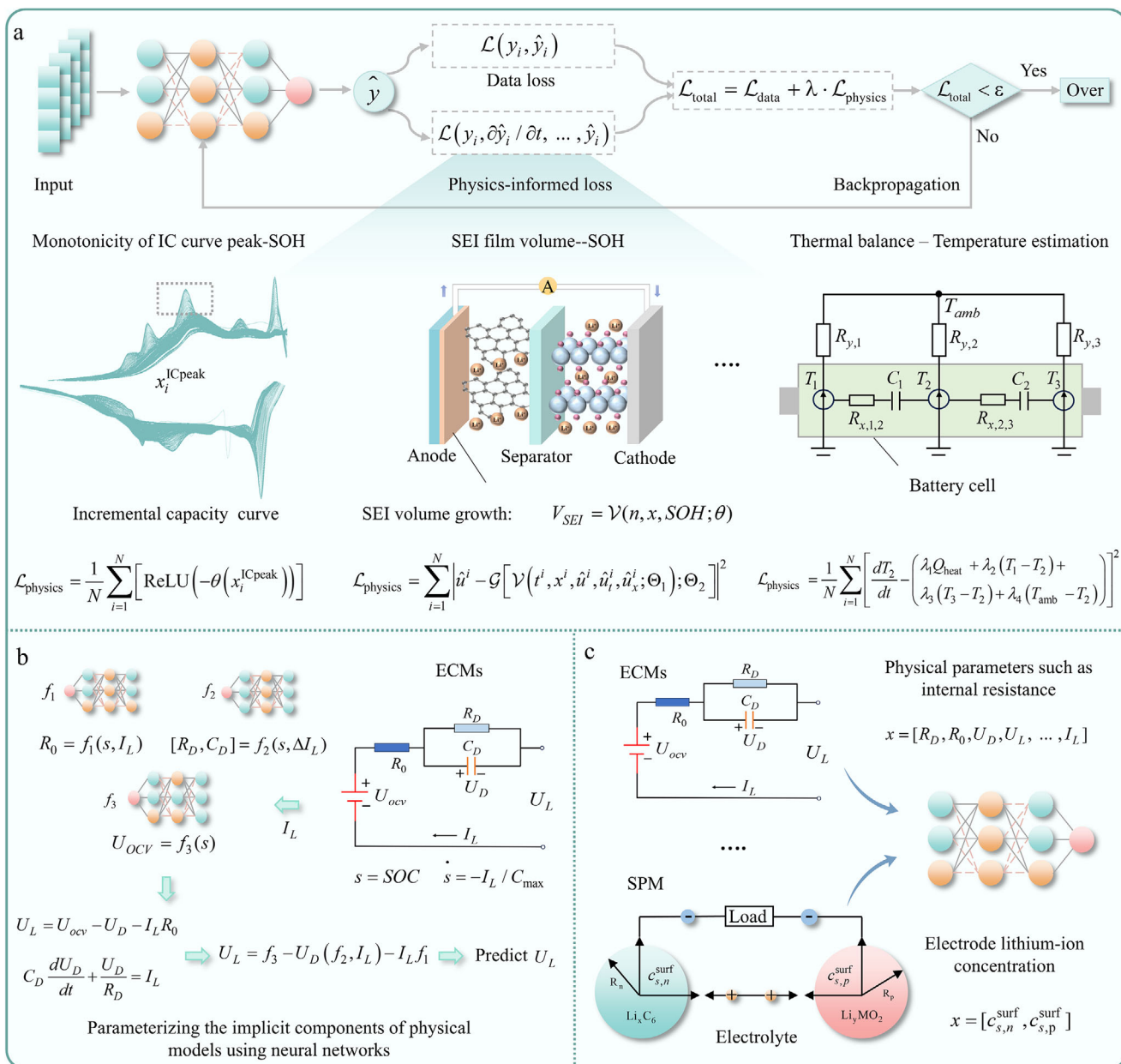


FIGURE 7 | Representative applications of PINNs in battery safety monitoring and diagnostics. (a) Paradigm I: Embedding physical constraints into the loss function. (b) Paradigm II: Neural parameterization of implicit components within physically structured models. (c) Paradigm III: Using physical-model-derived state or parameter variables as neural network inputs.

end-of-discharge predictions under randomized discharge conditions, reducing average MAE by approximately 70% compared with conventional LSTM-based approaches [353]. For the third category of methods that incorporate physically meaningful state variables as explicit model features, existing studies demonstrate that such approaches improve the adaptability of the model to complex operating conditions as well as its capability to represent internal states. For example, one study conducted online identification of ohmic resistance, polarization capacitance, and OCV in a Thevenin-type ECM. It used these parameters as physical priors for the PINN inputs, enabling decoupled learning of the individual voltage components. The resulting model effectively suppressed measurement noise and model bias, maintaining SOC and capacity estimation errors within 2% across diverse operating conditions [354]. Another study developed a PINN that integrates

a single-particle model (SPM) with a BiLSTM, using mechanistic variables such as electrode-surface lithium concentration as inputs to estimate heat-generation rates of LIBs across multiple operating conditions. Bayesian optimization was employed to select network hyperparameters, and the model achieved a minimum MAE of 0.542 kW/m³ under dynamic stress test conditions, substantially outperforming conventional LSTM methods [355]. Furthermore, another study addressed the complex conversion reactions of lithium-sulfur batteries by physically segmenting the discharge curves according to the underlying electrochemical phase-transition mechanisms, and then using the extracted trend and seasonal features as inputs to a recurrent neural network (RNN). This physics-inspired feature-engineering framework not only reduced the test MAE for EOL prediction to 8.9% but also further identified the ratio of electrolyte amount to

high-voltage-region capacity as a new key physical indicator, thereby moving beyond the limitation of purely data-driven models that remain confined to correlation fitting [356].

In conclusion, by incorporating physical mechanisms across multiple dimensions, including loss function regularization, model structure embedding, and feature space enhancement, PINNs have successfully established a unified modeling framework that integrates the flexibility of data-driven approaches with the rigor of physical models. This paradigm not only significantly enhances model robustness under extreme operating conditions and out-of-distribution scenarios but also provides an interpretable basis for decision-making in battery TR early warning and full lifecycle management. However, this field continues to face significant challenges as it transitions toward large-scale engineering implementation. Primarily, the disparity in gradient magnitudes between physical constraint terms and data fitting terms frequently induces optimization pathology. This phenomenon makes it difficult for the model to balance physical consistency and data accuracy simultaneously during training, thereby preventing convergence to the Pareto-optimal solution. Furthermore, the calculation of high-order physical residuals based on automatic differentiation entails substantial computational overhead. This limitation severely constrains the capability for real-time deployment on edge BMS chips, which are characterized by limited computational power. Future research directions involve integrating PINNs with neural operator technologies. By learning operator mappings between function spaces to substitute for the pointwise solution of traditional partial differential equations, this approach is expected to achieve millisecond-level inference while maintaining physical precision, thereby overcoming multiscale computational bottlenecks. Simultaneously, the deep integration of Bayesian uncertainty quantification frameworks can provide rigorous probabilistic confidence intervals for high-risk safety decisions. This integration is expected to facilitate a leapfrog development in battery management, transitioning the field from passive monitoring toward active physical perception and highly credible autonomous decision-making.

5.3.2 | Digital Twins

As a high-level application form deeply integrating mechanistic models and data-driven methods, digital twin technology constructs a closed-loop system characterized by virtual-physical symbiosis and dynamic feedback for intelligent safety monitoring and full-lifecycle management of batteries [357]. This system aims to reconstruct a virtual model in the digital space that maps one-to-one with the physical battery entity with high fidelity. Through cloud-based data streams, it facilitates continuous synchronization and real-time interaction between the physical entity and the virtual mirror, thereby fundamentally transcending the spatiotemporal limitations of traditional static modeling methods. As illustrated in Figure 6c, this channel of virtual-physical fusion enables the twin to map the complete trajectory of the physical entity, ranging from microscopic electrochemical states to macroscopic performance evolution in real time. This lays a dynamic foundation for achieving precise SOH prediction, cross-validation of early anomaly trends, and simulation optimization of control strategies. Notably, unlike PINNs, which focus on embedding

physical laws within a single model to enhance generalizability, digital twin technology constructs a more macroscopic, continuously evolving, system-level application architecture. Within this framework, it not only compatibly integrates SPMs, ECMs, and various data-driven algorithms to synchronously monitor key parameters such as SOH, three-dimensional temperature fields, and internal resistance with high precision, but also possesses robust generative simulation capabilities. Leveraging this capability, researchers can directly construct virtual battery prototypes with different material systems or topological structures on the digital twin. This enables the simulation of coupled electrical-thermal-mechanical-chemical behaviors and safety boundaries under conventional operating conditions and even extreme abuse conditions, with zero trial-and-error cost. This virtual validation mechanism significantly accelerates the design iteration cycle of new batteries and identifies potential design defects and safety risks before physical prototyping, providing prospective guidance for the research, development, and management of the full battery lifecycle [358, 359].

Leveraging its full-lifecycle mapping capabilities, digital twin technology has been widely applied in intelligent battery management and design, spanning multiple dimensions from macroscopic state estimation to the elucidation of microscopic mechanisms. Regarding battery state estimation during the operation phase, one study proposed a real-time degradation prediction method based on a digital twin framework and hybrid deep learning models. This method used a backpropagation neural network to reconstruct partially missing discharge voltage curves and, combined with real-time SOC data, drove a hybrid network comprising CNNs, LSTM networks, and attention mechanisms to predict the maximum available capacity of the battery. Experiments indicated that this framework could reveal the degradation state of the battery with an accuracy exceeding 99%, with the prediction error strictly controlled within 3 mAh [360]. Extending from electrochemical states to thermal safety management, another study developed a deep digital twin model that combines CNNs and finite-element-method thermal models to reconstruct three-dimensional temperature distributions in real time for large-scale battery systems. This model replaced expensive, high-density physical sensor deployment with efficient surrogate solutions in the digital domain, enabling rapid and precise temperature field prediction. The MAE was less than 0.73°C, significantly outperforming traditional coupled electro-thermal models [361]. Beyond state monitoring, digital twin technology further expands its application scenarios to the level of decision optimization in vehicle energy management. In the context of EV energy management, prior work proposed a decision framework that fuses digital twins with deep deterministic policy gradient reinforcement learning algorithms. Through real-time data fusion, this system not only accurately estimates SOH and SOC but also dynamically optimizes the trade-off between fuel consumption and maintenance strategies, demonstrating superior adaptability and computational efficiency, particularly in dynamic, time-varying driving environments [362]. To address complex fast-charging strategy optimization problems, another study proposed an online closed-loop framework based on a battery digital twin and Bayesian optimization. This method used an electrochemical-thermal coupled model that incorporated SEI film growth and lithium plating mechanisms as the digital twin. By employing Bayesian optimization algorithms

to efficiently search for Pareto-optimal solutions within a vast strategy space, it avoided the immense computational burden of directly solving complex systems of differential-algebraic equations. Furthermore, to further enhance optimization efficiency, the study introduced a parallel multi-channel optimization strategy, increasing the search convergence speed by a factor of 2.5. Validation results showed that protocols optimized using the Doyle-Fuller-Newman model reduced lithium inventory loss by 4.76% relative to benchmark fast-charging strategies over 90 cycles, achieving an effective balance between computational efficiency and battery health protection [363].

Beyond the operational domain, digital twin technology plays a crucial role in research on microscopic mechanisms and material design within the research and development domain. In the frontier field of solid-state batteries, although large-scale commercialization will take more time, digital twin technology has begun to assist in exploring microscopic mechanisms. For instance, research utilized synchrotron radiation X-ray computed tomography to acquire battery microstructure data. Combined with digital model-driven electrochemical simulations, this successfully revealed the lithium trapping effect in high-loading electrodes and subsequently proposed a localized ion path activation strategy, which significantly enhanced the reversibility and performance of solid-state batteries [364]. To address the bottleneck in which high-power battery development relies excessively on trial-and-error experiments and lacks insight into complex internal physicochemical processes, a study proposed a digital twin-assisted design framework based on electrochemical-thermal coupled models. This method pre-screened optimal electrode structural parameters via virtual simulation. It used the model to decompose the internal overpotential, precisely identifying that lithium-ion transport in the electrolyte is the key rate-determining step limiting ultra-high-rate performance. LFP batteries manufactured based on the guidance of this model achieved a high energy density of 92.38 Wh kg^{-1} under 50 C ultra-fast discharge and could even withstand pulse discharges as high as 150 C [365].

Although digital twin technology demonstrates immense potential for connecting the physical world and the digital space, its large-scale engineering implementation still faces the inherent trade-off between high fidelity and real-time performance. Existing high-precision multiphysics twin models often involve solving complex partial differential equations, entailing substantial computational overhead that is difficult to meet millisecond-level real-time safety monitoring requirements. Simultaneously, as batteries age, the parameters of the physical entity drift, and achieving online adaptive correction and continuous evolution of the twin model remain critical challenges. In the future, digital twin technology is expected to develop toward lightweighting and cognition. On the one hand, combining model order reduction technology with edge computing can enable efficient inference of complex physical field models at the edge, thereby resolving real-time bottlenecks. On the other hand, fusing generative AI and LLMs holds the promise of constructing a cognitive interface for digital twins. This would realize the automated interpretation of massive twin data and the AI-generated content-driven simulation of virtual extreme scenarios, thereby promoting more efficient real-time simulation and strategy optimization of battery systems in virtual space, accelerating the research, develop-

ment, and testing processes of new batteries, and significantly enhancing the intelligence level and safety throughout the full lifecycle.

5.3.3 | Post-Hoc Interpretability

Beyond physics-constrained hybrid modeling, post hoc interpretability provides another important route to mitigating the black-box nature of machine-learning models. These methods usually do not modify the training process itself. Instead, they explain model decisions after training by analyzing the relationships among input variables, feature contributions, and prediction outputs. Representative approaches include SHAP, feature-importance analysis, saliency maps, among others. SHAP and feature importance analysis can quantify the contributions of different input variables to model outputs. Saliency maps identify the temporal regions or feature segments to which model predictions are most sensitive. These methods can improve model transparency to some extent, support mechanistic analysis, and enhance model credibility in battery safety monitoring [344].

For example, one study proposed the symmetric-cell AI diagnostics framework, based on Li|Li symmetric cells. It used segmented voltage–time features to construct an RNN for prediction, and then applied feature importance analysis for post-hoc interpretation. This framework identified a key electrochemical fingerprint associated with the initial nucleation of lithium. The study showed that combining a simplified symmetric-cell platform with post hoc interpretability can not only improve the prediction of polarization acceleration in lithium metal batteries but also extract degradation descriptors with clear physical meaning. These descriptors provide mechanism-guided implications for interfacial regulation and electrolyte optimization. In addition, insights from saliency maps can also be used to optimize battery operating strategies [366]. Liu et al. proposed a sequential explainable learning framework. By calculating the saliency map of a one-dimensional CNN, they found that the final 10% depth-of-discharge region is closely associated with accelerated aging. Based on this interpretation, the authors further proposed a dual-cutoff discharge protocol. This protocol extended cycle life by up to 2.8 times, demonstrating the potential of interpretable machine learning to translate model interpretation into engineering optimization [367]. It is also worth noting that post-hoc interpretability can be further combined with the physics-constrained models discussed above to enable deeper mechanistic decoupling. For example, one study proposed a domain-adaptive deep-learning framework. This framework learned and reconstructed electrochemical impedance spectra in the hidden layer to embed physical constraints. It then combined SHAP analysis to achieve nondestructive diagnosis of aging mechanisms. The results showed that low-frequency impedance features play a dominant role in capacity fade under dynamic random operating conditions [368].

Beyond the methods discussed above, post-hoc interpretability also includes various other tools, such as layer-wise relevance propagation [344]. It should be noted that the interpretations generated by these methods usually depend directly on the training data itself. If the data are biased, the resulting

conclusions may also be affected. Therefore, relying solely on post-hoc interpretability is often insufficient to achieve a comprehensive understanding of model behavior. Domain knowledge and necessary experimental validation are still required to ensure the reliability and validity of the conclusions.

5.4 | Edge Deployment and Federated Learning for Fleet-wide Intelligence

As discussed in section 4.2.2.3, in current engineering practice for intelligent battery management algorithms, core data processing and model training remain highly dependent on cloud-based central servers. At the same time, edge devices predominantly perform basic data acquisition and instruction execution. This highly centralized architecture has significant limitations when dealing with large-scale, high-concurrency BMS. On the one hand, frequent data exchange between the cloud and the edge is constrained by bandwidth fluctuations and transmission delays inherent in communication networks, making it difficult to support real-time closed-loop updates and low-latency model control. On the other hand, centralized storage involves uploading massive amounts of sensitive operational data, posing severe risks of data privacy leakage and creating data silos. Consequently, constructing a cloud-edge collaboration computing architecture has become a critical pathway for enhancing the real-time performance, reliability, and security of BMS. In this architecture, edge computing effectively mitigates long-tail delays and bandwidth congestion in cloud communication by offloading inference tasks with extremely high real-time requirements, such as safety diagnosis and state estimation, to the edge BMS or local gateways. This achieves millisecond-level response speeds and highly reliable local control. Simultaneously, the cloud focuses on undertaking global model optimization tasks that are highly computationally complex and resource-intensive, and constructs an efficient collaborative paradigm of strong cloud training and fast edge inference through the federated learning mechanism. As shown in Figure 6d, unlike traditional centralized training, which requires uploading raw data, federated learning enables terminal devices to perform model updates locally using private data and to upload only encrypted model gradients or parameters to the cloud for secure aggregation. This distributed paradigm of moving models rather than data enables collaborative modeling across terminals and scenarios, assuming strict physical isolation of raw data, thereby establishing a solid data privacy defense line while achieving a Pareto-optimal balance between global model precision and real-time edge response [369–371].

At the application level, federated learning effectively addresses fundamental state-modeling problems in heterogeneous data environments by introducing distributed, collaborative mechanisms. Addressing the challenge of non-independent and identically distributed data common in lithium battery SOC estimation, a study proposed a collaborative battery estimation system based on federated learning. This method effectively corrected model deviation in heterogeneous data environments and improved training efficiency and stability by introducing strategies such as label standardization, regularization of proximal terms, and shared data. Experimental results indicated that this model achieved an RMSE below 4.5% on open-source

datasets across different ambient temperatures, thereby verifying the feasibility of efficient collaborative estimation under privacy-protection constraints [372]. While resolving basic state estimation, integrating transfer learning has become a frontier of exploration within the federated framework to further enhance the model's generalization capability and personalized adaptability across operating conditions and individual scenarios. Regarding SOH estimation, prior work proposed a decentralized, peer-to-peer, personalized federated transfer learning framework (P2P-PerFTL). This method employs a CNN-BiLSTM-Attention hybrid network locally to extract temporal features and achieves personalized adaptation by freezing base layers and fine-tuning fully connected layers. In the global aggregation phase, it innovatively designed a weighted aggregation mechanism based on domain shift (introducing maximum mean discrepancy and correlation alignment distance metrics) to adaptively balance the contribution weights of models from different clients. Validation results demonstrated that this method significantly reduced SOH estimation errors compared with traditional federated learning and centralized training across four transfer scenarios with different operating conditions and battery types, effectively overcoming the challenge of distributional discrepancy in distributed environments [373]. Furthermore, to address the challenges of scarce labeled data and feature mining in distributed environments, the deep integration of Self-SL and federated learning offers new solutions for low-resource scenarios. One study further enhanced the robustness of feature extraction by introducing contrastive learning and proposing a dynamically weighted federated contrastive Self-SL framework. This method first uses time-frequency mixing data augmentation and temporal information reconstruction modules on local clients to self-supervise the extraction of multi-level features from unlabeled data. Subsequently, it collaboratively optimizes the global model on the central server using a process-aware, dynamically weighted aggregation algorithm, effectively mitigating the negative impact of low-quality client data on model performance. Validation results indicated that, using only 20% labeled samples, the MAE for SOH estimation of this model on a self-built dataset was 2.80%, significantly improving the model's convergence speed and generalization accuracy [374].

In summary, the deep integration of edge computing and federated learning provides an efficient and secure solution for large-scale battery management across devices and fleets by organically combining computational power offloading with data privacy protection. However, further development in this field still faces several key challenges. First, the frequent interaction of massive terminal parameters entails huge communication overhead, which may lead to training latency in bandwidth-constrained scenarios. Second, differences in the computational power of edge devices across vehicles and non-uniform battery aging rates easily induce the “straggler effect” in federated training, slowing the convergence of the global model. Finally, the distributed architecture itself harbors security risks of malicious nodes conducting “poisoning attacks” or “gradient leakage”. In the future, combining model compression techniques (such as quantization and pruning) with asynchronous aggregation strategies is expected to significantly reduce communication overhead and enhance compatibility across heterogeneous systems. Simultaneously, introducing blockchain technology to build a trusted federated network is expected to further strengthen the system's

TABLE 3 | Comparison of machine intelligence and conventional approaches in battery safety-related tasks.

Specific task	Machine intelligence approach/paradigm	Representative machine-intelligence method and result	Conventional method and result
External short circuit fault diagnosis	Supervised deep learning	CNN-LSTM-Autoencoder: Precision = 91.33% [276].	Pearson correlation coefficient: Precision = 55.76% [276].
Early warning of TR risk	Multimodal deep learning	Dual-domain time-frequency fusion network: the average response time precedes the onset of TR by 7954 s [315].	Online dynamic impedance: the warning time is 580 s ahead of the TR [375].
RUL prediction	Semi-supervised learning	Semi-SL-LSTM: achieves comparable accuracy with only one-third of the labeled data, with a RUL prediction MAE = 2.53 cycles [321].	Particle filter: prediction MAE = 4.5 cycles [376].
Connection fault diagnosis	Self-supervised learning	Self-supervised domain adaptation network: achieves 100% recall with only 50% target-domain training data [337].	Pearson correlation coefficient: Recall = 90.33% [276].
Temperature distribution estimation	Physics-informed learning	PINN: temperature estimation RMSE = 0.57°C [350].	Electrochemical-thermal coupling model: temperature estimation RMSE = 1.27°C [377].
Real-time battery health monitoring	Federated learning	P2P-PerFTL: SOH-estimation RMSE = 1.33% without raw data sharing [373].	Internal-resistance ECM using constant voltage phase charging data: SOH-estimation RMSE = 3.95% [378].

anti-attack capability and data traceability, thereby promoting the evolution of battery management from an isolated, static, single-body mode toward a truly collaborative, dynamic, and highly credible swarm intelligence paradigm.

In summary, to present more directly the demonstrated performance of machine-intelligence methods in battery safety-related tasks and their differences from conventional approaches, selected representative cases discussed in Sections 4 and 5 are consolidated in Table 3 and summarized in a results-oriented comparative manner. Specifically, Table 3 is organized around the BMS monitoring discussed in Section 4, together with the four dimensions discussed in Section 5, namely Perception, Algorithms, Mechanisms, and Deployment. It summarizes several representative battery safety-related tasks and compares specific algorithms under different machine-intelligence paradigms with conventional methods. It should be noted that the safety-related tasks considered here include not only tasks directly oriented toward fault warning and fault diagnosis, but also lifetime prediction and real-time health monitoring, which support preventive safety management. As shown in Table 3, for the representative tasks listed, machine-intelligence methods generally outperform conventional approaches in terms of TR warning lead time, temperature-distribution estimation, lifetime prediction, and fault identification. Moreover, these advantages are reflected not only in improvements in predictive accuracy or diagnostic performance, but also in the ability to make effective use of limited labeled data and to adapt to scenarios subject to data-privacy constraints.

6 | Outlook

Despite significant progress in algorithmic development and real-time implementation, bridging the gap between model performance in controlled environments and safe operation in real-world scenarios remains a major challenge. Existing diagnostic frameworks, although increasingly accurate and scalable, often struggle with generalization across chemistries and operational contexts. Furthermore, many safety strategies still rely on post-hoc detection and reactive measures, lacking proactive control. To enable robust and autonomous battery safety management, future efforts should focus on integrating predictive algorithms into certification protocols, designing control architectures that intervene before failure onset, and building transferable models that operate reliably across diverse battery types and use cases. Ensuring safe and intelligent battery operation at scale calls for more than algorithmic progress. It requires systemic reform in how safety is defined, predicted, and controlled. The following outlook articulates strategic pathways to realize this vision, spanning test protocols, self-healing technology, autonomous control frameworks, and transferable prognostics (Figure 8).

6.1 | Testing Protocols and Standards

Current battery certification frameworks remain largely rooted in deterministic testing philosophies that were designed for an era of simpler electrochemical systems. Standards such as Underwriters Laboratories (UL) 2580, Society of Automotive Engineers (SAE)

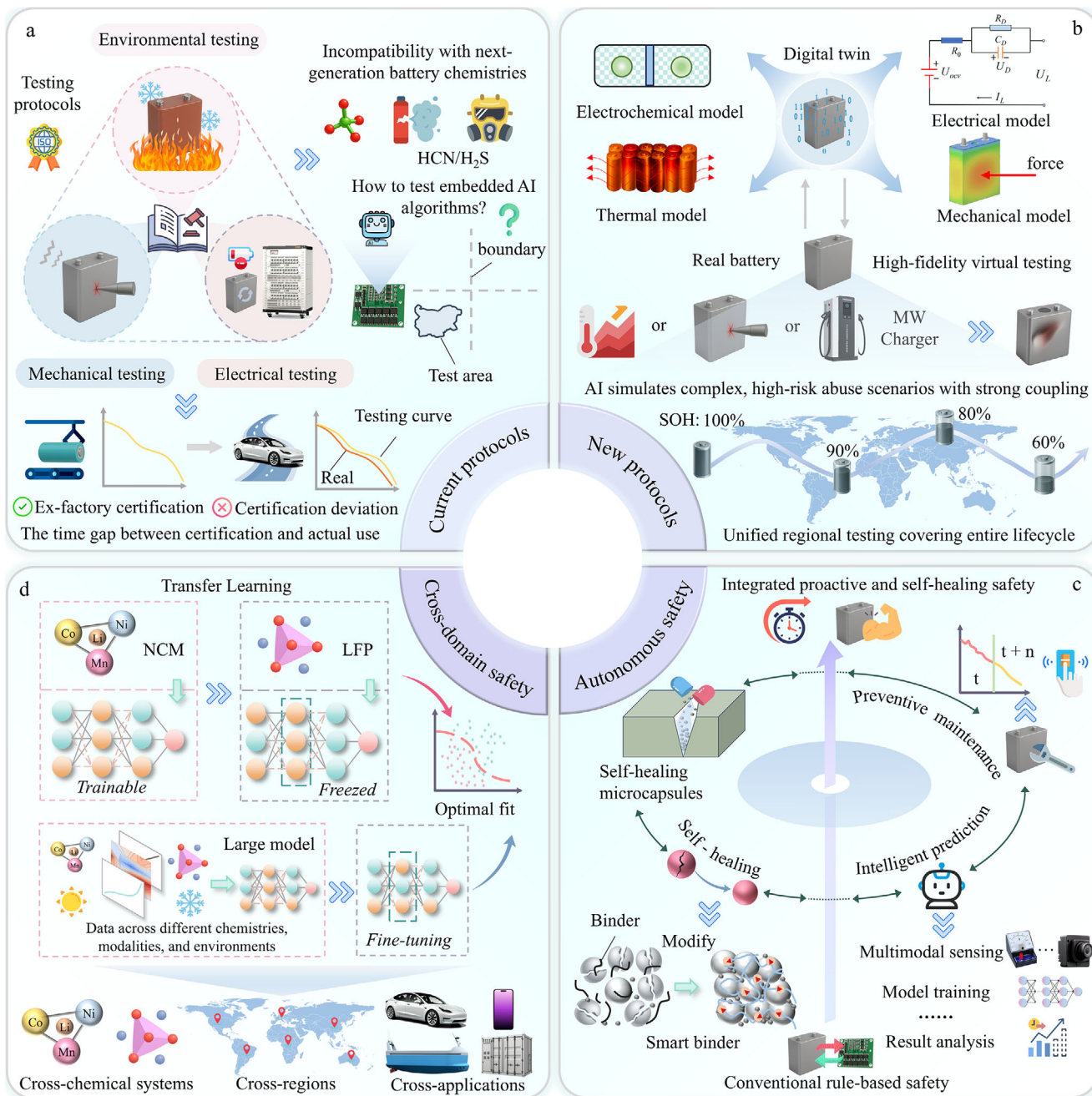


FIGURE 8 | Framework for intelligent and autonomous battery safety management. (a) Limitations of current testing protocols under real operating conditions and emerging battery systems. (b) Next-generation AI-integrated testing procedures based on digital twins and lifecycle-spanning validation. (c) Integrated proactive battery safety framework combining multimodal sensing, intelligent prediction, preventive maintenance, and self-healing-enabled active fault mitigation. (d) Cross-domain safety intelligence and transferable models across chemistries, regions, and applications.

J2464, and International Electrotechnical Commission (IEC) 62660 specify a fixed set of abuse tests including overcharge, short circuit, crush, and penetration (Figure 8a) [379–382]. These procedures are invaluable for establishing baseline safety thresholds, yet they represent static evaluations performed under highly controlled laboratory conditions. In practical operation, battery degradation is a continuous, dynamic process influenced by stochastic variations in temperature, load cycles, and manufacturing heterogeneity. Consequently, the conventional pass–fail structure of existing standards cannot fully represent the probabilistic nature of battery safety risk in the field. This limitation

becomes more pronounced for next-generation electrochemical systems, whose failure behaviors are increasingly chemistry-specific. In such systems, safety risk is not solely determined by the occurrence of fire or explosion. Still, it may instead be dominated by the release of toxic, corrosive gaseous species upon failure (Figure 8a). The composition, release rate, and persistence of these gases vary substantially across chemistries, introducing hazard dimensions—such as acute toxicity and environmental exposure—that are not explicitly addressed within existing fire-centric certification criteria. As a result, a design that formally satisfies current standards may still pose unquantified risks

in confined or semi-confined environments, underscoring a fundamental mismatch between legacy testing paradigms and emerging battery technologies [122, 124]. A more fundamental limitation arises from the temporal gap between the certification event and the battery system's real-time evolution. Once a design is certified, its compliance is assumed to persist throughout its service life, even though operational stresses, environmental conditions, and usage behaviors can significantly alter its risk profile (Figure 8a). As machine learning and data-driven diagnostic algorithms are integrated into BMS, this static approach to safety assurance is becoming increasingly inadequate [48, 383, 384]. The validation of such intelligent systems requires dynamic assessment protocols that evaluate how algorithms respond to uncertainty, adapt to unseen scenarios, and maintain reliability in the presence of partial or corrupted data streams. Future testing standards should therefore transition from single-event verification toward continuous, AI-integrated validation. Instead of focusing solely on material or structural resilience, new protocols are needed to assess the predictive performance of embedded algorithms and their interactions with sensing hardware. Key evaluation metrics should include predictive lead time before fault onset, false-alarm sensitivity, recovery behavior after algorithmic misclassification, and latency of protective action during real-time operation. These indicators provide a more holistic picture of safety performance, linking data interpretation with physical response.

To achieve this transformation, certification bodies may adopt a hybrid validation framework that combines experimental testing with high-fidelity simulation. Digital twins, constructed from coupled electrochemical–thermal–mechanical models, can replicate complex abuse conditions that are impractical or hazardous to reproduce in physical experiments (Figure 8b) [358, 362, 385, 386]. When synchronized with real sensor data, these virtual environments allow systematic exploration of algorithm robustness across varying chemistries, pack architectures, and ambient conditions. The outcome of such tests would not merely confirm structural safety but would quantify the confidence level of algorithmic predictions, forming a “safety envelope” that evolves with accumulated field evidence. The institutional aspect of testing also requires rethinking. Present standards evaluate hardware components in isolation, whereas intelligent safety management is inherently systemic. A next-generation framework should extend certification to the software logic embedded in BMS. This necessitates the creation of standardized digital testbeds where AI-driven controllers can be benchmarked using harmonized datasets [104]. Within these testbeds, model updates could be validated through controlled shadow operation in parallel with certified systems, ensuring algorithmic improvements do not compromise safety compliance. Finally, global harmonization of these emerging standards is essential. Batteries deployed across EVs, grid storage, and portable electronics operate in diverse thermal and regulatory environments. Fragmented regional certification practices impose redundant costs and complicate cross-border product deployment. Establishing unified, data-centric, and AI-compatible safety testing protocols would enable consistent benchmarking of both hardware and intelligence layers, fostering trust and transparency in large-scale battery deployment. This paradigm would transform certification from a one-time requirement into a living framework that continuously verifies safety as systems evolve in real operation.

6.2 | Toward Autonomous Safety Management

A future-oriented battery safety architecture should treat autonomy as a core design principle. Autonomous safety systems should not rely solely on predefined thresholds or static intervention routines. Instead, they are required to continuously monitor both internal and external states, assess emerging risks, and dynamically select mitigation strategies in real time. This closed-loop paradigm integrates high-fidelity sensing, predictive analytics, and adaptive response mechanisms to create systems capable of maintaining stability under uncertain and rapidly changing conditions. In the battery domain, this vision translates to continuous integration of data from distributed sensors, including voltage, current, temperature, pressure, gas evolution, and mechanical strain, into predictive models that detect unsafe trajectories before they escalate into failures [29, 387–389]. Batteries, in this emerging framework, evolve from passively monitored devices to active participants in their own protection [390, 391]. They are expected to interpret their own state, forecast potential hazards, and implement intelligent responses to minimize risk. This redefinition of safety logic calls for a fundamental shift. Systems should not initiate full shutdowns at the first sign of parameter violations. Rather, they should consider a broader context of risk before taking action. For instance, in response to localized thermal stress, appropriate measures may include reducing the charging current, activating localized cooling, or electrically isolating specific modules, all while maintaining overall system function [392]. These decisions are necessary to be coordinated across multiple layers, spanning cells, modules, and the pack, to preserve safety margins while minimizing disruption.

Emerging AI methods are accelerating this transformation. Real-time risk modeling enables probabilistic predictions of safety margins based on evolving operational data. Machine learning algorithms, especially those incorporating continual learning, enable the system to adapt its safety strategies to long-term degradation patterns and varying use cases. PINNs can detect subtle early indicators of failure, such as micro-level impedance changes or local temperature anomalies, that would be difficult to capture through conventional rule-based monitoring [341, 393, 394]. Hybrid reasoning frameworks that combine symbolic logic with data-driven inference offer improved transparency and traceability in safety decisions. Multiscale safety graphs help map fault propagation pathways across cells, modules, and subsystems, enabling targeted containment strategies. Federated safety learning across distributed battery systems can identify rare but critical failure modes without requiring centralized data aggregation, preserving both data privacy and representational diversity [395]. These technological advances should be accompanied by corresponding shifts in certification protocols. Safety assurance processes must evolve to account for algorithms that learn and adapt over time. This includes defining acceptable boundaries for online model updates, establishing rigorous auditing procedures, and ensuring robust fallback mechanisms when model uncertainty is high. Ultimately, autonomous battery safety management is not merely an automation of existing workflows. It represents a broader shift in engineering philosophy. Safety is no longer a static condition verified through compliance testing. It becomes a dynamic property embedded within the system itself. Future battery systems are expected to increasingly

function as intelligent agents that continuously monitor their own state, reason about emerging risks, and execute optimal interventions that balance safety, performance, and longevity (Figure 8c). This paradigm shift is expected to play a central role in enabling the resilient operation of electrified infrastructure at scale.

6.3 | Autonomous Self-healing for Active Fault Mitigation

Autonomous safety should rely not only on risk forecasting, decision-making, and externally actuated interventions, but also on active fault-mitigation capabilities embedded within battery materials and cell architectures. Such capabilities are expected to attenuate the amplification of failure cascades at the onset or early stages of damage evolution. Self-healing technologies represent a prominent pathway in this direction. By introducing reversible reconstruction at the material and interfacial levels, self-healing may enable batteries to partially recover structural integrity and interfacial continuity during cycling and service perturbations (Figure 8c). This, in turn, is likely to suppress the accumulation of localized electrochemical heterogeneity and may reduce the likelihood that microscopic defects escalate into severe failure events. In contrast to external protection strategies, self-healing seeks to internalize safety resilience within the battery cell itself, thereby enhancing fault tolerance and buffering degradation under complex operating conditions [396].

Self-healing strategies can be broadly categorized into extrinsic and intrinsic approaches. Extrinsic approaches typically rely on pre-embedded or releasable healing components to deliver localized compensatory repair once damage occurs, as exemplified in Figure 8c by microcapsule-based healing systems. Intrinsic approaches instead leverage reversible interactions and network reconfiguration inherent to the host material, enabling repeatable sequences of damage, reconstruction, and reconnection. For engineering integration in batteries, a particularly promising and generalizable route is the development of intrinsically self-healing material systems. Through this route, self-healing functionality can be incorporated without excessive structural complexity into key constituents such as electrolytes, smart binders (Figure 8c), coatings, and critical interfacial layers, while remaining effective over extended cycling [396, 397].

At the mechanistic level, intrinsic self-healing is commonly supported by the synergy of reversible dynamic covalent bonding and noncovalent interactions. Dynamic covalent motifs such as Diels–Alder chemistry, acylhydrazone linkages, disulfide exchange, and borate ester bonding can permit controlled rearrangement while maintaining network robustness. Noncovalent interactions such as hydrogen bonding, metal–ligand coordination, π – π stacking, and ionic interactions provide rapidly reversible connections and efficient energy-dissipation pathways. Through judicious combination and tuning of these interactions, a designable balance can be established between structural stability and dynamic reparability. This balance is expected to offer a broadly applicable materials toolkit to sustain interfacial contact, relax stress concentrations, and impede defect propagation [397]. Moreover, for solid-state batteries characterized by solid–solid interfaces and

strongly coupled thermo-electro-mechanical service conditions, adaptive reconfiguration in response to interfacial defects and contact loss may suppress local current focusing and defect amplification induced by contact inhomogeneity. Such suppression is likely to reduce penetration-related risks and may render the safety margin less dependent on the timeliness of externally imposed responses [175, 398].

Nevertheless, elevating self-healing from a material function to a deployable safety capability requires systematic, cross-scale advancement. First, healing kinetics should be co-optimized with ionic and electronic transport. Healing rates, triggering conditions, and long-term stability need to align with the tempo of damage accumulation. Otherwise, repair may lag behind damage evolution, or transport may be compromised, eroding practical benefit [397]. Second, evaluation protocols should shift from a singular focus on healing efficiency toward resilience metrics directly aligned with safety objectives. These metrics are expected to include the recoverability of interfacial impedance and contact, robustness under repeated damage–healing cycles, and reliability boundaries under realistic thermo-electro-mechanical disturbances. Third, scalability, cost, and recycling compatibility need to be incorporated as early design constraints. The additional material complexity introduced by self-healing functionalities is required to remain compatible with manufacturable process windows to progress from laboratory feasibility to engineering viability [399].

6.4 | Cross-domain Battery Safety Prognostics

As battery systems diversify in both chemistry and deployment environment, safety prognostics should evolve from narrowly trained models toward architectures that are inherently transferable, adaptable, and generalizable. The conventional focus on lithium-ion cells has led to safety models that are often not robust when applied to other battery chemistries, such as sodium-ion, zinc-based, or all-solid-state systems (Figure 8d). Moreover, real-world deployments now span a growing array of operational domains, from sub-zero grid storage installations to high-temperature aerospace systems, and from ruggedized portable electronics to maritime propulsion. In these settings, failure mechanisms can differ substantially, and assumptions valid in one context may not hold in another. Addressing this challenge requires a shift toward cross-domain safety intelligence that can learn from one application and apply that knowledge to others. Transfer learning is a foundational strategy in this transition. Models trained on large lithium-ion datasets can be adapted to new chemistries with minimal data by leveraging shared degradation signatures and structural priors [400, 401]. For example, patterns in internal resistance growth or gas evolution may manifest differently across materials, yet can still be interpreted using domain-informed embedding spaces. Equally important is the adoption of multimodal prognostics frameworks. Safety-critical signals often arise not from a single sensor channel but from the interactions between electrochemical, thermal, mechanical, and contextual data. By combining voltage dynamics, acoustic emissions, vibration signatures, and ambient metadata, models can identify failure onset mechanisms that would otherwise remain latent [402, 403]. Cross-modal fusion also enhances the ability of the system to operate under

sensor failure or data sparsity, increasing robustness in field conditions (Figure 8d).

Another emerging trajectory is the use of foundation models tailored for battery safety tasks. Inspired by breakthroughs in language and vision domains, these large-scale models (Figure 8d) are pretrained on diverse battery datasets—spanning chemistries, failure events, and operating conditions—and then adapted to specific prognostic tasks with minimal tuning [302, 404–406]. Such models can internalize broad patterns of degradation and hazard formation, enabling few-shot learning in underrepresented chemistries or novel usage environments. Their scalability and generalization capabilities make them promising candidates for unifying safety intelligence across disparate systems. Multilingual knowledge integration also presents a compelling opportunity, especially in global battery deployment. Incorporating textual manuals, maintenance logs, and regulatory documents into the prognostic pipeline models can align operational semantics with sensor data [407]. This allows safety systems to interpret alerts, recall relevant mitigation strategies, and comply with location-specific safety mandates. The development of such cross-domain safety models must be accompanied by infrastructure capable of supporting them. This includes federated learning platforms that allow distributed model training across devices and organizations without exposing raw data, as well as standardized ontologies for representing battery metadata across manufacturers and chemistries. Only through such coordinated efforts can we build a globally scalable battery safety infrastructure, capable of adapting to the accelerating pace of technological and environmental change. However, the practical realization of these capabilities is fundamentally constrained by the limited availability of open and standardized datasets for emerging battery chemistries. While lithium-ion systems benefit from relatively mature and extensive data resources, experimental and operational data for next-generation batteries, including sodium-ion, zinc-based, metal-anode, and solid-state systems, remain fragmented, heterogeneous, and often inaccessible. This data scarcity restricts the effectiveness of transfer learning and large battery models, hampers the pretraining of foundation models, and impedes the systematic characterization of chemistry-specific failure modes, such as toxic gas release and non-ignition hazards. Establishing open, unified, and chemistry-inclusive battery safety databases with standardized representations of electrochemical, thermal, mechanical, and gaseous signatures is therefore a prerequisite for scalable and generalizable safety intelligence [104].

Acknowledgements

This work is supported by the National Key Research and Development Program of China (2024YFE0115800) and the Introduced Innovative R&D Team of Guangdong (2023ZT10L145). All opinions expressed in this paper are the authors' and do not necessarily reflect the policies and views of sponsors.

Funding

This work is supported by the National Key Research and Development Program of China (2024YFE0115800) and the Introduced Innovative R&D Team of Guangdong (2023ZT10L145). All opinions expressed in this paper

are the authors' and do not necessarily reflect the policies and views of sponsors.

Conflicts of Interest

The authors declare no conflicts of interest.

Data Availability Statement

Data sharing not applicable to this article as no datasets were generated or analysed during the current study.

References

1. Y. Zheng, Y. Che, X. Hu, X. Sui, D. I. Stroe, and R. Teodorescu, "Thermal state Monitoring of Lithium-ion Batteries: Progress, Challenges, and Opportunities," *Progress in Energy and Combustion Science* 100 (2024): 101120, <https://doi.org/10.1016/j.pecs.2023.101120>.
2. Y. Guo, Y. Li, K. Qiu, et al., "Removal of Residual Contaminants by Minute-level Washing Facilitates the Direct Regeneration of Spent Cathodes from Retired EV Li-ion Batteries," *Energy & Environmental Science* 18, no. 1 (2025): 264–274, <https://doi.org/10.1039/D4EE03021D>.
3. K. Li, X. Li, Z. Xiong, et al., "Unlocking Vehicle-to-grid Potential of Load Shifting in China's Megacities Considering Comprehensive Real-world Behaviors," *Nature Communications* 16, no. 1 (2025): 10087, <https://doi.org/10.1038/s41467-025-65073-8>.
4. Y. Sun, C. Zuo, H. Wang, et al., "Designing Safe and Long-life Lithium-ion Batteries via a Solvent-relay Strategy," *Nature Energy* 10 (2025): 1–8.
5. D. Shi, M. Cai, Y. Che, L. Xie, and J. Zhao, "Towards Artificial Intelligence-enabled Autonomous Battery Prognostics and Management," *Journal of Energy Chemistry* 113 (2025): 905–939.
6. H. Jo, M. Gong, S. Y. Kim, D. H. Seo, and S. K. Jung, "Guided Phase Transition for Mitigating Voltage Hysteresis of Iron Fluoride Positive Electrodes in Lithium-ion Batteries," *Nature Communications* 16, no. 1 (2025): 8596, <https://doi.org/10.1038/s41467-025-63676-9>.
7. International Energy Agency Global EV Outlook 2025. Available at: <https://www.iea.org/reports/global-ev-outlook-2025> [accessed 24 November 2025].
8. China Energy Storage Alliance. China new energy storage development report (2025), https://henb.nea.gov.cn/hdhy/zlxz/202509/t20250902_286682.html; 2025 [accessed 24 November 2025].
9. J. Zhao, X. Feng, Q. Pang, et al., "Battery Safety: Machine Learning-based Prognostics," *Progress in Energy and Combustion Science* 102 (2024): 101142, <https://doi.org/10.1016/j.pecs.2023.101142>.
10. S. Y. Kim, S. W. Kwon, M. Nasir Bashir, and J. S. Lee, "Predicting Dendrite Growth in Lithium Metal Batteries through Iterative Neural Networks and Voltage Embedding," *npj Computational Materials* 11, no. 1 (2025): 337, <https://doi.org/10.1038/s41524-025-01824-x>.
11. Z. Wang, D. Shi, et al., "Battery Health Diagnostics: Bridging the Gap between Academia and Industry," *ETransportation* 19 (2024): 100309.
12. Y. Li, H. Shi, S. Wang, et al., "A Comprehensive Review of Remaining Useful Life Prediction Methods for Lithium-ion Batteries: Models, Trends, and Engineering Applications," *Journal of Energy Chemistry* 112 (2025): 384–414.
13. J. Zhu, L. Huang, L. Xu, et al., "Bio-based Furan Aramid/Ceramic-coated Lithium-ion Battery Separators with High Ionic Conductivity, Wettability and Safety via in Situ Lithium Compensation Strategy," *Journal of Energy Chemistry* 114 (2025): 630–638.
14. Y. Wang, X. Feng, Y. Peng, et al., "Reductive Gas Manipulation at Early Self-heating Stage Enables Controllable Battery Thermal Failure," *Joule* 6, no. 12 (2022): 2810–2820, <https://doi.org/10.1016/j.joule.2022.10.010>.
15. S. Chen, X. Wei, H. Wu, et al., "Multi-functional Thermal Barrier Suppresses Battery Thermal Runaway Propagation and Degradation,"

- Renewable and Sustainable Energy Reviews* 223 (2025): 116056, <https://doi.org/10.1016/j.rser.2025.116056>.
16. C. Jin, X. Feng, Y. Sun, et al., “High-Frequency Induction Heating: a Breakthrough for Reliable Thermal Runaway Triggering in Battery Safety Testing,” *ACS Energy Letters* 10 (2025): 6054–6063.
 17. J. Zhao, Z. Lv, D. Li, et al., “Battery Engineering Safety Technologies (BEST): M5 Framework of Mechanisms, Modes, Metrics, Modeling, and Mitigation,” *ETransportation* 22 (2024): 100364.
 18. EV FireSafe. Passenger EV LIB fire incidents, https://www.evfiresafe.com/_files/ugd/8b9ad1_1e058681d2e447fdbe00fce9c46d4ec8.pdf; 2024 [accessed 24 November 2025].
 19. Q. Wang, B. Mao, S. I. Stoliarov, and J. Sun, “A Review of Lithium Ion Battery Failure Mechanisms and Fire Prevention Strategies,” *Progress in Energy and Combustion Science* 73 (2019): 95–131, <https://doi.org/10.1016/j.pecs.2019.03.002>.
 20. M. R. Palacín and A. de Guibert, “Why Do Batteries Fail?,” *Science* 351, no. 6273 (2016): 1253292.
 21. Y. Zhang, P. Ping, X. Dai, et al., “Failure Mechanism and Thermal Runaway Behavior of Lithium-ion Battery Induced by Arc Faults,” *Renewable and Sustainable Energy Reviews* 207 (2025): 114914, <https://doi.org/10.1016/j.rser.2024.114914>.
 22. G. Zhang, X. Wei, X. Wang, et al., “Lithium-ion Battery Sudden Death: Safety Degradation and Failure Mechanism,” *ETransportation* 20 (2024): 100333.
 23. S. Chen, X. Wei, G. Zhang, et al., “Active and Passive Safety Enhancement for Batteries from Force Perspective,” *Renewable and Sustainable Energy Reviews* 187 (2023): 113740, <https://doi.org/10.1016/j.rser.2023.113740>.
 24. L. Chen, S. Zeng, J. Li, et al., “Safety Assessment of Overcharged Batteries and a Novel Passive Warning Method Based on Relaxation Expansion Force,” *Journal of Energy Chemistry* 105 (2025): 595–607, <https://doi.org/10.1016/j.jechem.2025.02.016>.
 25. K. Liu, Y. Liu, D. Lin, A. Pei, and Y. Cui, “Materials for Lithium-ion Battery Safety,” *Science advances* 4, no. 6 (2018): aas9820, <https://doi.org/10.1126/sciadv.aas9820>.
 26. P. Li, M. Xu, X. Guo, et al., “Thermal Switches for Lithium-ion Battery Thermal Management: Principle, Performance and Application,” *Energy Storage Materials* 81 (2025): 104481, <https://doi.org/10.1016/j.ensm.2025.104481>.
 27. C. Hu, B. Zhang, M. Leng, et al., “Multiscale Strategies for Low-temperature Heating to Break the Cold Barrier of Lithium-Ion Batteries: from Material Design to System Integration,” *Advanced Energy Materials* 15 (2025): 04155.
 28. O. ElJarray, H. Dai, Z. Chen, et al., “Ensuring Battery Safety in Electric Vehicles: Challenges, Developments, and Future Perspectives,” *Small* 22 (2025): 2503406.
 29. Y. Wei, M. Wang, M. Zhang, T. Cai, Y. Huang, and M. Xu, “Advancements, Challenges, and Future Trajectories in Advanced Battery Safety Detection,” *Electrochemical Energy Reviews* 8, no. 1 (2025): 10, <https://doi.org/10.1007/s41918-025-00245-0>.
 30. X. Zhang, S. Chen, J. Zhu, and Y. Gao, “A Critical Review of Thermal Runaway Prediction and Early-warning Methods for Lithium-ion Batteries,” *Energy Material Advances* 4 (2023): 0008, <https://doi.org/10.34133/energymatadv.0008>.
 31. G. Wang, P. Ping, D. Kong, et al., “Advances and Challenges in Thermal Runaway Modeling of Lithium-Ion Batteries,” *The Innovation* 5, no. 4 (2024): 100624.
 32. J. Zhao, M. Liu, B. Zhang, et al., “Review of Lithium-ion Battery Fault Features, Diagnosis Methods, and Diagnosis Procedures,” *IEEE Internet of Things Journal* 11, no. 11 (2023): 18936–18950, <https://doi.org/10.1109/JIOT.2023.3324322>.
 33. N. Lin, K. Chen, Z. Zhang, S. Chen, and Z. Wang, “Beyond Diagnosis: Why Current Fault Diagnosis Methods for Power Batteries Fall Short,” *Journal of Energy Storage* 130 (2025): 117225, <https://doi.org/10.1016/j.est.2025.117225>.
 34. V. Sulzer, P. Mohtat, A. Aitio, et al., “The Challenge and Opportunity of Battery Lifetime Prediction from Field Data,” *Joule* 5, no. 8 (2021): 1934–1955, <https://doi.org/10.1016/j.joule.2021.06.005>.
 35. Z. Lv and J. Zhao, “Resource-efficient Artificial Intelligence for Battery Capacity Estimation Using Convolutional FlashAttention Fusion Networks,” *eTransportation* 23 (2025): 100383.
 36. J. Zhao, X. Feng, J. Wang, Y. Lian, M. Ouyang, and A. F. Burke, “Battery Fault Diagnosis and Failure Prognosis for Electric Vehicles Using Spatio-temporal Transformer Networks,” *Applied Energy* 352 (2023): 121949, <https://doi.org/10.1016/j.apenergy.2023.121949>.
 37. Q. Hu, J. Lu, J. Hui, Z. Rao, Y. Ren, and H. Wang, “Artificial Intelligence-Driven Development in Rechargeable Battery Materials: Progress, Challenges, and Future Perspectives,” *Advanced Functional Materials* 35 (2025): 08438, <https://doi.org/10.1002/adfm.202508438>.
 38. J. Zhao, X. Qu, Y. Wu, M. Fowler, and A. F. Burke, “Artificial Intelligence-driven Real-world Battery Diagnostics,” *Energy and AI* 18 (2024): 100419, <https://doi.org/10.1016/j.egyai.2024.100419>.
 39. Y. C. Gao, X. Chen, Y. H. Yuan, et al., “Accelerating Battery Innovation: AI-powered Molecular Discovery,” *Chemical Society Reviews* 54 (2025): 9630–9684.
 40. Y. Li, C. Wu, Y. Wang, N. Li, T. Liu, and J. Lu, “Accelerating the Battery Revolution: AI-driven Multiscale Innovation from Material Discovery to Smart Manufacturing,” *Advanced Functional Materials* 36 (2025): 14830.
 41. T. Raoofi and M. Yildiz, “Comprehensive Review of Battery state Estimation Strategies Using Machine Learning for Battery Management Systems of Aircraft Propulsion Batteries,” *Journal of Energy Storage* 59 (2023): 106486, <https://doi.org/10.1016/j.est.2022.106486>.
 42. O. Demirci, S. Taskin, E. Schaltz, and B. A. Demirci, “Review of Battery state Estimation Methods for Electric Vehicles-Part I: SOC Estimation,” *Journal of energy storage* 87 (2024): 111435, <https://doi.org/10.1016/j.est.2024.111435>.
 43. O. Demirci, S. Taskin, E. Schaltz, and B. A. Demirci, “Review of Battery state Estimation Methods for Electric Vehicles-Part II: SOH Estimation,” *Journal of Energy Storage* 96 (2024): 112703, <https://doi.org/10.1016/j.est.2024.112703>.
 44. J. Rhyu, J. Schaeffer, M. L. Li, et al., “Systematic Feature Design for Cycle Life Prediction of Lithium-ion Batteries during Formation,” *Joule* 9, no. 5 (2025): 101884.
 45. J. Zhao, Z. Wang, Y. Wu, and A. F. Burke, “Predictive Pretrained Transformer (PPT) for Real-time Battery Health Diagnostics,” *Applied Energy* 377 (2025): 124746, <https://doi.org/10.1016/j.apenergy.2024.124746>.
 46. Y. Wang, X. Feng, D. Guo, et al., “Temperature Excavation to Boost Machine Learning Battery Thermochemical Predictions,” *Joule* 8, no. 9 (2024): 2639–2651, <https://doi.org/10.1016/j.joule.2024.07.002>.
 47. S. Ji, J. Zhu, Y. Yang, G. Dos Reis, and Z. Zhang, “Data-Driven Battery Characterization and Prognosis: Recent Progress, Challenges, and Prospects,” *Small Methods* 8, no. 7 (2024): 2301021, <https://doi.org/10.1002/smt.202301021>.
 48. D. P. Finegan, J. Zhu, X. Feng, et al., “The Application of Data-driven Methods and Physics-based Learning for Improving Battery Safety,” *Joule* 5, no. 2 (2021): 316–329, <https://doi.org/10.1016/j.joule.2020.11.018>.
 49. M. F. Ng, J. Zhao, Q. Yan, G. J. Conduit, and Z. W. Seh, “Predicting the state of Charge and Health of Batteries Using Data-driven Machine Learning,” *Nature Machine Intelligence* 2, no. 3 (2020): 161–170, <https://doi.org/10.1038/s42256-020-0156-7>.
 50. B. Liaw, W. Li, L. Raijmakers, et al., “Demystifying Data-driven Approaches for Battery Electric Transportation: Challenges and Future Directions,” *eTransportation* 26 (2025): 100501.

51. Y. Chen, Y. Kang, Y. Zhao, et al., "A Review of Lithium-ion Battery Safety Concerns: the Issues, Strategies, and Testing Standards," *Journal of Energy Chemistry* 59 (2021): 83–99, <https://doi.org/10.1016/j.jechem.2020.10.017>.
52. W. Lu, I. Belharouak, J. Liu, and K. Amine, "Thermal Properties of Li₄/3Ti₅/3O₄/LiMn₂O₄ Cell," *Journal of Power Sources* 174, no. 2 (2007): 673–677.
53. S. Wu, Y. Chen, W. Luan, et al., "A Review of Multiscale Mechanical Failures in Lithium-Ion Batteries: Implications for Performance, Lifetime and Safety," *Electrochemical Energy Reviews* 7, no. 1 (2024): 35, <https://doi.org/10.1007/s41918-024-00233-w>.
54. W. Huang, X. Feng, X. Han, W. Zhang, and F. Jiang, "Questions and Answers Relating to Lithium-Ion Battery Safety Issues," *Cell Reports Physical Science* 2, no. 1 (2021): 100285, <https://doi.org/10.1016/j.xcrp.2020.100285>.
55. H. Sun, W. Tian, J. Yue, and F. Su, "Lithium-ion Battery Heterogeneous Electrochemical-thermal-mechanical Multiphysics Coupling Model and Characterization of Microscopic Properties," *Journal of Power Sources* 629 (2025): 235970, <https://doi.org/10.1016/j.jpowsour.2024.235970>.
56. K. Amine, I. Belharouak, Z. Chen, et al., "Nanostructured Anode Material for High-Power Battery System in Electric Vehicles," *Advanced materials* 22, no. 28 (2010): 3052–3057, <https://doi.org/10.1002/adma.201000441>.
57. J. Zhao, X. Feng, M. K. Tran, M. Fowler, M. Ouyang, and A. F. Burke, "Battery Safety: Fault Diagnosis from Laboratory to Real World," *Journal of Power Sources* 598, no. 234111 (2024): 10–1016, <https://doi.org/10.1016/j.jpowsour.2024.234111>.
58. S. Rana, R. Kumar, and R. S. Bharj, "Current Trends, Challenges, and Prospects in Material Advances for Improving the Overall Safety of Lithium-ion Battery Pack," *Chemical Engineering Journal* 463 (2023): 142336, <https://doi.org/10.1016/j.cej.2023.142336>.
59. S. S. Zhang, "A Review on Electrolyte Additives for Lithium-ion Batteries," *Journal of Power Sources* 162, no. 2 (2006): 1379–1394, <https://doi.org/10.1016/j.jpowsour.2006.07.074>.
60. R. Li, W. Li, A. Singh, D. Ren, Z. Hou, and M. Ouyang, "Effect of External Pressure and Internal Stress on Battery Performance and Lifespan," *Energy Storage Materials* 52 (2022): 395–429, <https://doi.org/10.1016/j.ensm.2022.07.034>.
61. S. Chen, G. Fan, Y. Wang, et al., "The Impact of Intermittent Overcharging on Battery Capacity and Reliability: Electrochemical Performance Analysis and Failure Prediction," *Journal of Power Sources* 591 (2024): 233800, <https://doi.org/10.1016/j.jpowsour.2023.233800>.
62. Y. Xie, S. Wang, R. Li, et al., "Inhomogeneous Degradation Induced by Lithium Plating in a Large-format Lithium-ion Battery," *Journal of Power Sources* 542 (2022): 231753, <https://doi.org/10.1016/j.jpowsour.2022.231753>.
63. P. Röder, N. Baba, and H. D. Wiemhöfer, "A Detailed Thermal Study of a Li [Ni_{0.33}Co_{0.33}Mn_{0.33}] O₂/LiMn₂O₄-based Lithium Ion Cell by Accelerating Rate and Differential Scanning Calorimetry," *Journal of Power Sources* 248 (2014): 978–987.
64. G. Tang, J. Zhang, S. Ma, J. Li, Z. Peng, and W. Chen, "Unveiling Gas Production in Rechargeable Batteries via in Situ Differential Electrochemical Mass Spectrometry," *Chemical Society Reviews* 54, no. 15 (2025): 7216–7251, <https://doi.org/10.1039/D5CS00276A>.
65. W. Wang, W. Li, F. Yu, et al., "Unravelling Gas Evolution Mechanisms in Battery Electrode Materials," *Nature Chemistry* 18 (2026): 1–12.
66. Y. Liao, H. Zhang, Y. Peng, et al., "Electrolyte Degradation during Aging Process of Lithium-Ion Batteries: Mechanisms, Characterization, and Quantitative Analysis," *Advanced Energy Materials* 14, no. 18 (2024): 2304295, <https://doi.org/10.1002/aenm.202304295>.
67. D. Li, C. Shen, Y. Zheng, and J. Xu, "Electrochemo-Mechanical Degradation and Failure of Active Particles in High Energy Density Batteries: a Review," *Small* 21, no. 8 (2025): 2407740, <https://doi.org/10.1002/sml.202407740>.
68. D. Lisbona and T. Snee, "A Review of Hazards Associated with Primary Lithium and Lithium-ion Batteries," *Process safety and environmental protection* 89, no. 6 (2011): 434–442, <https://doi.org/10.1016/j.psep.2011.06.022>.
69. P. Liu, L. Yang, B. Xiao, et al., "Revealing Lithium Battery Gas Generation for Safer Practical Applications," *Advanced Functional Materials* 32, no. 47 (2022): 2208586, <https://doi.org/10.1002/adfm.202208586>.
70. H. Liu, C. Li, X. Hu, et al., "Multi-modal Framework for Battery state of Health Evaluation Using Open-source Electric Vehicle Data," *Nature Communications* 16, no. 1 (2025): 1137, <https://doi.org/10.1038/s41467-025-56485-7>.
71. J. Nanda and S. Kalnaus, "Cracking the Failure of Lithium Batteries," *Science* 388, no. 6744 (2025): 255–255, <https://doi.org/10.1126/science.adw9437>.
72. M. Bao, E. W. Chen, Y. M. Lu, Z. S. Liu, and S. Liu, "Vibration and Noise Analysis for a Motor of Pure Electric Vehicle," *Advanced Materials Research* 915-916 (2014): 98–102, <https://doi.org/10.4028/www.scientific.net/AMR.915-916.98>.
73. M. J. Brand, S. F. Schuster, T. Bach, et al., "Effects of Vibrations and Shocks on Lithium-ion Cells," *Journal of Power Sources* 288 (2015): 62–69, <https://doi.org/10.1016/j.jpowsour.2015.04.107>.
74. J. M. Hooper, J. Marco, G. H. Chouchelamane, J. S. Chevalier, and D. Williams, "Multi-axis Vibration Durability Testing of Lithium Ion 18650 NCA Cylindrical Cells," *Journal of energy storage* 15 (2018): 103–123, <https://doi.org/10.1016/j.est.2017.11.006>.
75. L. Li, X. Chen, R. Hu, et al., "Aging Mechanisms and Thermal Characteristics of Commercial 18650 Lithium-Ion Battery Induced by Minor Mechanical Deformation," *Journal of Electrochemical Energy Conversion and Storage* 18, no. 2 (2021): 021010, <https://doi.org/10.1115/1.4048703>.
76. G. Qian, F. Monaco, D. Meng, et al., "The Role of Structural Defects in Commercial Lithium-ion Batteries," *Cell Reports Physical Science* 2, no. 9 (2021): 100554, <https://doi.org/10.1016/j.xcrp.2021.100554>.
77. R. Zhao, J. Liu, and J. Gu, "Simulation and Experimental Study on Lithium Ion Battery Short Circuit," *Applied Energy* 173 (2016): 29–39, <https://doi.org/10.1016/j.apenergy.2016.04.016>.
78. E. Jiaqiang, H. Xiao, S. Tian, and Y. Huang, "A Comprehensive Review on Thermal Runaway Model of a Lithium-ion Battery: Mechanism, Thermal, Mechanical, Propagation, Gas Venting and Combustion," *Renewable Energy* 229 (2024): 120762.
79. R. Spotnitz and J. Franklin, "Abuse Behavior of High-power, Lithium-ion Cells," *Journal of power sources* 113, no. 1 (2003): 81–100, [https://doi.org/10.1016/S0378-7753\(02\)00488-3](https://doi.org/10.1016/S0378-7753(02)00488-3).
80. L. Kong, C. Li, J. Jiang, and M. G. Pecht, "Li-ion Battery Fire Hazards and Safety Strategies," *Energies* 11, no. 9 (2018): 2191, <https://doi.org/10.3390/en11092191>.
81. R. Jung, M. Metzger, F. Maglia, C. Stinner, and H. A. Gasteiger, "Oxygen Release and Its Effect on the Cycling Stability of LiNi_xMn_y-Co_zO₂ (NMC) Cathode Materials for Li-ion Batteries," *Journal of The Electrochemical Society* 164, no. 7 (2017): A1361–A1377, <https://doi.org/10.1149/2.0021707jes>.
82. X. Feng, M. Ouyang, X. Liu, L. Lu, Y. Xia, and X. He, "Thermal Runaway Mechanism of Lithium Ion Battery for Electric Vehicles: a Review," *Energy storage materials* 10 (2018): 246–267, <https://doi.org/10.1016/j.ensm.2017.05.013>.
83. Z. Rao, P. Lyu, M. Li, X. Liu, and X. Feng, "A Thermal Perspective on Battery Safety," *Nature Reviews Clean Technology* 1, no. 7 (2025): 511–524, <https://doi.org/10.1038/s44359-025-00073-x>.
84. B. Xiong, R. Chen, F. Zeng, J. Kang, and Y. Men, "Thermal Shrinkage and Microscopic Shutdown Mechanism of Polypropylene Separator for Lithium-ion Battery: in-situ Ultra-small Angle X-ray Scattering Study," *Journal of Membrane Science* 545 (2018): 213–220, <https://doi.org/10.1016/j.memsci.2017.10.001>.

85. L. S. de Vasconcelos, R. Xu, Z. Xu, et al., “Chemomechanics of Rechargeable Batteries: Status, Theories, and Perspectives,” *Chemical Reviews* 122, no. 15 (2022): 13043–13107.
86. H. Du, Y. Wang, Y. Kang, et al., “Side Reactions/Changes in Lithium-Ion Batteries: Mechanisms and Strategies for Creating Safer and Better Batteries,” *Advanced Materials* 36, no. 29 (2024): 2401482, <https://doi.org/10.1002/adma.202401482>.
87. K. Yang, L. Zhang, W. Wang, et al., “Multiscale Modeling for Enhanced Battery Health Analysis: Pathways to Longevity,” *Carbon Neutralization* 3, no. 3 (2024): 348–385, <https://doi.org/10.1002/cnl2.124>.
88. B. Nie, Y. Dong, and L. Chang, “The Evolution of Thermal Runaway Parameters of Lithium-ion Batteries under Different Abuse Conditions: a Review,” *Journal of Energy Storage* 96 (2024): 112624, <https://doi.org/10.1016/j.est.2024.112624>.
89. A. C. Walk, M. Huttin, and M. Kamlah, “Comparison of a Phase-field Model for Intercalation Induced Stresses in Electrode Particles of Lithium Ion Batteries for Small and Finite Deformation Theory,” *European Journal of Mechanics—A/Solids* 48 (2014): 74–82, <https://doi.org/10.1016/j.euromechsol.2014.02.020>.
90. Y. Wang, H. Li, Z. Wang, C. Lian, and Z. Xie, “Factors Affecting Stress in Anode Particles during Charging Process of Lithium Ion Battery,” *Journal of Energy Storage* 43 (2021): 103214, <https://doi.org/10.1016/j.est.2021.103214>.
91. X. Gao, Y. Jia, W. Zhang, C. Yuan, and J. Xu, “Mechanics-driven Anode Material Failure in Battery Safety and Capacity Deterioration Issues: a Review,” *Applied Mechanics Reviews* 74, no. 6 (2022): 060801, <https://doi.org/10.1115/1.4054566>.
92. J. G. Swallow, W. H. Woodford, F. P. McGrogan, N. Ferralis, Y. M. Chiang, and K. J. Van Vliet, “Effect of Electrochemical Charging on Elastoplastic Properties and Fracture Toughness of LiXCoO₂,” *Journal of the electrochemical society* 161, no. 11 (2014): F3084–F3090, <https://doi.org/10.1149/2.014141jes>.
93. S. Xia, L. Mu, Z. Xu, et al., “Chemomechanical Interplay of Layered Cathode Materials Undergoing Fast Charging in Lithium Batteries,” *Nano energy* 53 (2018): 753–762, <https://doi.org/10.1016/j.nanoen.2018.09.051>.
94. Z. Ren, X. Zhang, M. Liu, et al., “Constant Dripping Wears away a Stone: Fatigue Damage Causing Particles’ cracking,” *Journal of Power Sources* 416 (2019): 104–110, <https://doi.org/10.1016/j.jpowsour.2019.01.084>.
95. H. Wu, H. Jia, C. Wang, J. G. Zhang, and W. Xu, “Recent Progress in Understanding Solid Electrolyte Interphase on Lithium Metal Anodes,” *Advanced Energy Materials* 11, no. 5 (2021): 2003092, <https://doi.org/10.1002/aenm.202003092>.
96. G. Pozzato, A. Allam, L. Pulvirenti, G. A. Negoita, W. A. Paxton, and S. Onori, “Analysis and Key Findings from Real-world EV Field Data,” *Joule* 7, no. 9 (2023): 2035–2053.
97. J. Vazquez-Arenas, L. E. Gimenez, M. Fowler, T. Han, and S. K. Chen, “A Rapid Estimation and Sensitivity Analysis of Parameters Describing the Behavior of Commercial Li-ion Batteries Including Thermal Analysis,” *Energy Conversion and Management* 87 (2014): 472–482, <https://doi.org/10.1016/j.enconman.2014.06.076>.
98. W. Mroziak, J. McDonald, E. Shuttleworth, and A. Ankowski, “Comparative Safety Analysis of Current and next-generation Battery Technologies,” *Journal of Power Sources* 670 (2026): 239428, <https://doi.org/10.1016/j.jpowsour.2026.239428>.
99. Y. Zhang, T. Mo, X. Wu, H. Yu, and B. Mao, “Comparative Study of Gas Generation during Thermal Runaway in High-capacity Sodium-ion Batteries and Lithium Iron Phosphate Battery for Energy Storage Applications,” *Journal of Power Sources* 662 (2026): 238780, <https://doi.org/10.1016/j.jpowsour.2025.238780>.
100. Y. Yue, Z. Jia, Y. Li, et al., “Thermal Runaway Hazards Comparison between Sodium-ion and Lithium-ion Batteries Using Accelerating Rate Calorimetry,” *Process Safety and Environmental Protection* 189 (2024): 61–70, <https://doi.org/10.1016/j.psep.2024.06.032>.
101. W. Mei, Z. Cheng, L. Wang, et al., “Thermal Hazard Comparison and Assessment of Li-ion Battery and Na-ion Battery,” *Journal of Energy Chemistry* 102 (2025): 18–26, <https://doi.org/10.1016/j.jechem.2024.10.036>.
102. W. Chen, S. Shen, B. Ma, et al., “Comparative Study on Thermal Runaway and Gas Generation Behavior between Sodium Ion Battery and Lithium Iron Phosphate/Ternary Lithium Ion Battery,” *Energy Storage* 8, no. 1 (2026): 70340, <https://doi.org/10.1002/est2.70340>.
103. Q. Chuang, W. Qian, L. Chunjing, Y. Hongtao, and L. Zhenyan, “Comparison of Thermal Runaway and Gas Production Behavior between Copper-based/Hard Carbon Sodium Ion Battery and Lithium-Iron Phosphate/Graphite Lithium-ion Battery,” *Journal of Energy Storage* 132 (2025): 117848, <https://doi.org/10.1016/j.est.2025.117848>.
104. C. Yang, A. Singh, X. Pu, et al., “Addressing the Safety of next-generation Batteries,” *Nature* 645, no. 8081 (2025): 603–613, <https://doi.org/10.1038/s41586-025-09358-4>.
105. L. Lin and O. A. Ezekoye, “Time-resolved Characterization of Toxic and Flammable Gases during Venting of Li-ion Cylindrical Cells with Current Interrupt Devices,” *Journal of Loss Prevention in the Process Industries* 94 (2025): 105488, <https://doi.org/10.1016/j.jlp.2024.105488>.
106. S. J. Yang, J. K. Hu, F. N. Jiang, et al., “Oxygen-induced Thermal Runaway Mechanisms of Ah-level Solid-state Lithium Metal Pouch Cells,” *Etransportation* 18 (2023): 100279, <https://doi.org/10.1016/j.etrans.2023.100279>.
107. T. Kim, K. Kim, S. Lee, G. Song, M. S. Jung, and K. T. Lee, “Thermal Runaway Behavior of Li₆PS₅Cl Solid Electrolytes for LiNi_{0.8}Co_{0.1}Mn_{0.1}O₂ and LiFePO₄ in all-solid-state Batteries,” *Chemistry of Materials* 34, no. 20 (2022): 9159–9171, <https://doi.org/10.1021/acs.chemmater.2c02106>.
108. Y. Wu, S. Zhang, Sun, Huang, J. Xu, C. Liu, and G. Cui, “Electrochemical Initiation and Chemical Reaction Cascades in Dual-stage Thermal Runaway in Sulfide-based all-solid-state Batteries,” *Nature Communications* 17 (2026): 2928.
109. T. Liu, L. W. Kum, D. K. Singh, and J. Kumar, “Thermal, Electrical, and Environmental Safeties of Sulfide Electrolyte-based All-solid-state Li-ion Batteries,” *ACS omega* 8, no. 13 (2023): 12411–12417, <https://doi.org/10.1021/acsomega.3c00261>.
110. Z. Li, Z. Cheng, Y. Yu, et al., “Thermal Runaway Comparison and Assessment between Sodium-ion and Lithium-ion Batteries,” *Process Safety and Environmental Protection* 193 (2025): 842–855, <https://doi.org/10.1016/j.psep.2024.11.118>.
111. Z. Li, M. Dadsetan, J. Gao, et al., “Revealing the Thermal Safety of Prussian Blue Cathode for Safer Nonaqueous Batteries,” *Advanced Energy Materials* 11, no. 42 (2021): 2101764, <https://doi.org/10.1002/aenm.202101764>.
112. R. A. Adams, A. Varma, and V. G. Pol, “Mechanistic Elucidation of Thermal Runaway in Potassium-ion Batteries,” *Journal of Power Sources* 375 (2018): 131–137, <https://doi.org/10.1016/j.jpowsour.2017.11.065>.
113. S. Nanda, A. Dolocan, A. Yanyachi, et al., “Thermal Decomposition Pathways and Interfacial Reactivity in Potassium-ion Batteries: Focus on the Electrolyte and Anode,” *Energy & Environmental Science* 19 (2026): 1215–1236, <https://doi.org/10.1039/D5EE06908D>.
114. P. Xu, F. Huang, Y. Sun, et al., “Anode-Free Alkali Metal Batteries: from Laboratory to Practicability,” *Advanced Functional Materials* 34, no. 44 (2024): 2406080, <https://doi.org/10.1002/adfm.202406080>.
115. E. Wang, S. Ge, W. Li, B. Fu, F. Zhou, and W. Chen, “Precisely Deciphering Solid Electrolyte Interphase,” *Matter* 8, no. 11 (2025): 102368.
116. C. D. Fincher, C. E. Athanasiou, C. Gilgenbach, et al., “Controlling Dendrite Propagation in Solid-state Batteries with Engineered Stress,” *Joule* 6, no. 12 (2022): 2794–2809, <https://doi.org/10.1016/j.joule.2022.10.011>.
117. Z. Ning, G. Li, D. L. Melvin, et al., “Dendrite Initiation and Propagation in Lithium Metal Solid-state Batteries,” *Nature* 618, no. 7964 (2023): 287–293, <https://doi.org/10.1038/s41586-023-05970-4>.

118. G. McConohy, X. Xu, T. Cui, et al., “Mechanical Regulation of Lithium Intrusion Probability in Garnet Solid Electrolytes,” *Nature energy* 8, no. 3 (2023): 241–250.
119. B. Zhang, B. Yuan, X. Yan, et al., “Atomic Mechanism of Lithium Dendrite Penetration in Solid Electrolytes,” *Nature Communications* 16, no. 1 (2025): 1906, <https://doi.org/10.1038/s41467-025-57259-x>.
120. L. Gan, X. Xu, X. Yu, and H. Li, “Assessing the Thermal Runaway Characteristics of Solid-state Lithium Batteries Based on Thermochemical Reaction Properties at Material Level,” *Energy Storage Materials* 78 (2025): 104223, <https://doi.org/10.1016/j.ensm.2025.104223>.
121. N. Darmet, J. Charbonnel, M. Reytier, L. Broche, and R. Vincent, “First Experimental Assessment of all-solid-state Battery Thermal Runaway Propagation in a Battery Pack,” *ACS Applied Energy Materials* 7, no. 10 (2024): 4365–4375, <https://doi.org/10.1021/acsaem.4c00248>.
122. W. G. Lim, S. Kim, E. A. Wu, D. H. Tan, S. Peng, and X. Li, “Safety of Sodium-ion Batteries: Evaluation and Perspective from Component Materials to Cells, Modules, and Packs,” *Advanced Energy Materials* (2025): e05016, <https://doi.org/10.1002/aenm.202505016>.
123. NIOSH. Immediately Dangerous to Life or Health (IDLH) Values, <https://www.cdc.gov/niosh/idlh/>; 2024 [accessed 22 March 2026].
124. M. D. Bouguern, N. G. Ningappa, K. Vishweswariah, A. K. Kumar M R, R. Kanno, and K. Zaghbi, “Comparative Advances in Sulfide and Halide Electrolytes for Commercialization of all-solid-state Lithium Batteries,” *Advanced Materials* 38 (2025): 13255.
125. H. Wang, D. Yu, C. Kuang, et al., “Alkali Metal Anodes for Rechargeable Batteries,” *Chemistry* 5, no. 2 (2019): 313–338, <https://doi.org/10.1016/j.chempr.2018.11.005>.
126. Y. Cui, W. Song, J. Liu, and B. Cong, “Research Progress on Thermal Runaway Mechanisms of all-solid-state Lithium Batteries,” *ACS Energy Letters* 10, no. 11 (2025): 5282–5303, <https://doi.org/10.1021/acsenrgylett.5c00503>.
127. D. He, J. Wang, Y. Peng, et al., “Research Advances on Thermal Runaway Mechanism of LIBs and Safety Improvement,” *Sustainable Materials and Technologies* 41 (2024): 01017.
128. L. Wang, Z. Su, R. Wang, H. Liang, B. Fang, and R. Mo, “Recent Status, Key Strategies and Challenging Perspectives of Smart Batteries for next-generation Batteries,” *Journal of Materials Chemistry A* 13 (2025): 21116–21171.
129. K. T. Selvi, K. A. Mangai, J. A. Lett, I. Fatimah, and S. Sagadevan, “Exploring the Electrode Materials for High-performance Lithium-ion Batteries for Energy Storage Application,” *Journal of Energy Storage* 92 (2024): 112208, <https://doi.org/10.1016/j.est.2024.112208>.
130. Z. Wu, C. Zhang, F. Yuan, et al., “Ni-rich Cathode Materials for Stable High-energy LIBs,” *Nano Energy* 126 (2024): 109620.
131. S. Zhang, Z. Yang, Y. Lu, W. Xie, Z. Yan, and J. Chen, “Insights into Cation Migration and Intermixing in Advanced Cathode Materials for Lithium-Ion Batteries,” *Advanced Energy Materials* 14, no. 36 (2024): 2402068, <https://doi.org/10.1002/aenm.202402068>.
132. D. Versaci, R. Colombo, G. Montinaro, et al., “Tailoring Cathode Materials: a Comprehensive Study on LNMO/LFP Blending for next Generation Lithium-ion Batteries,” *Journal of Power Sources* 613 (2024): 234955, <https://doi.org/10.1016/j.jpowsour.2024.234955>.
133. J. C. Stallard, L. Wheatcroft, S. G. Booth, et al., “Mechanical Properties of Cathode Materials for Lithium-ion Batteries,” *Joule* 6, no. 5 (2022): 984–1007, <https://doi.org/10.1016/j.joule.2022.04.001>.
134. Y. H. Luo, H. X. Wei, L. B. Tang, et al., “Nickel-rich and Cobalt-free Layered Oxide Cathode Materials for Lithium Ion Batteries,” *Energy storage materials* 50 (2022): 274–307, <https://doi.org/10.1016/j.ensm.2022.05.019>.
135. J. Li, W. Zhong, Q. Deng, Q. Zhang, and C. Yang, “Recent Progress in Synthesis and Surface Modification of Nickel-rich Layered Oxide Cathode Materials for Lithium-ion Batteries,” *International Journal of Extreme Manufacturing* 4, no. 4 (2022): 042004, <https://doi.org/10.1088/2631-7990/ac92ef>.
136. G. Ko, S. Jeong, S. Park, et al., “Doping Strategies for Enhancing the Performance of Lithium Nickel Manganese Cobalt Oxide Cathode Materials in Lithium-ion Batteries,” *Energy Storage Materials* 60 (2023): 102840, <https://doi.org/10.1016/j.ensm.2023.102840>.
137. C. U. Mulik, R. S. Kamat, X. Wang, et al., “High-performance Li-ion Battery Cathode: Mn-doped LiFePO₄ via Solution Combustion Synthesis Method,” *Journal of Electroanalytical Chemistry* 971 (2024): 118568, <https://doi.org/10.1016/j.jelechem.2024.118568>.
138. W. He, P. Liu, Y. Zhou, et al., “A Novel Morphology-controlled Synthesis of Na⁺-doped Li- and Mn-rich Cathodes by the Self-assembly of Amphiphilic Spherical Micelles,” *Sustainable Materials and Technologies* 25 (2020): e00171, <https://doi.org/10.1016/j.susmat.2020.e00171>.
139. W. Yu, C. Li, Y. Li, et al., “Research Progress on Lithium-rich Cathode Materials for High Energy Density Lithium-ion Batteries,” *Journal of Alloys and Compounds* 986 (2024): 174156, <https://doi.org/10.1016/j.jallcom.2024.174156>.
140. W. Guo, W. Wei, H. Zhu, Y. Hu, H. Jiang, and C. Li, “In Situ Surface Engineering Enables High Interface Stability and Rapid Reaction Kinetics for Ni-rich Cathodes,” *eScience* 3, no. 1 (2023): 100082, <https://doi.org/10.1016/j.esci.2022.10.008>.
141. T. Zhao, L. Li, R. Chen, et al., “Design of Surface Protective Layer of LiF/FeF₃ Nanoparticles in Li-rich Cathode for High-capacity Li-ion Batteries,” *Nano Energy* 15 (2015): 164–176, <https://doi.org/10.1016/j.nanoen.2015.04.013>.
142. W. Zhao, C. Zhao, H. Wu, L. Li, and C. Zhang, “Progress, Challenge and Perspective of Graphite-based Anode Materials for Lithium Batteries: a Review,” *Journal of Energy Storage* 81 (2024): 110409, <https://doi.org/10.1016/j.est.2023.110409>.
143. B. Li, Y. Chao, M. Li, et al., “A Review of Solid Electrolyte Interphase (SEI) and Dendrite Formation in Lithium Batteries,” *Electrochemical Energy Reviews* 6, no. 1 (2023): 7, <https://doi.org/10.1007/s41918-022-00147-5>.
144. H. Liu, Z. Wei, W. He, and J. Zhao, “Thermal Issues about Li-ion Batteries and Recent Progress in Battery Thermal Management Systems: a Review,” *Energy conversion and management* 150 (2017): 304–330, <https://doi.org/10.1016/j.enconman.2017.08.016>.
145. H. Adenusi, G. A. Chass, S. Passerini, K. V. Tian, and G. Chen, “Lithium Batteries and the Solid Electrolyte Interphase (SEI)—Progress and Outlook,” *Advanced energy materials* 13, no. 10 (2023): 2203307, <https://doi.org/10.1002/aenm.202203307>.
146. J. Xu, Y. Hu, and X. Wu, “Improvement of Cycle Stability for High-voltage Lithium-ion Batteries by in-situ Growth of SEI Film on Cathode,” *Nano Energy* 5 (2014): 67–73, <https://doi.org/10.1016/j.nanoen.2014.02.004>.
147. N. W. Li, Y. X. Yin, C. P. Yang, and Y. G. Guo, “An Artificial Solid Electrolyte Interphase Layer for Stable Lithium Metal Anodes,” *Advanced materials* 28, no. 9 (2016): 1853–1858, <https://doi.org/10.1002/adma.201504526>.
148. W. Mo, S. Hu, H. Li, X. Zhu, and L. Zhang, “Designing Multifunctional Artificial SEI Layers for Long-term Stability of Sodium Metal Anodes,” *Journal of Colloid and Interface Science* 683 (2025): 600–609, <https://doi.org/10.1016/j.jcis.2024.12.100>.
149. S. J. Park, J. Y. Hwang, C. S. Yoon, H. G. Jung, and Y. K. Sun, “Stabilization of Lithium-metal Batteries Based on the in Situ Formation of a Stable Solid Electrolyte Interphase Layer,” *ACS Applied Materials & Interfaces* 10, no. 21 (2018): 17985–17993, <https://doi.org/10.1021/acsaami.8b04592>.
150. S. H. Pan, S. Nachimuthu, B. J. Hwang, G. Bruncklaus, and J. C. Jiang, “Synergistic Dual Electrolyte Additives for Fluoride Rich Solid-electrolyte Interface on Li Metal Anode Surface: Mechanistic Understanding of Electrolyte Decomposition,” *Journal of Colloid and Interface Science* 649 (2023): 804–814, <https://doi.org/10.1016/j.jcis.2023.06.147>.

151. Z. Xu, Y. Yu, Y. Huang, et al., “Recent Advances in Protecting Li-anode via Establishing Nitrides as Stable Solid Electrolyte Interphases,” *Journal of Power Sources* 579 (2023): 233274, <https://doi.org/10.1016/j.jpowsour.2023.233274>.
152. C. Zhang, S. Gu, D. Zhang, et al., “Nonflammable, Localized High-concentration Electrolyte towards a High-safety Lithium Metal Battery,” *Energy Storage Materials* 52 (2022): 355–364, <https://doi.org/10.1016/j.ensm.2022.08.018>.
153. K. Song, X. Wang, Z. Xie, et al., “Ultrathin CuF₂-Rich Solid-Electrolyte Interphase Induced by Cation-Tailored Double Electrical Layer Toward Durable Sodium Storage,” *Angewandte Chemie International Edition* 62, no. 10 (2023): 202216450, <https://doi.org/10.1002/anie.202216450>.
154. B. Ahmed, C. Xia, and H. N. Alshareef, “Electrode Surface Engineering by Atomic Layer Deposition: a Promising Pathway toward Better Energy Storage,” *Nano Today* 11, no. 2 (2016): 250–271, <https://doi.org/10.1016/j.nantod.2016.04.004>.
155. L. Zhao, G. Chen, Y. Weng, et al., “Precise Al₂O₃ Coating on LiNi_{0.5}Co_{0.2}Mn_{0.3}O₂ by Atomic Layer Deposition Restrains the Shuttle Effect of Transition Metals in Li-ion Capacitors,” *Chemical Engineering Journal* 401 (2020): 126138, <https://doi.org/10.1016/j.cej.2020.126138>.
156. Y. Cao, X. Meng, and A. Li, “Atomic Layer Deposition of High-Capacity Anodes for Next-Generation Lithium-Ion Batteries and Beyond,” *Energy & Environmental Materials* 4, no. 3 (2021): 363–391, <https://doi.org/10.1002/eem2.12132>.
157. T. Zhang, T. Wang, Y. Zheng, et al., “Atomic Layer Deposition for Sodium-Ion Batteries,” *Advanced Energy Materials* 15 (2025): 01760, <https://doi.org/10.1002/aenm.202501760>.
158. E. Adhitama, F. Dias Brandao, I. Dienwiebel, et al., “Pre-Lithiation of Silicon Anodes by Thermal Evaporation of Lithium for Boosting the Energy Density of Lithium Ion Cells,” *Advanced functional materials* 32, no. 22 (2022): 2201455, <https://doi.org/10.1002/adfm.202201455>.
159. L. Jin, C. Shen, Q. Wu, et al., “Pre-Lithiation Strategies for Next-Generation Practical Lithium-Ion Batteries,” *Advanced Science* 8, no. 12 (2021): 2005031, <https://doi.org/10.1002/adv.202005031>.
160. M. Li, J. Yuan, M. Jin, et al., “Elucidating the Chemical Pre-Lithiation Mechanism of Hard Carbon Anodes for Ultra-High Stability Lithium-Ion Batteries,” *Small* 21, no. 2 (2025): 2407919, <https://doi.org/10.1002/sml.202407919>.
161. M. Bai, M. Zhong, X. Tang, W. Shen, J. Zhang, and S. Guo, “Heteroatoms Doped Holey Graphene Enhanced Carbon Frameworks with Chemical Pre-lithiation Affording Reversible Lithium Plating/Stripping in Anode-free Lithium Metal Batteries,” *Energy Storage Materials* 82 (2025): 104648, <https://doi.org/10.1016/j.ensm.2025.104648>.
162. S. Bai, W. Bao, K. Qian, et al., “Elucidating the Role of Prelithiation in Si-Based Anodes for Interface Stabilization,” *Advanced Energy Materials* 13, no. 28 (2023): 2301041, <https://doi.org/10.1002/aenm.202301041>.
163. F. Wang, B. Wang, J. Li, et al., “Prelithiation: a Crucial Strategy for Boosting the Practical Application of next-generation Lithium Ion Battery,” *ACS nano* 15, no. 2 (2021): 2197–2218, <https://doi.org/10.1021/acsnano.0c10664>.
164. S. Chen, G. Wu, H. Jiang, et al., “External Li Supply Reshapes Li Deficiency and Lifetime Limit of Batteries,” *Nature* 638, no. 8051 (2025): 676–683, <https://doi.org/10.1038/s41586-024-08465-y>.
165. X. Fan, C. Zhong, J. Liu, et al., “Opportunities of Flexible and Portable Electrochemical Devices for Energy Storage: Expanding the Spotlight onto Semi-solid/Solid Electrolytes,” *Chemical Reviews* 122, no. 23 (2022): 17155–17239, <https://doi.org/10.1021/acs.chemrev.2c00196>.
166. M. Yuan and K. Liu, “Rational Design on Separators and Liquid Electrolytes for Safer Lithium-ion Batteries,” *Journal of Energy Chemistry* 43 (2020): 58–70, <https://doi.org/10.1016/j.jechem.2019.08.008>.
167. W. Ren, C. Ding, X. Fu, and Y. Huang, “Advanced Gel Polymer Electrolytes for Safe and Durable Lithium Metal Batteries: Challenges, Strategies, and Perspectives,” *Energy Storage Materials* 34 (2021): 515–535, <https://doi.org/10.1016/j.ensm.2020.10.018>.
168. W. Liang, K. Zhao, L. Ouyang, M. Zhu, and J. Liu, “A Review of Functional Group Selection and Design Strategies for Gel Polymer Electrolytes for Metal Batteries,” *Materials Science and Engineering: R: Reports* 164 (2025): 100973, <https://doi.org/10.1016/j.mserr.2025.100973>.
169. X. Y. Huang, C. Z. Zhao, W. J. Kong, et al., “Tailoring Polymer Electrolyte Solvation for 600 Wh Kg⁻¹ Lithium Batteries,” *Nature* 646 (2025): 1–8.
170. Q. Zhao, S. Stalin, C. Z. Zhao, and L. A. Archer, “Designing Solid-state Electrolytes for Safe, Energy-dense Batteries,” *Nature Reviews Materials* 5, no. 3 (2020): 229–252, <https://doi.org/10.1038/s41578-019-0165-5>.
171. X. Zhu, J. Wu, and J. Lu, “Insight into Inorganic Solid-State Electrolytes: Ionic Transport and Failure Mechanisms,” *Advanced Functional Materials* 34, no. 49 (2024): 2409547, <https://doi.org/10.1002/adfm.202409547>.
172. K. Wu, J. Tan, Z. Liu, et al., “Incombustible Solid Polymer Electrolytes: a Critical Review and Perspective,” *Journal of Energy Chemistry* 93 (2024): 264–281, <https://doi.org/10.1016/j.jechem.2024.01.013>.
173. H. Lv, X. Chu, Y. Zhang, Q. Liu, F. Wu, and D. Mu, “Self-healing Solid-state Polymer Electrolytes for High-safety and Long-cycle Lithium-ion Batteries,” *Materials Today* 78 (2024): 181–208, <https://doi.org/10.1016/j.mattod.2024.06.018>.
174. J. Li, X. Zhu, Z. Xu, et al., “Dynamic Metal-Ligand Coordinated Self-Healing Polymer Electrolytes for Lithium-Ion Batteries: Correlating Coordination Mechanisms with Electrochemical Properties,” *Advanced Functional Materials* 35 (2025): 10177, <https://doi.org/10.1002/adfm.202510177>.
175. F. Pei, L. Wu, Y. Zhang, et al., “Interfacial Self-healing Polymer Electrolytes for Long-cycle Solid-state Lithium-sulfur Batteries,” *Nature Communications* 15, no. 1 (2024): 351, <https://doi.org/10.1038/s41467-023-43467-w>.
176. X. Ge, F. Zhang, L. Wu, Z. Yang, and T. Xu, “Current Challenges and Perspectives of Polymer Electrolyte Membranes,” *Macromolecules* 55, no. 10 (2022): 3773–3787, <https://doi.org/10.1021/acs.macromol.1c02053>.
177. X. Chen, W. He, L. X. Ding, S. Wang, and H. Wang, “Enhancing Interfacial Contact in all Solid state Batteries with a Cathode-supported Solid Electrolyte Membrane Framework,” *Energy & Environmental Science* 12, no. 3 (2019): 938–944, <https://doi.org/10.1039/C8EE02617C>.
178. D. Xu, B. Wang, Q. Wang, et al., “High-strength Internal Cross-linking Bacterial Cellulose-network-based Gel Polymer Electrolyte for Dendrite-suppressing and High-rate Lithium Batteries,” *ACS applied materials & interfaces* 10, no. 21 (2018): 17809–17819, <https://doi.org/10.1021/acsami.8b00034>.
179. D. Yang, L. He, Y. Liu, et al., “An Acetylene Black Modified Gel Polymer Electrolyte for High-performance Lithium-sulfur Batteries,” *Journal of Materials Chemistry A* 7, no. 22 (2019): 13679–13686, <https://doi.org/10.1039/C9TA03123E>.
180. L. Long, S. Wang, M. Xiao, and Y. Meng, “Polymer Electrolytes for Lithium Polymer Batteries,” *Journal of Materials Chemistry A* 4, no. 26 (2016): 10038–10069, <https://doi.org/10.1039/C6TA02621D>.
181. G. Cheng, Z. Wang, X. Wang, and Y. He, “All-climate Thermal Management Structure for Batteries Based on Expanded Graphite/Polymer Composite Phase Change Material with a High Thermal and Electrical Conductivity,” *Applied Energy* 322 (2022): 119509, <https://doi.org/10.1016/j.apenergy.2022.119509>.
182. J. Luo, D. Zou, Y. Wang, S. Wang, and L. Huang, “Battery Thermal Management Systems (BTMs) Based on Phase Change Material (PCM): a Comprehensive Review,” *Chemical Engineering Journal* 430 (2022): 132741, <https://doi.org/10.1016/j.cej.2021.132741>.
183. Z. Li, Y. Zhang, S. Zhang, and B. Tang, “Phase Change Materials for Lithium-ion Battery Thermal Management Systems: a Review,” *Journal of Energy Storage* 80 (2024): 110259, <https://doi.org/10.1016/j.est.2023.110259>.

184. P. GaneshKumar, V. Sivalingam, S. Divya, T. H. Oh, V. S. Vigneswaran, and R. Velraj, "Thermophysical Exploration: State-of-the-art Review on Phase Change Materials for Effective Thermal Management in Lithium-ion Battery Systems," *Journal of Energy Storage* 87 (2024): 111412, <https://doi.org/10.1016/j.est.2024.111412>.
185. M. Malik, I. Dincer, M. Rosen, and M. Fowler, "Experimental Investigation of a New Passive Thermal Management System for a Li-ion Battery Pack Using Phase Change Composite Material," *Electrochimica Acta* 257 (2017): 345–355, <https://doi.org/10.1016/j.electacta.2017.10.051>.
186. W. Luo, L. Zhao, and M. Chen, "The Effect of PCM on Mitigating Thermal Runaway Propagation in Lithium-ion Battery Modules," *Applied Thermal Engineering* 236 (2024): 121608.
187. A. Wang, J. Jiang, Y. Liu, et al., "Research Progress of Aerogel Used in Lithium-ion Power Batteries," *Journal of Loss Prevention in the Process Industries* 92 (2024): 105433, <https://doi.org/10.1016/j.jlp.2024.105433>.
188. L. Ge, S. Shang, Y. Ma, et al., "Overview of Aerogels for Thermal Insulation," *ACS Applied Materials & Interfaces* 17, no. 18 (2025): 26091–26116, <https://doi.org/10.1021/acsmi.4c22957>.
189. P. V. Chombo and Y. Laoonual, "A Review of Safety Strategies of a Li-ion Battery," *Journal of Power Sources* 478 (2020): 228649, <https://doi.org/10.1016/j.jpowsour.2020.228649>.
190. C. F. Lopez, J. A. Jeevarajan, and P. P. Mukherjee, "Experimental Analysis of Thermal Runaway and Propagation in Lithium-ion Battery Modules," *Journal of the electrochemical society* 162, no. 9 (2015): A1905–A1915, <https://doi.org/10.1149/2.0921509jes>.
191. W. Zhang, L. Huang, Z. Zhang, et al., "Non-uniform Phase Change Material Strategy for Directional Mitigation of Battery Thermal Runaway Propagation," *Renewable Energy* 200 (2022): 1338–1351, <https://doi.org/10.1016/j.renene.2022.10.070>.
192. H. He, F. Sun, Z. Wang, et al., "China's Battery Electric Vehicles Lead the World: Achievements in Technology System Architecture and Technological Breakthroughs," *Green Energy and Intelligent Transportation* 1, no. 1 (2022): 100020, <https://doi.org/10.1016/j.geits.2022.100020>.
193. H. Lian, C. Liu, D. Xiong, et al., "Engineering Ultra-Stable Solid Electrolyte Interphase via Strong Crystal Face Coupling for High-Rate Solid Lithium Batteries," *Advanced Functional Materials* 36 (2026): 30233, <https://doi.org/10.1002/adfm.202530233>.
194. S. Lou, F. Zhang, C. Fu, et al., "Interface Issues and Challenges in all-Solid-State Batteries: Lithium, Sodium, and Beyond," *Advanced Materials* 33, no. 6 (2021): 2000721, <https://doi.org/10.1002/adma.202000721>.
195. L. Peng, T. Lei, C. Liao, S. Chen, S. Cheng, and J. Xie, "Fluorine-doped Electrolyte and Artificial SEI for Enhanced Interfacial Stability in all-solid-state Lithium Metal Batteries," *ACS Applied Engineering Materials* 2, no. 6 (2024): 1698–1705, <https://doi.org/10.1021/acsaenm.4c00279>.
196. T. Ma, D. Wu, Z. Wang, et al., "In-situ Cathode Coating for all-solid-state Batteries by Freeze-drying Technology," *Nano Energy* 124 (2024): 109522, <https://doi.org/10.1016/j.nanoen.2024.109522>.
197. Y. Morino, A. Shiota, S. Kanada, et al., "Design of Cathode Coating Using Niobate and Phosphate Hybrid Material for Sulfide-based Solid-state Battery," *ACS Applied Materials & Interfaces* 15, no. 30 (2023): 36086–36095, <https://doi.org/10.1021/acsmi.3c02827>.
198. Y. Huang, S. Cao, X. Xie, et al., "Improving the Structure and Cycling Stability of Ni-rich Layered Cathodes by Dual Modification of Yttrium Doping and Surface Coating," *ACS applied materials & interfaces* 12, no. 17 (2020): 19483–19494, <https://doi.org/10.1021/acsmi.0c01558>.
199. X. Zhang, T. Wu, J. Jian, et al., "Dual Modification Strategy for Enhanced Cycling and Rate Performance of Ni-Rich Cathode Materials in Lithium-Ion Batteries," *Small* 20, no. 45 (2024): 2404488, <https://doi.org/10.1002/smll.202404488>.
200. X. Yan, K. Chen, Z. Chen, X. Ai, and Y. Cao, "Uncoupling Solvent Intercalation on Graphite Anode in Lithium-ion Batteries," *Advanced Energy Materials* 16 (2026): 05287.
201. X. Zheng, S. Weng, W. Luo, et al., "Deciphering the Role of Fluoroethylene Carbonate towards Highly Reversible Sodium Metal Anodes," *Research* 2022 (2022), <https://doi.org/10.34133/2022/9754612>.
202. R. Wang, H. Li, Y. Wu, et al., "How to Promote the Industrial Application of SiOx Anode Prelithiation: Capability, Accuracy, Stability, Uniformity, Cost, and Safety," *Advanced Energy Materials* 12, no. 48 (2022): 2202342, <https://doi.org/10.1002/aenm.202202342>.
203. Z. Huang, Z. Deng, Y. Zhong, et al., "Progress and Challenges of Prelithiation Technology for Lithium-Ion Battery," *Carbon Energy* 4, no. 6 (2022): 1107–1132, <https://doi.org/10.1002/cey2.256>.
204. X. Guo, Z. Xie, R. Wang, et al., "Interface-Compatible Gel-Polymer Electrolyte Enabled by NaF-Solubility-Regulation toward all-Climate Solid-State Sodium Batteries," *Angewandte Chemie International Edition* 63, no. 18 (2024): 202402245, <https://doi.org/10.1002/anie.202402245>.
205. E. Hosseinzadeh, S. Arias, M. Krishna, et al., "Quantifying Cell-to-cell Variations of a Parallel Battery Module for Different Pack Configurations," *Applied Energy* 282 (2021): 115859, <https://doi.org/10.1016/j.apenergy.2020.115859>.
206. Z. Ji and C. Zhang, "Study on the Impact of Battery Pack Arrangement on Temperature Uniformity Distribution," *Sustainable Energy & Fuels* 8, no. 19 (2024): 4519–4532, <https://doi.org/10.1039/D4SE00459K>.
207. A. Kurzawski, L. Torres-Castro, R. Shurtz, J. Lamb, and J. C. Hewson, "Predicting Cell-to-cell Failure Propagation and Limits of Propagation in Lithium-ion Cell Stacks," *Proceedings of the Combustion Institute* 38, no. 3 (2021): 4737–4745, <https://doi.org/10.1016/j.proci.2020.06.270>.
208. S. Nyamathulla and C. Dhanamjayulu, "A Review of Battery Energy Storage Systems and Advanced Battery Management System for Different Applications: Challenges and Recommendations," *Journal of Energy Storage* 86 (2024): 111179, <https://doi.org/10.1016/j.est.2024.111179>.
209. M. Waseem, M. Ahmad, A. Parveen, and M. Suhaib, "Battery Technologies and Functionality of Battery Management System for EVs: Current Status, Key Challenges, and Future Perspectives," *Journal of Power Sources* 580 (2023): 233349, <https://doi.org/10.1016/j.jpowsour.2023.233349>.
210. M. Manas, R. Yadav, and R. K. Dubey, "Designing a Battery Management System for Electric Vehicles: a Congregated Approach," *Journal of Energy Storage* 74 (2023): 109439, <https://doi.org/10.1016/j.est.2023.109439>.
211. B. Gou, Y. He, P. Huang, W. Zhang, Y. Zhang, and Z. Bai, "Understanding the Voltage Inconsistency Features in Lithium-ion Battery Module," *Journal of Energy Storage* 115 (2025): 116007, <https://doi.org/10.1016/j.est.2025.116007>.
212. K. Shen, W. Liu, X. Lai, et al., "Investigation of Inhomogeneous Temperature Characteristics and Estimation Method for Temperature Distribution in Aging Large-size Blade Cells," *Journal of Energy Storage* 113 (2025): 115648, <https://doi.org/10.1016/j.est.2025.115648>.
213. H. Su, H. Yang, C. Ma, et al., "High Response and Selectivity of the SnO₂ Nanobox Gas Sensor for Ethyl Methyl Carbonate Leakage Detection in a Lithium-ion Battery," *ACS sensors* 9, no. 1 (2024): 444–454, <https://doi.org/10.1021/acssensors.3c02230>.
214. S. M. Lee, J. Y. Kim, J. Lee, and J. W. Byeon, "Evaluation of Cracking Damage in Electrode Materials of a Lmo/al-lix Lithium-ion Battery through Analysis of Acoustic Emission Signals," *Journal of Materials Research and Technology* 24 (2023): 5235–5249, <https://doi.org/10.1016/j.jmrt.2023.04.121>.
215. X. Guo, S. Guo, C. Wu, J. Li, C. Liu, and W. Chen, "Intelligent Monitoring for Safety-Enhanced Lithium-Ion/Sodium-Ion Batteries," *Advanced Energy Materials* 13, no. 10 (2023): 2203903, <https://doi.org/10.1002/aenm.202203903>.
216. Y. Iwasaki, M. Misumi, and T. Nakamiya, "Robust Vehicle Detection under Various Environments to Realize Road Traffic Flow Surveillance Using an Infrared Thermal Camera," *The Scientific World Journal* 2015, no. 1 (2015): 947272, <https://doi.org/10.1155/2015/947272>.

217. S. Masuch, P. Gümbel, N. Kaden, and K. Dröder, "Applications and Development of X-ray Inspection Techniques in Battery Cell Production," *Processes* 11, no. 1 (2022): 10, <https://doi.org/10.3390/pr11010010>.
218. W. Sterkens, D. Diaz-Romero, T. Goedemé, W. Dewulf, and J. R. Peeters, "Detection and Recognition of Batteries on X-Ray Images of Waste Electrical and Electronic Equipment Using Deep Learning Resources," *Conservation and Recycling* 168 (2021): 105246.
219. P. L. dos Santos, T. A. Perdicoulis, P. A. Salgado, and J. C. Azevedo, "Kalman Filter for Noise Reduction of Li-Ion Cell Discharge Current," *IFAC-PapersOnLine* 56, no. 2 (2023): 9582–9587.
220. Y. Wang, S. H. He, and B. C. Wang, "Evolutionary Sensor Placement for Spatiotemporal Modeling of Battery Thermal Process," *IEEE Transactions on Industrial Informatics* 18, no. 4 (2021): 2223–2232, <https://doi.org/10.1109/TII.2021.3084133>.
221. J. Huang, S. T. Boles, and J. M. Tarascon, "Sensing as the Key to Battery Lifetime and Sustainability," *Nature Sustainability* 5, no. 3 (2022): 194–204, <https://doi.org/10.1038/s41893-022-00859-y>.
222. C. Huang and B. Shen, "Event-based Fusion Estimation for Multi-rate Systems Subject to Sensor Degradations," *Journal of the Franklin Institute* 358, no. 16 (2021): 8754–8771, <https://doi.org/10.1016/j.franklin.2021.08.011>.
223. J. Fan, C. Liu, N. Li, et al., "Wireless Transmission of Internal Hazard Signals in Li-ion Batteries," *Nature* 641, no. 8063 (2025): 639–645, <https://doi.org/10.1038/s41586-025-08785-7>.
224. E. Miele, W. M. Dose, I. Manyakin, et al., "Hollow-core Optical Fibre Sensors for Operando Raman Spectroscopy Investigation of Li-ion Battery Liquid Electrolytes," *Nature Communications* 13, no. 1 (2022): 1651, <https://doi.org/10.1038/s41467-022-29330-4>.
225. N. Sun, Q. Rong, J. Wu, et al., "Fully Printable Integrated Multifunctional Sensor Arrays for Intelligent Lithium-ion Batteries," *Nature Communications* 16, no. 1 (2025): 7361, <https://doi.org/10.1038/s41467-025-62657-2>.
226. S. E. Crawford, G. R. Lander, H. P. Paudel, et al., "Quantum Sensing for Emerging Energy Technologies," *Nature Reviews Clean Technology* 1 (2025): 1–16.
227. K. W. See, G. Wang, Y. Zhang, et al., "Critical Review and Functional Safety of a Battery Management System for Large-scale Lithium-ion Battery Pack Technologies," *International Journal of Coal Science & Technology* 9, no. 1 (2022): 36, <https://doi.org/10.1007/s40789-022-00494-0>.
228. A. A. de França, J. M. M. Villanueva, and E. C. T. de Macêdo, "Cloud Battery Management System Development," in *2024 8th International Symposium on Instrumentation Systems, Circuits and Transducers (INSCIT)* (IEEE, 2024), 1–6, <https://doi.org/10.1109/INSCIT62583.2024.10693411>.
229. M. S. Ramkumar, C. S. R. Reddy, A. Ramakrishnan, et al., "Review on Li-ion Battery with Battery Management Dystem in Electrical Vehicle," *Advances in Materials Science and Engineering* 2022, no. 1 (2022): 3379574.
230. G. L. Plett and G. McVeigh, "Sensitivity of Lithium-ion Battery SOH Estimates to Sensor Measurement Error and Latency," in *2024 International Conference on Electrical, Computer and Energy Technologies (IEEE, 2024)*, 1–6.
231. S. Arandhakar and J. Nakka, "State of Charge Estimation of Lithium Ion Battery for Electric Vehicle Using Cutting Edge Machine Learning Algorithms: a Review," *Journal of Energy Storage* 103 (2024): 114281, <https://doi.org/10.1016/j.est.2024.114281>.
232. P. Reshma and V. J. Manohar, "Collaborative Evaluation of SoC, SoP and SoH of Lithium-ion Battery in an Electric Bus through Improved Remora Optimization Algorithm and Dual Adaptive Kalman Filtering Algorithm," *Journal of Energy Storage* 68 (2023): 107573, <https://doi.org/10.1016/j.est.2023.107573>.
233. M. Wu, L. Qin, and G. Wu, "State of Power Estimation of Power Lithium-ion Battery Based on an Equivalent Circuit Model," *Journal of Energy Storage* 51 (2022): 104538, <https://doi.org/10.1016/j.est.2022.104538>.
234. X. Yang, S. Wang, W. Xu, et al., "A Novel Fuzzy Adaptive Cubature Kalman Filtering Method for the state of Charge and state of Energy co-estimation of Lithium-ion Batteries," *Electrochimica Acta* 415 (2022): 140241, <https://doi.org/10.1016/j.electacta.2022.140241>.
235. M. Jiang, D. Li, Z. Li, et al., "Advances in Battery State Estimation of Battery Management System in Electric Vehicles," *Journal of Power Sources* 612 (2024): 234781, <https://doi.org/10.1016/j.jpowsour.2024.234781>.
236. Z. Wang, D. T. Gladwin, M. J. Smith, and S. Haass, "Practical state Estimation Using Kalman Filter Methods for Large-scale Battery Systems," *Applied Energy* 294 (2021): 117022, <https://doi.org/10.1016/j.apenergy.2021.117022>.
237. M. Zhang and X. Fan, "Design of Battery Management System Based on Improved Ampere-hour Integration Method," *International Journal of Electric and Hybrid Vehicles* 14, no. 1-2 (2022): 1–29, <https://doi.org/10.1504/IJEHV.2022.125249>.
238. D. Chen, W. Gao, C. Zhang, and L. Chen, "SOC Estimation of Lithium Battery Based on Double Modified Ampere-hour Integral Method," in *2022 37th Youth Academic Annual Conference of Chinese Association of Automation (YAC)* (IEEE, 2022), 1093–1098.
239. M. U. Hassan, S. Saha, M. E. Haque, S. Islam, A. Mahmud, and N. Mendis, "A Comprehensive Review of Battery state of Charge Estimation Techniques," *Sustainable Energy Technologies and Assessments* 54 (2022): 102801, <https://doi.org/10.1016/j.seta.2022.102801>.
240. S. Peng, Y. Miao, R. Xiong, J. Bai, M. Cheng, and M. Pecht, "State of Charge Estimation for a Parallel Battery Pack Jointly by Fuzzy-PI Model Regulator and Adaptive Unscented Kalman Filter," *Applied energy* 360 (2024): 122807.
241. J. Wang, J. Meng, Q. Peng, T. Liu, and J. Peng, "An Electrochemical-thermal Coupling Model for Lithium-ion Battery state-of-charge Estimation with Improve Dual Particle Filter Framework," *Journal of Energy Storage* 87 (2024): 111473, <https://doi.org/10.1016/j.est.2024.111473>.
242. X. Liu, X. Q. Zhang, X. Chen, et al., "A Generalizable, Data-driven Online Approach to Forecast Capacity Degradation Trajectory of Lithium Batteries," *Journal of Energy Chemistry* 68 (2022): 548–555, <https://doi.org/10.1016/j.jechem.2021.12.004>.
243. Y. Zhang, T. Wik, J. Bergström, M. Pecht, and C. Zou, "A Machine Learning-based Framework for Online Prediction of Battery Ageing Trajectory and Lifetime Using Histogram Data," *Journal of Power Sources* 526 (2022): 231110, <https://doi.org/10.1016/j.jpowsour.2022.231110>.
244. K. Y. Liu, T. T. Wang, B. B. Zou, H. J. Peng, and X. Liu, "TELL-Me: T Time-series-decomposition-based Ensembled Lightweight Learning Model for Diverse Battery Prognosis and Diagnosis," *Journal of Energy Chemistry* 106 (2025): 1–8, <https://doi.org/10.1016/j.jechem.2025.01.063>.
245. K. Y. Liu, T. T. Wang, X. Liu, and H. J. Peng, "Data-Driven Online Prognosis of Rechargeable Batteries: Prospect and Perspective," *Batteries & Supercaps* 7, no. 3 (2024): 202300596, <https://doi.org/10.1002/batt.202300596>.
246. A. Vasylyev, A. Vannoni, and A. Sorce, "Optimal Dispatch of Li-Ion Battery Energy Storage, Reviewing and Considering Cycling and Calendar Ageing Models," *Applied Thermal Engineering* 265 (2025): 125597.
247. H. Zhu, C. Yin, M. Lu, et al., "A Critical Review on Operating Parameter Monitoring/Estimation, Battery Management and Control System for Redox Flow Batteries," *Journal of Energy Storage* 102 (2024): 114029, <https://doi.org/10.1016/j.est.2024.114029>.
248. Z. M. Ali, F. Jurado, F. H. Gandoman, and M. Čalasan, "Advancements in Battery Thermal Management for Electric Vehicles: Types, Technologies, and Control Strategies Including Deep Learning Methods," *Ain Shams Engineering Journal* 15, no. 9 (2024): 102908, <https://doi.org/10.1016/j.asej.2024.102908>.

249. K. Liu, Q. Peng, Z. Liu, W. Li, N. Cui, and C. Zhang, "Adaptive Battery Thermal Management Systems in Unsteady Thermal Application Contexts," *Journal of Energy Chemistry* 97 (2024): 650–668, <https://doi.org/10.1016/j.jechem.2024.07.004>.
250. K. Chen, Z. Zhang, B. Wu, M. Song, and X. Wu, "An Air-cooled System with a Control Strategy for Efficient Battery Thermal Management," *Applied Thermal Engineering* 236 (2024): 121578, <https://doi.org/10.1016/j.applthermaleng.2023.121578>.
251. R. J. Wang, Y. H. Pan, and W. L. Cheng, "A Dimensionless Study on Thermal Control of Positive Temperature Coefficient (PTC) Materials," *International Communications in Heat and Mass Transfer* 120 (2021): 104987, <https://doi.org/10.1016/j.icheatmasstransfer.2020.104987>.
252. J. Feng, A. Yu, L. Zhang, F. Liu, and Z. Zhan, "Adaptive Self-preheating Lithium-ion Battery System Based on Positive Temperature Coefficient Material at Sub-freezing Temperatures," *Applied Thermal Engineering* 278 (2025): 127319.
253. T. Wang, J. Wu, J. Wu, et al., "Energy Consumption Analysis and Performance Evaluation of Electric Vehicle Integrated Thermal Management System Experiments," *Applied Thermal Engineering* 269 (2025): 126002, <https://doi.org/10.1016/j.applthermaleng.2025.126002>.
254. L. He, H. Jing, Y. Zhang, P. Li, and Z. Gu, "Performance Research of Integrated Thermal Management System for Battery Electric Vehicles with Motor Waste Heat Recovery," *Journal of Energy Storage* 84 (2024): 110893, <https://doi.org/10.1016/j.est.2024.110893>.
255. F. Fei and D. Wang, "PTC Power Control of Electric Vehicle Thermal Management System Based on Neural Network Feedforward," *Applied Thermal Engineering* 253 (2024): 123803.
256. H. Togun, A. Basem, H. I. Mohammed, et al., "A Comprehensive Review of Battery Thermal Management Systems for Electric Vehicles: Enhancing Performance, Sustainability, and Future Trends," *International Journal of Hydrogen Energy* 97 (2025): 1077–1107, <https://doi.org/10.1016/j.ijhydene.2024.11.093>.
257. F. S. Hwang, T. Confrey, C. Reidy, et al., "Review of Battery Thermal Management Systems in Electric Vehicles," *Renewable and Sustainable Energy Reviews* 192 (2024): 114171, <https://doi.org/10.1016/j.rser.2023.114171>.
258. Z. Rao and S. Wang, "A Review of Power Battery Thermal Energy Management," *Renewable and Sustainable Energy Reviews* 15, no. 9 (2011): 4554–4571, <https://doi.org/10.1016/j.rser.2011.07.096>.
259. Z. Yu, J. Zhang, and W. Pan, "A Review of Battery Thermal Management Systems about Heat Pipe and Phase Change Materials," *Journal of Energy Storage* 62 (2023): 106827, <https://doi.org/10.1016/j.est.2023.106827>.
260. Y. Wu, A. C. Y. Yuen, C. Mo, Q. Chen, and X. Huang, "An Advanced BPNN/RVEA Coupled Control Strategy for Novel Immersed Liquid Cooling Battery Thermal Management System," *Journal of Energy Storage* 125 (2025): 117008, <https://doi.org/10.1016/j.est.2025.117008>.
261. N. Khan, C. A. Ooi, A. Alturki, M. Amir, and T. Alharbi, "A Critical Review of Battery Cell Balancing Techniques, Optimal Design, Converter Topologies, and Performance Evaluation for Optimizing Storage System in Electric Vehicles," *Energy Reports* 11 (2024): 4999–5032, <https://doi.org/10.1016/j.egy.2024.04.041>.
262. E. Jiaqiang, B. Zhang, Y. Zeng, et al., "Effects Analysis on Active Equalization Control of Lithium-ion Batteries Based on Intelligent Estimation of the state-of-charge," *Energy* 238 (2022): 121822.
263. A. K. Singh, K. Kumar, U. Choudhury, A. K. Yadav, A. Ahmad, and K. Surender, "Applications of Artificial Intelligence and Cell Balancing Techniques for Battery Management System (BMS) in Electric Vehicles: a Comprehensive Review," *Process Safety and Environmental Protection* 191 (2024): 2247–2265, <https://doi.org/10.1016/j.psep.2024.09.105>.
264. S. Kivrak, T. Özer, Y. Oğuz, and E. B. Erken, "Battery Management System Implementation with the Passive Control Method Using MOSFET as a Load," *Measurement and Control* 53, no. 1-2 (2020): 205–213, <https://doi.org/10.1177/0020294019883401>.
265. D. Shylla, R. Harikrishnan, and R. Swarnkar, "Comparative Analysis and Evaluation of the Different Active Cell Balancing Topologies in Lithium Ions Batteries," *Journal of The Electrochemical Society* 170, no. 8 (2023): 080501, <https://doi.org/10.1149/1945-7111/ace958>.
266. M. M. Hoque, M. A. Hannan, A. Mohamed, and A. Ayob, "Battery Charge Equalization Controller in Electric Vehicle Applications: a Review," *Renewable and Sustainable Energy Reviews* 75 (2017): 1363–1385, <https://doi.org/10.1016/j.rser.2016.11.126>.
267. M. Daowd, M. Antoine, N. Omar, P. Van den Bossche, and J. Van Mierlo, "Single Switched Capacitor Battery Balancing System Enhancements," *Energies* 6, no. 4 (2013): 2149–2174, <https://doi.org/10.3390/en6042149>.
268. S. Goodarzi, R. Beiranvand, S. M. Mousavi, and M. Mohamadian, "A New Algorithm for Increasing Balancing Speed of Switched-capacitor Lithium-ion Battery Cell Equalizers," in *The 6th Power Electronics, Drive Systems & Technologies Conference (PEDSTC2015) (IEEE, 2015)*, 292–297.
269. C. S. Lim, K. J. Lee, N. J. Ku, D. S. Hyun, and R. Y. Kim, "A Modularized Equalization Method Based on Magnetizing Energy for a Series-connected Lithium-ion Battery String," *IEEE Transactions on Power Electronics* 29, no. 4 (2013): 1791–1799, <https://doi.org/10.1109/TPEL.2013.2270000>.
270. J. Sun and D. Dai, "An Equalization Topology Based on Multi-winding Transformer and Flyback Converter for Series-connected Lithium-ion Battery Packs," *Journal of Energy Storage* 125 (2025): 116963, <https://doi.org/10.1016/j.est.2025.116963>.
271. B. Wang, D. Xuan, X. Zhao, J. Chen, and C. Lu, "Dynamic Battery Equalization Scheme of Multi-cell Lithium-ion Battery Pack Based on PSO and VUFLC," *International Journal of Electrical Power & Energy Systems* 136 (2022): 107760, <https://doi.org/10.1016/j.ijepes.2021.107760>.
272. Q. Yu, C. Wang, J. Li, R. Xiong, and M. Pecht, "Challenges and Outlook for Lithium-ion Battery Fault Diagnosis Methods from the Laboratory to Real World Applications," *ETransportation* 17 (2023): 100254.
273. Z. Sun, Z. Wang, P. Liu, et al., "An Online Data-driven Fault Diagnosis and Thermal Runaway Early Warning for Electric Vehicle Batteries," *IEEE transactions on power electronics* 37, no. 10 (2022): 12636–12646.
274. L. Jiang, Z. Deng, X. Tang, L. Hu, X. Lin, and X. Hu, "Data-driven Fault Diagnosis and Thermal Runaway Warning for Battery Packs Using Real-world Vehicle Data," *Energy* 234 (2021): 121266.
275. D. Li, P. Liu, Z. Zhang, et al., "Battery Thermal Runaway Fault Prognosis in Electric Vehicles Based on Abnormal Heat Generation and Deep Learning Algorithms," *IEEE Transactions on Power Electronics* 37, no. 7 (2022): 8513–8525, <https://doi.org/10.1109/TPEL.2022.3150026>.
276. H. Zhao, C. Zhang, L. Xu, C. Liao, L. Wang, and L. Wang, "A Deep Neural Network for Multi-fault Diagnosis of Battery Packs Based on an Incremental Voltage Measurement Topology," *Energy* 316 (2025): 134590.
277. P. Mei, H. R. Karimi, J. Xie, et al., "Battery state Estimation Methods and Management System under Vehicle–cloud Collaboration: a Survey," *Renewable and Sustainable Energy Reviews* 206 (2024): 114857, <https://doi.org/10.1016/j.rser.2024.114857>.
278. GB/T 32960.3-2025, Technical Specifications for Remote Service and Management System for Electric Vehicles—Part 3: Communication Protocol and Data Format (Standards Press of China, 2025).
279. H. Jing, H. U. Jianyao, J. Ouyang, and S. S. Ou, "An Integrated Data-driven and Physics-based Approach for Dynamic Operation Simulation of Electric Vehicles (No. 2025-01-8604)," *SAE Technical Paper* (2025), <https://doi.org/10.4271/2025-01-8604>.
280. Q. Li, Y. Wang, Z. Pu, S. Wang, and W. Zhang, "Time Series Association state Analysis Method for Attacks on the Smart Internet of Electric Vehicle Charging Network," *Transportation Research Record: Journal of the Transportation Research Board* 2673, no. 4 (2019): 217–228, <https://doi.org/10.1177/0361198119837180>.

281. X. Ding, D. Zhang, J. Cheng, B. Wang, and P. C. K. Luk, "An Improved Thevenin Model of Lithium-ion Battery with High Accuracy for Electric Vehicles," *Applied Energy* 254 (2019): 113615, <https://doi.org/10.1016/j.apenergy.2019.113615>.
282. S. Li, H. He, P. Zhao, and S. Cheng, "Data Cleaning and Restoring Method for Vehicle Battery Big Data Platform," *Applied Energy* 320 (2022): 119292, <https://doi.org/10.1016/j.apenergy.2022.119292>.
283. J. Hong, K. Li, F. Liang, et al., "A Novel state of Health Prediction Method for Battery System in Real-world Vehicles Based on Gated Recurrent Unit Neural Networks," *Energy* 289 (2024): 129918.
284. Y. Zhao, Z. Jiang, X. Chen, P. Liu, T. Peng, and Z. Shu, "Toward Environmental Sustainability: Data-driven Analysis of Energy Use Patterns and Load Profiles for Urban Electric Vehicle Fleets," *Energy* 285 (2023): 129465.
285. X. Yang, Z. Peng, P. Wang, and C. Zhuge, "Seasonal Variance in Electric Vehicle Charging Demand and Its Impacts on Infrastructure Deployment: a Big Data Approach," *Energy* 280 (2023): 128230.
286. Y. Zhao, Z. Wang, Z. J. M. Shen, L. Zhang, D. G. Dorrell, and F. Sun, "Big Data-driven Decoupling Framework Enabling Quantitative Assessments of Electric Vehicle Performance Degradation," *Applied Energy* 327 (2022): 120083, <https://doi.org/10.1016/j.apenergy.2022.120083>.
287. D. Cui, Z. Wang, P. Liu, et al., "Battery Electric Vehicle Usage Pattern Analysis Driven by Massive Real-world Data," *Energy* 250 (2022): 123837.
288. B. Li, M. C. Kisacikoglu, C. Liu, N. Singh, and M. Erol-Kantarci, "Big Data Analytics for Electric Vehicle Integration in Green Smart Cities," *IEEE Communications Magazine* 55, no. 11 (2017): 19–25, <https://doi.org/10.1109/MCOM.2017.1700133>.
289. D. Cui, Z. Wang, Z. Zhang, P. Liu, S. Wang, and D. G. Dorrell, "Driving Event Recognition of Battery Electric Taxi Based on Big Data Analysis," *IEEE Transactions on Intelligent Transportation Systems* 23, no. 7 (2021): 9200–9209, <https://doi.org/10.1109/TITS.2021.3092756>.
290. X. Wu, Z. Zuo, and P. Liu, "User Behavior Optimization Strategy for Electric Vehicle Based on Improving Battery SOH," in *Proceedings of China SAE Congress 2021: Selected Papers* (Singapore: Springer Nature Singapore, 2022, October), 1223–1236.
291. F. Rücker, J. Figgner, I. Schoeneberger, and D. U. Sauer, "Battery Electric Vehicles in Commercial Fleets: Use Profiles, Battery Aging, and Open-access Data," *Journal of Energy Storage* 86 (2024): 111030.
292. R. Sun, J. Chen, and C. Piao, "Battery Health Features Extraction and state of Health Estimation Based on Real-time Online Vehicle Driving Data," *Journal of Power Sources* 645 (2025): 236784, <https://doi.org/10.1016/j.jpowsour.2025.236784>.
293. D. Kumar and M. K. Sharma, "Early Prediction of Battery Swelling via Delta Resistance Features and Optimized Machine Learning Models to Avoid Thermal Runaway," *Franklin Open* 12 (2025): 100389.
294. J. Tan, Z. Wei, R. Wang, C. Zhang, and H. He, "Data Restoration and Aging Classification Warning within Cloud-edge Battery Management System," *Journal of Energy Storage* 118 (2025): 116186, <https://doi.org/10.1016/j.est.2025.116186>.
295. J. Hong, F. Liang, H. Yang, et al., "Multi-forward-step state of Charge Prediction for Real-world Electric Vehicles Battery Systems Using a Novel LSTM-GRU Hybrid Neural Network," *Etransportation* 20 (2024): 100322.
296. W. Li, M. Rentemeister, J. Badeda, D. Jöst, D. Schulte, and D. U. Sauer, "Digital Twin for Battery Systems: Cloud Battery Management System with Online state-of-charge and state-of-health Estimation," *Journal of energy storage* 30 (2020): 101557, <https://doi.org/10.1016/j.est.2020.101557>.
297. H. Jing, J. Hu, S. S. Ou, Z. Lv, R. Lyu, and J. Zhao, "Scalable and Generalizable Deep Learning for Battery state of Health Estimation in on-road Electric Vehicles," *Journal of Energy Chemistry* 110 (2025): 823–841.
298. B. Ma, L. Zhang, H. Yu, et al., "End-cloud Collaboration Method Enables Accurate state of Health and Remaining Useful Life Online Estimation in Lithium-ion Batteries," *Journal of Energy Chemistry* 82 (2023): 1–17, <https://doi.org/10.1016/j.jechem.2023.02.052>.
299. W. Wang, K. Yang, L. Zhang, et al., "An End-cloud Collaboration Approach for Online state-of-health Estimation of Lithium-ion Batteries Based on Multi-feature and Transformer," *Journal of Power Sources* 608 (2024): 234669, <https://doi.org/10.1016/j.jpowsour.2024.234669>.
300. S. Yang, Z. Zhang, R. Cao, et al., "Implementation for a Cloud Battery Management System Based on the CHAIN Framework," *Energy and AI* 5 (2021): 100088, <https://doi.org/10.1016/j.egyai.2021.100088>.
301. I. Altiner and S. S. Ou, "Reinforcement Learning in Optimizing the Electric Vehicle Battery System Coupling with Driving Behaviors (No. 2024-01-2006)," *SAE Technical Paper* (2024), <https://doi.org/10.4271/2024-01-2006>.
302. D. Ding, Z. Li, L. Luo, et al., "Large Lithium-ion Battery Model for Secure Shared Electric Bike Battery in Smart Cities," *Nature Communications* 16, no. 1 (2025): 8415, <https://doi.org/10.1038/s41467-025-63678-7>.
303. H. Yu, H. Dai, G. Tian, et al., "Big-data-based Power Battery Recycling for New Energy Vehicles: Information Sharing Platform and Intelligent Transportation Optimization," *IEEE Access* 8 (2020): 99605–99623, <https://doi.org/10.1109/ACCESS.2020.2998178>.
304. Y. Hua, X. Liu, S. Zhou, Y. Huang, H. Ling, and S. Yang, "Toward Sustainable Reuse of Retired Lithium-ion Batteries from Electric Vehicles," *Resources, Conservation and Recycling* 168 (2021): 105249, <https://doi.org/10.1016/j.resconrec.2020.105249>.
305. H. Wang, T. Liu, B. Kim, et al., "Architectural Design Alternatives Based on Cloud/Edge/Fog Computing for Connected Vehicles," *IEEE Communications Surveys & Tutorials* 22, no. 4 (2020): 2349–2377, <https://doi.org/10.1109/COMST.2020.3020854>.
306. A. S. Ramesh, S. Vigneshwar, S. Vickram, et al., "Artificial Intelligence Driven Hydrogen and Battery Technologies—A Review," *Fuel* 337 (2023): 126862.
307. V. B. Korde, A. B. Khelkar, S. Khot, P. Malavadakar, P. Deshmukh, and S. Amalraj, "Advancements of Lithium-ion Battery Recycling: Transitioning from Traditional Methods to AI and Machine Learning Techniques," *Renewable and Sustainable Energy Reviews* 225 (2026): 116180, <https://doi.org/10.1016/j.rser.2025.116180>.
308. Y. Xiong, D. Zhang, X. Ruan, et al., "Artificial Intelligence in Rechargeable Battery: Advancements and Prospects," *Energy Storage Materials* 73 (2024): 103860, <https://doi.org/10.1016/j.ensm.2024.103860>.
309. J. Park and J. Lee, "Electrochemical Energy Conversion and Storage Processes with Machine Learning," *Trends in Chemistry* 6, no. 6 (2024): 302–313, <https://doi.org/10.1016/j.trechm.2024.04.007>.
310. K. Liu, J. Fang, S. Zhao, et al., "Battery state-of-health Estimation: an Ultrasonic Detection Method with Explainable AI," *Energy* 319 (2025): 134923.
311. Z. Liu, Y. Lu, X. Ma, et al., "Advanced Functional Optical fiber Sensors for Smart Battery Monitoring," *Energy Material Advances* 5 (2024): 0142, <https://doi.org/10.34133/energymatadv.0142>.
312. M. Aery, I. Vashishat, S. Malik, N. Jindal, and M. Singh, "Predicting EV Li-ion Battery Fires: an Integrated Approach Using Generative AI and Machine Learning Based on Vented Gas Emissions," *IEEE Transactions on Intelligent Transportation Systems* 26 (2025): 12121–12131, <https://doi.org/10.1109/TITS.2025.3562181>.
313. D. Huang, M. Qin, D. Liu, Q. Sun, S. Hu, and Y. Zhang, "Multi-step Ahead SOH Prediction for Vehicle Batteries Based on Multimodal Feature Fusion and Spatio-temporal Attention Neural Network," *Journal of Energy Storage* 124 (2025): 116837, <https://doi.org/10.1016/j.est.2025.116837>.
314. X. Li, C. Gwan, S. Zhao, X. Gao, and Y. Zhu, "Multimodal Temperature Prediction for Lithium-ion Battery Thermal Runaway Using Multi-scale Gated Fusion and Bidirectional Cross-attention Mechanisms,"

- Journal of Energy Storage* 116 (2025): 116098, <https://doi.org/10.1016/j.est.2025.116098>.
315. H. Liu, Y. Wang, X. Li, Y. Li, and Y. Shang, "Early Warning of Thermal Runaway for Lithium-ion Batteries Based on Multimodal Reconstruction Fusion of Acoustic Signals," *Journal of Energy Storage* 137 (2025): 118497, <https://doi.org/10.1016/j.est.2025.118497>.
316. Y. Zeng, S. Mai, W. Yan, and H. Hu, "Multimodal Reaction: Information Modulation for Cross-modal Representation Learning," *IEEE Transactions on Multimedia* 26 (2023): 2178–2191, <https://doi.org/10.1109/TMM.2023.3293335>.
317. L. Ma, J. Tian, T. Zhang, Q. Guo, and C. Y. Chung, "Enhanced Battery Life Prediction with Reduced Data Demand via Semi-supervised Representation Learning," *Journal of Energy Chemistry* 101 (2025): 524–534, <https://doi.org/10.1016/j.jechem.2024.10.001>.
318. X. Yang, Z. Song, I. King, and Z. Xu, "A Survey on Deep Semi-supervised Learning," *IEEE transactions on knowledge and data engineering* 35, no. 9 (2022): 8934–8954, <https://doi.org/10.1109/TKDE.2022.3220219>.
319. G. Kim, "Recent deep semi-supervised learning approaches and related works arXiv preprint," (2021), *arXiv:2106.11528*.
320. M. R. Amini, V. Feofanov, L. Pauletto, L. Hadjadj, E. Devijver, and Y. Maximov, "Self-training: a Survey," *Neurocomputing* 616 (2025): 128904, <https://doi.org/10.1016/j.neucom.2024.128904>.
321. X. Li, M. Lyv, X. Gao, K. Li, and Y. Zhu, "A co-estimation Framework of state of Health and Remaining Useful Life for Lithium-ion Batteries Using the Semi-supervised Learning Algorithm," *Energy and AI* 19 (2025): 100458, <https://doi.org/10.1016/j.egyai.2024.100458>.
322. N. Guo, S. Chen, J. Tao, Y. Liu, J. Wan, and X. Li, "Semi-supervised Learning for Explainable Few-shot Battery Lifetime Prediction," *Joule* 8, no. 6 (2024): 1820–1836, <https://doi.org/10.1016/j.joule.2024.02.020>.
323. W. Liu, S. Yue, P. Yang, R. Zhou, and J. Yu, "Densely-connected Contrastive Observer for Fault Diagnosis of VRLA Battery in Large Data Center Based on Semisupervised Few-shot Learning," *IEEE Transactions on Power Electronics* 39, no. 10 (2024): 13758–13770, <https://doi.org/10.1109/TPEL.2024.3414135>.
324. Y. Song, T. Wang, P. Cai, S. K. Mondal, and J. P. Sahoo, "A Comprehensive Survey of Few-shot Learning: Evolution, Applications, Challenges, and Opportunities," *ACM Computing Surveys* 55, no. 13s (2023): 1–40, <https://doi.org/10.1145/3582688>.
325. H. Gharoun, F. Momenifar, F. Chen, and A. H. Gandomi, "Meta-learning Approaches for Few-shot Learning: a Survey of Recent Advances," *ACM Computing Surveys* 56, no. 12 (2024): 1–41, <https://doi.org/10.1145/3659943>.
326. A. Hosna, E. Merry, J. Gyalmo, Z. Alom, Z. Aung, and M. A. Azim, "Transfer Learning: a Friendly Introduction," *Journal of Big Data* 9, no. 1 (2022): 102, <https://doi.org/10.1186/s40537-022-00652-w>.
327. J. Meng, Y. You, M. Lin, J. Wu, and Z. Song, "Multi-scenarios Transferable Learning Framework with Few-shot for Early Lithium-ion Battery Lifespan Trajectory Prediction," *Energy* 286 (2024): 129682.
328. C. Dong and D. Sun, "Multi-source Domain Transfer Learning with Small Sample Learning for Thermal Runaway Diagnosis of Lithium-ion Battery," *Applied Energy* 365 (2024): 123248, <https://doi.org/10.1016/j.apenergy.2024.123248>.
329. J. Zhao, L. Kong, and J. Lv, "An Overview of Deep Neural Networks for Few-shot Learning," *Big Data Mining and Analytics* 8, no. 1 (2024): 145–188, <https://doi.org/10.26599/BDMA.2024.9020049>.
330. A. Vettoruzzo, M. R. Bouguelia, J. Vanschoren, T. Rognvaldsson, and K. C. Santosh, "Advances and Challenges in Meta-learning: a Technical Review," *IEEE transactions on pattern analysis and machine intelligence* 46, no. 7 (2024): 4763–4779, <https://doi.org/10.1109/TPAMI.2024.3357847>.
331. H. Xue, Y. An, Y. Qin, et al., "Toward Few-Shot Learning in the Open World: a Review and beyond," *IEEE Transactions on Pattern Analysis and Machine Intelligence* 47 (2025): 10420–10440, <https://doi.org/10.1109/TPAMI.2025.3594686>.
332. X. Sun, C. Zhao, S. Yang, G. Wang, and H. Yu, "ShotAdpt: Few-shot Early Prediction of Battery Cycle Life with Adaptive Feature Reduction," *IEEE Transactions on Transportation Electrification* 11 (2025): 12874–12886, <https://doi.org/10.1109/TTE.2025.3596992>.
333. J. Yang, X. Wang, M. Zhang, and L. Jiang, "Bayesian Meta Random Graph Implicit Enhanced Network for Lithium-ion Batteries Remaining Useful Life Prediction with Few-shot and Uncertainty Interference," *IEEE Transactions on Transportation Electrification* 11 (2025): 9877–9889, <https://doi.org/10.1109/TTE.2025.3563217>.
334. V. Rani, S. T. Nabi, M. Kumar, A. Mittal, and K. Kumar, "Self-supervised Learning: a Succinct Review," *Archives of Computational Methods in Engineering* 30, no. 4 (2023): 2761–2775, <https://doi.org/10.1007/s11831-023-09884-2>.
335. J. Gui, T. Chen, J. Zhang, et al., "A Survey on Self-supervised Learning: Algorithms, Applications, and Future Trends," *IEEE Transactions on Pattern Analysis and Machine Intelligence* 46, no. 12 (2024): 9052–9071, <https://doi.org/10.1109/TPAMI.2024.3415112>.
336. K. Zhang, Q. Wen, C. Zhang, et al., "Self-supervised Learning for Time Series Analysis: Taxonomy, Progress, and Prospects," *IEEE transactions on pattern analysis and machine intelligence* 46, no. 10 (2024): 6775–6794, <https://doi.org/10.1109/TPAMI.2024.3387317>.
337. M. Miao, P. Yang, S. Yue, R. Zhou, and J. Yu, "Multi-source Self-supervised Domain Adaptation Network for VRLA Battery Anomaly Detection of Data Center under Non-ideal Conditions," *Energy* 299 (2024): 131392.
338. T. Wang, Z. Ma, S. Zou, Z. Chen, and P. Wang, "Lithium-ion Battery state-of-health Estimation: a Self-supervised Framework Incorporating Weak Labels," *Applied Energy* 355 (2024): 122332, <https://doi.org/10.1016/j.apenergy.2023.122332>.
339. A. Arunan, Y. Qin, X. Li, U. X. Tan, H. V. Poor, and C. Yuen, "Learning More with Less: a Generalizable, Self-supervised Framework for Privacy-preserving Capacity Estimation with EV Charging Data," *IEEE Transactions on Industrial Informatics* 22 (2025): 543–554.
340. Q. Wang, M. Ye, S. Celik, et al., "Unlocking the Potential of Unlabeled Data: Self-supervised Machine Learning for Battery Aging Diagnosis with Real-world Field Data," *Journal of Energy Chemistry* 99 (2024): 681–691, <https://doi.org/10.1016/j.jechem.2024.08.037>.
341. R. Xiong, Y. He, Y. Sun, Y. Jia, and W. Shen, "Enhanced Electrode-level Diagnostics for Lithium-ion Battery Degradation Using Physics-informed Neural Networks," *Journal of Energy Chemistry* 104 (2025): 618–627.
342. L. Yang, M. He, Y. Ren, B. Gao, and H. Qi, "Physics-informed Neural Network for co-estimation of state of Health, Remaining Useful Life, and Short-term Degradation Path in Lithium-ion Batteries," *Applied Energy* 398 (2025): 126427, <https://doi.org/10.1016/j.apenergy.2025.126427>.
343. Y. Luo, S. Ju, P. Li, and H. Zhang, "A Method for Estimating Lithium-ion Battery state of Health Based on Physics-informed Hybrid Neural Network," *Electrochimica Acta* 525 (2025): 146110, <https://doi.org/10.1016/j.electacta.2025.146110>.
344. T. T. Wang, K. Y. Liu, H. J. Peng, and X. Liu, "Interpretable Machine Learning for Battery Prognosis: Retrospect and Prospect," *Advanced Energy Materials* 15, no. 48 (2025): 03067, <https://doi.org/10.1002/aenm.202503067>.
345. R. Lian and W. Li, "Unlocking Battery Insights with Interpretable Machine Learning," *Joule* 9, no. 9 (2025): 102131, <https://doi.org/10.1016/j.joule.2025.102131>.
346. X. Ye, Y. Cheng, X. Lan, et al., "Interpretable Machine Learning for Solid-state Batteries," *ACS nano* 20 (2026): 4637–4647, <https://doi.org/10.1021/acsnano.5c21738>.

347. K. Luo, J. Zhao, Y. Wang, et al., “Physics-informed Neural Networks for PDE Problems: a Comprehensive Review,” *Artificial Intelligence Review* 58, no. 10 (2025): 323.
348. G. E. Karniadakis, I. G. Kevrekidis, L. Lu, P. Perdikaris, S. Wang, and L. Yang, “Physics-informed Machine Learning,” *Nature Reviews Physics* 3, no. 6 (2021): 422–440, <https://doi.org/10.1038/s42254-021-00314-5>.
349. C. Lin, L. Wu, X. Tuo, et al., “A Lightweight Two-stage Physics-informed Neural Network for SOH Estimation of Lithium-ion Batteries with Different Chemistries,” *Journal of Energy Chemistry* 105 (2025): 261–279, <https://doi.org/10.1016/j.jechem.2025.01.057>.
350. K. Shen, W. Xu, X. Lai, et al., “Physics-informed Machine Learning Estimation of the Temperature of Large-format Lithium-ion Batteries under Various Operating Conditions,” *Applied Thermal Engineering* 269 (2025): 126200, <https://doi.org/10.1016/j.applthermaleng.2025.126200>.
351. F. Wang, Z. Zhai, Z. Zhao, Y. Di, and X. Chen, “Physics-informed Neural Network for Lithium-ion Battery Degradation Stable Modeling and Prognosis,” *Nature Communications* 15, no. 1 (2024): 4332, <https://doi.org/10.1038/s41467-024-48779-z>.
352. R. Zhu, J. Hu, and W. Peng, “Bayesian Calibrated Physics-informed Neural Networks for Second-life Battery SOH Estimation,” *Reliability Engineering & System Safety* 264 (2025): 111432, <https://doi.org/10.1016/j.res.2025.111432>.
353. F. Wang, Q. Zhi, Z. Zhao, et al., “Inherently Interpretable Physics-informed Neural Network for Battery Modeling and Prognosis,” *IEEE Transactions on Neural Networks and Learning Systems* 36 (2023): 1145–1159.
354. Q. Wang, M. Ye, B. Li, G. Lian, and Y. Li, “Co-estimation of state of Charge and Capacity for Battery Packs in Real Electric Vehicles with Few Representative Cells and Physics-informed Machine Learning,” *Energy* 306 (2024): 132520.
355. H. Pang, L. Wu, J. Liu, X. Liu, and K. Liu, “Physics-informed Neural Network Approach for Heat Generation Rate Estimation of Lithium-ion Battery under Various Driving Conditions,” *Journal of Energy Chemistry* 78 (2023): 1–12, <https://doi.org/10.1016/j.jechem.2022.11.036>.
356. X. Liu, H. J. Peng, B. Q. Li, et al., “Untangling Degradation Chemistries of Lithium-Sulfur Batteries through Interpretable Hybrid Machine Learning,” *Angewandte Chemie* 134, no. 48 (2022): 202214037, <https://doi.org/10.1002/ange.202214037>.
357. F. Naseri, S. Gil, C. Barbu, et al., “Digital Twin of Electric Vehicle Battery Systems: Comprehensive Review of the Use Cases, Requirements, and Platforms,” *Renewable and Sustainable Energy Reviews* 179 (2023): 113280, <https://doi.org/10.1016/j.rser.2023.113280>.
358. A. Bendaouia, F. Wang, H. Oufiak, and J. Li, “Digital Twin for Battery Energy Storage Systems,” *Renewable and Sustainable Energy Reviews* 226 (2026): 116347, <https://doi.org/10.1016/j.rser.2025.116347>.
359. M. Dubarry, D. Howey, and B. Wu, “Enabling Battery Digital Twins at the Industrial Scale,” *Joule* 7, no. 6 (2023): 1134–1144, <https://doi.org/10.1016/j.joule.2023.05.005>.
360. W. Li, Y. Li, A. Garg, and L. Gao, “Enhancing Real-time Degradation Prediction of Lithium-ion Battery: a Digital Twin Framework with CNN-LSTM-attention Model,” *Energy* 286 (2024): 129681.
361. K. Shen, Y. Ling, X. Meng, et al., “A Deep Learning-based Digital Twin Model for the Temperature Field of Large-scale Battery Systems,” *Journal of Energy Storage* 113 (2025): 115676, <https://doi.org/10.1016/j.est.2025.115676>.
362. I. Saba, M. Ullah, and M. Tariq, “Advancing Electric Vehicle Battery Analysis with Digital Twins in Intelligent Transportation Systems,” *IEEE Transactions on Intelligent Transportation Systems* 25, no. 9 (2024): 12141–12150, <https://doi.org/10.1109/TITS.2024.3361807>.
363. G. Luo, D. Han, Y. Zhang, and H. Ruan, “A Digital Twin for Advancing Battery Fast Charging Based on a Bayesian Optimization-based Method,” *Journal of Energy Storage* 93 (2024): 112365, <https://doi.org/10.1016/j.est.2024.112365>.
364. Y. Sun, Y. Ning, Z. Qiang, et al., “Digital-Twin-Assisted Insights into Irreversible Capacity and Activation Strategy Power High-Loading Solid-State Batteries,” *Angewandte Chemie International Edition* 64, no. 36 (2025): 202502169, <https://doi.org/10.1002/anie.202502169>.
365. H. Zhang, D. Ren, H. Ming, et al., “Digital Twin Enables Rational Design of Ultrahigh-Power Lithium-Ion Batteries,” *Advanced Energy Materials* 13, no. 1 (2023): 2202660, <https://doi.org/10.1002/aenm.202202660>.
366. B. B. Zou, K. Y. Liu, Y. Yan, et al., “Decoding Lithium Metal Battery Degradation with Symmetric-cell Artificial Intelligence Diagnostics (SAID),” *Advanced Materials* 38 (2025): 12041.
367. X. Liu, B. B. Zou, Y. N. Wang, et al., “Interpretable Learning of Accelerated Aging in Lithium Metal Batteries,” *Journal of the American Chemical Society* 146, no. 48 (2024): 33012–33021, <https://doi.org/10.1021/jacs.4c09363>.
368. Y. Che, J. Guo, Y. Zheng, et al., “Unlocking Interpretable Prediction of Battery Random Discharge Capacity with Domain Adaptive Physics Constraint,” *Advanced Energy Materials* 15, no. 13 (2025): 2405506, <https://doi.org/10.1002/aenm.202405506>.
369. L. Li, Y. Fan, M. Tse, and K. Y. Lin, “A Review of Applications in Federated Learning,” *Computers & Industrial Engineering* 149 (2020): 106854, <https://doi.org/10.1016/j.cie.2020.106854>.
370. D. C. Nguyen Ding, Q. V. Pham, P. N. Pathirana, L. B. Le, A. Seneviratne, and H. V. Poor, “Federated Learning Meets Blockchain in Edge Computing: Opportunities and Challenges,” *IEEE Internet of Things Journal* 8, no. 16 (2021): 12806–12825, <https://doi.org/10.1109/JIOT.2021.3072611>.
371. M. K. Hasan, N. Jahan, M. Z. A. Nazri, et al., “Federated Learning for Computational Offloading and Resource Management of Vehicular Edge Computing in 6G-V2X Network,” *IEEE Transactions on Consumer Electronics* 70, no. 1 (2024): 3827–3847.
372. R. Lai, J. Wang, Y. Tian, and J. Tian, “FedCBE: a Federated-learning-based Collaborative Battery Estimation System with Non-IID Data,” *Applied Energy* 368 (2024): 123534, <https://doi.org/10.1016/j.apenergy.2024.123534>.
373. T. Wang and Z. Dong, “Peer-to-peer Personalized Federated Transfer Learning for Battery state of Health Estimation of Vehicles,” *IEEE Transactions on Intelligent Vehicles* 10 (2024): 3195–3207.
374. T. Han, Z. Lu, and J. Yu, “Dynamic Weighted Federated Contrastive Self-supervised Learning for state-of-health Estimation of Lithium-ion Battery with Insufficient Labeled Samples,” *Applied Energy* 383 (2025): 125336, <https://doi.org/10.1016/j.apenergy.2025.125336>.
375. N. Lyu, Y. Jin, R. Xiong, S. Miao, and J. Gao, “Real-time Overcharge Warning and Early Thermal Runaway Prediction of Li-ion Battery by Online Impedance Measurement,” *IEEE transactions on industrial electronics* 69, no. 2 (2021): 1929–1936.
376. L. Zhang, Z. Mu, and C. Sun, “Remaining Useful Life Prediction for Lithium-ion Batteries Based on Exponential Model and Particle Filter,” *IEEE Access* 6 (2018): 17729–17740, <https://doi.org/10.1109/ACCESS.2018.2816684>.
377. Y. Huang, X. Lai, D. Ren, et al., “Thermal and Stoichiometry Inhomogeneity Investigation of Large-format Lithium-ion Batteries via a Three-dimensional Electrochemical-thermal Coupling Model,” *Electrochimica Acta* 468 (2023): 143212, <https://doi.org/10.1016/j.electacta.2023.143212>.
378. A. I. Rodriguez-Cea, D. Morinigo-Sotelo, and F. V. Tinaut, “A Procedure for Evaluating the SOH of Li-ion Batteries from Data during the Constant Voltage Charge Phase and the Use of an ECM with Internal Resistance,” *Journal of Energy Storage* 108 (2025): 115074, <https://doi.org/10.1016/j.est.2024.115074>.
379. V. Ruiz, A. Pfrang, A. Kriston, N. Omar, P. Van den Bossche, and L. Boon-Brett, “A Review of International Abuse Testing Standards and Regulations for Lithium Ion Batteries in Electric and Hybrid Electric Vehicles,” *Renewable and Sustainable Energy Reviews* 81 (2018): 1427–1452, <https://doi.org/10.1016/j.rser.2017.05.195>.

380. UL 2580; Safety Requirements for Vehicle Power Batteries. Underwriter laboratories inc.: Chicago, IL, USA, 2020.
381. IEC 62660-2; Secondary Lithium-Ion Cells for the Propulsion of Electric Road Vehicles-part 2: Reliability and Abuse Testing. International Electrical Commission: Geneva, Switzerland, 2018.
382. SAE J2464; Electric and Hybrid Electric Vehicle Rechargeable Energy Storage System (RESS) Safety and Abuse Testing. Society of Automotive Engineers: Pittsburgh, PA, USA, 2021. <https://www.mdpi.com/2313-0105/8/11/248#B67-batteries-08-00248>.
383. H. Meng, M. Hu, Z. Kong, et al., "Risk Analysis of Lithium-ion Battery Accidents Based on Physics-informed Data-driven Bayesian Networks," *Reliability Engineering & System Safety* 251 (2024): 110294, <https://doi.org/10.1016/j.res.2024.110294>.
384. X. Qu, J. Zhao, H. Pang, M. Fowler, and A. F. Burke, "Real-world Battery Diagnostics in Industry 4.0," *Green Energy and Intelligent Transportation* 5 (2025): 100298.
385. H. Tang, Y. Wu, Y. Cai, F. Wang, Z. Lin, and Y. Pei, "Design of Power Lithium Battery Management System Based on Digital Twin," *Journal of Energy Storage* 47 (2022): 103679, <https://doi.org/10.1016/j.est.2021.103679>.
386. J. M. Reniers and D. A. Howey, "Digital Twin of a MWh-scale Grid Battery System for Efficiency and Degradation Analysis," *Applied Energy* 336 (2023): 120774, <https://doi.org/10.1016/j.apenergy.2023.120774>.
387. Z. Li, J. Cong, Y. Ding, et al., "Strategies for Intelligent Detection and Fire Suppression of Lithium-ion Batteries," *Electrochemical Energy Reviews* 7, no. 1 (2024): 32, <https://doi.org/10.1007/s41918-024-00232-x>.
388. W. Mei, Z. Liu, C. Wang, et al., "Operando Monitoring of Thermal Runaway in Commercial Lithium-ion Cells via Advanced Lab-on-fiber Technologies," *Nature communications* 14, no. 1 (2023): 5251, <https://doi.org/10.1038/s41467-023-40995-3>.
389. J. Deng, X. Yu, D. Pang, B. Fei, and J. Mo, "Cutting-edge Gas Sensor Design for Monitoring Thermal Runaway in Lithium-ion Batteries: a Critical Review," *Journal of Energy Chemistry* 109 (2025): 769–785.
390. M. Schmid, E. Gebauer, C. Hanzl, and C. Endisch, "Active Model-based Fault Diagnosis in Reconfigurable Battery Systems," *IEEE Transactions on Power Electronics* 36, no. 3 (2020): 2584–2597, <https://doi.org/10.1109/TPEL.2020.3012964>.
391. M. Schmid, E. Gebauer, and C. Endisch, "Structural Analysis in Reconfigurable Battery Systems for Active Fault Diagnosis," *IEEE Transactions on Power Electronics* 36, no. 8 (2021): 8672–8684, <https://doi.org/10.1109/TPEL.2021.3049573>.
392. D. Luo, L. Jiang, H. Chen, et al., "Enhanced Energy Efficiency and Thermal Performance of a Hybrid Battery Thermal Management System by a Delay Control Strategy of Thermoelectric Coolers," *Renewable Energy* 253 (2025): 123607.
393. P. Wen, Z. S. Ye, Y. Li, S. Chen, P. Xie, and S. Zhao, "Physics-informed Neural Networks for Prognostics and Health Management of Lithium-ion Batteries," *IEEE Transactions on Intelligent Vehicles* 9, no. 1 (2023): 2276–2289, <https://doi.org/10.1109/TIV.2023.3315548>.
394. A. Tang, Y. Xu, J. Tian, X. Shu, and Q. Yu, "Physics-informed Battery Degradation Prediction: Forecasting Charging Curves Using One-cycle Data," *Journal of Energy Chemistry* 101 (2025): 825–836, <https://doi.org/10.1016/j.jechem.2024.10.018>.
395. J. Li, A. Khalatbarisoltani, Y. Che, Y. Yang, and X. Hu, "Data-Secure and Privacy-Protected Electric Vehicle Battery Fault Detection Using Decentralized Federated Learning with Differential Privacy," *Energy Storage Materials* 83 (2025): 104681, <https://doi.org/10.1016/j.ensm.2025.104681>.
396. W. Ma, S. Wan, X. Cui, et al., "Exploration and Application of Self-Healing Strategies in Lithium Batteries," *Advanced Functional Materials* 33, no. 15 (2023): 2212821, <https://doi.org/10.1002/adfm.202212821>.
397. X. Yang, Z. Zhang, X. Xu, et al., "Self-healing Functional Materials for Advanced Batteries: Mechanisms, Dynamics, and Applications," *Energy Storage Materials* 75 (2025): 103992, <https://doi.org/10.1016/j.ensm.2024.103992>.
398. Y. He, C. Wang, R. Zhang, et al., "A Self-healing Plastic Ceramic Electrolyte by an Aprotic Dynamic Polymer Network for Lithium Metal Batteries," *Nature Communications* 15, no. 1 (2024): 10015, <https://doi.org/10.1038/s41467-024-53869-z>.
399. R. Narayan, C. Laberty-Robert, J. Pelta, J. M. Tarascon, and R. Dominko, "Self-Healing: an Emerging Technology for Next-Generation Smart Batteries," *Advanced Energy Materials* 12, no. 17 (2022): 2102652, <https://doi.org/10.1002/aenm.202102652>.
400. H. Zhang, Y. Li, S. Zheng, et al., "Battery Lifetime Prediction across Diverse Ageing Conditions with Inter-cell Deep Learning," *Nature Machine Intelligence* 7, no. 2 (2025): 270–277, <https://doi.org/10.1038/s42256-024-00972-x>.
401. Y. Li, G. Gao, K. Chen, et al., "A Hybrid AFM-BiLSTM Model for Lithium-ion Battery Capacity Prediction Using Fused Features," *Energy* 338 (2025): 138888.
402. Y. Ning, F. Yang, Y. Zhang, et al., "Bridging Multimodal Data and Battery Science with Machine Learning," *Matter* 7, no. 6 (2024): 2011–2203.
403. S. Ding, C. Dong, T. Zhao, L. Koh, X. Bai, and J. Luo, "A Meta-learning Based Multimodal Neural Network for Multistep Ahead Battery Thermal Runaway Forecasting," *IEEE Transactions on Industrial Informatics* 17, no. 7 (July 2021): 4503–4511, <https://doi.org/10.1109/TII.2020.3015555>.
404. C. Bian, X. Han, Z. Duan, C. Deng, S. Yang, and J. Feng, "Hybrid Prompt-driven Large Language Model for Robust state-of-charge Estimation of Multitype li-ion Batteries," *IEEE Transactions on Transportation Electrification* 11, no. 1 (2024): 426–437, <https://doi.org/10.1109/TTE.2024.3391938>.
405. B. Chen, H. Shao, Y. Qin, Y. Jin, and X. Hu, "A Domain Knowledge-guided Industrial Large Model Framework: A Case Study in Battery Health Estimation and Recycling," *IEEE Transactions on Industrial Informatics* 21 (2025): 8080–8090, <https://doi.org/10.1109/TII.2025.3584498>.
406. H. Peng, C. Liu, and H. Li, "Large Language Model Enabled Health Management for Internet of Batteries in Electric Vehicles," *IEEE Internet of Things Journal* 12 (2024): 6082–6094.
407. W. Zuo, H. Zheng, T. He, et al., "Large Language Models for Batteries," *Joule* 9, no. 8 (2025): 102037, <https://doi.org/10.1016/j.joule.2025.102037>.

Supporting Information

Additional supporting information can be found online in the Supporting Information section.

Supplementary File: aenm71093-sup-0001-SuppMat.docx.